Master's thesis

NTNU
Norwegian University of Science and Technology
Faculty of Engineering
Department of Energy and Process Engineering

Maximilian August Windingstad Sletbakk
Eskil Kvålsvold
Jonas Dalby

Energy and Climate Concept for the Development of a Zero-Emission Residential Area – Analysis of Energy Supply Solutions

Master's thesis in Energi og Miljø
Supervisor: Natasa Nord
June 2023

NTNU
Norwegian University of
Science and Technology

Maximilian August Windingstad Sletbakk
Eskil Kvålsvold
Jonas Dalby

Energy and Climate Concept for the Development of a Zero-Emission Residential Area – Analysis of Energy Supply Solutions

Master's thesis in Energi og Miljø
Supervisor: Natasa Nord
June 2023

Norwegian University of Science and Technology
Faculty of Engineering
Department of Energy and Process Engineering

Background

The future energy requirements for buildings are going to become stricter, both in terms of energy efficiency and requirements for renewable energy sources. Additionally, it is important to have high ambitions in the development of building and residential areas. Furthermore, it is crucial that the electrical power grid is not overloaded and that there is a balance between the supply of heat and electricity. This is important both in terms of investment and operation. *Fossen Utvikling* is developing all the infrastructure and outdoor areas, including the building structures. A zero-emission residential area will be built on Tanberghøgda, which will include 600 new homes in a new district in Hønefoss, Ringerike municipality. The goal of the assignment is to analyze and interpret a development plan for an energy and climate concept for this area related to electricity and heat supply. There are two groups of students working on this project. The students in this assignment will focus on energy supply solutions for both electricity and heat, as well as opportunities for reducing energy and power demands in the given area. The students will use energy demand profiles developed by another group of students working on energy demand in IDA-ICE. The work on energy supply should focus on reducing operating costs and power requirements in the area. Students are expected to use self-programmed codes in Python or MATLAB. Based on current relevant and future potential technologies, the students will define different scenarios to reduce operating costs and power requirements in the area. All scenarios will be simulated in the developed codes. Various time profiles and duration curves for heat and electricity will be analyzed. All results will be summarized and analyzed.

Goals

The goal of the thesis is to analyze and interpret the viability of the energy and climate concept preliminary development plan. Of which the operational costs and power demand are the main areas of focus.

Disclaimer

This Masters thesis is a continuation of previous works from the Project Thesis *Energy and Climate Concept for the Development of a Zero-Emission Residential Area - Analysis of Energy Supply Solutions*[1], submitted December 2022 by the authors of this Master Thesis. Despite the fact that this thesis is an independent academic production, some parts are largely based on previous efforts. These parts are mainly found in the chapters of introduction, theory, method, and some parts of results.

Acknowledgment

We would like to thank the following people for their great help during this Master thesis. Our Supervisor Natasa Nord, for her guidance and advice. Anders N. Gullhav and Xingji Yu for their help with the optimization model and implementation in *Gurobi* and *Pyomo* software. Frederik W Skarstein from Fossen Utvikling, for his help with acquiring relevant documents for the different systems at Tanberghøgda. Nils Rusås Ruud from COWI, for his help with photovoltaic production data. Jaromił Najman, Matthias Miltenberger, and Jonasz Staszek for their help with *Gurobi* related challenges.

M.A.W.S
E.K
J.D

Preface

Trondheim, 06-06-2023

Maximilian August Windingstad Sletbakk
Eskil Kvålsvold
Jonas Dalby

Glossary

CEEQUAL *The Civil Engineering Environmental Quality Assessment and Award Scheme (CEEQUAL)*, re-branded as *Building Research Establishment Environmental Assessment Method (BREEAM)* in October of 2022 [2]. 24

COP Coefficient of Performance. 35

COWI Engineering consulting firm, responsible for the concept report on Tanberghøgda [3]. 33

EPBD Energy Performance of Building Directive. 15

EPD Environmental Product Declaration. 24

EV Electric Vehicle. 46

FTP Free Transfer Protocol. 34

GHG Greenhouse Gas. 15

Group 2 Referring to the group working on the energy demand models for the buildings in Tanberghøgda. 35

HCV Higher Heating Value. 11

HOMER Hybrid Optimization of Multipe Energy Resources. 19

HSE Health, Safety and Environment. 3

IPCC International Panel on Climate Change. 15

LCA Life Cycle Assessment. 24

LCV Lower Heating Value. 11

LFP Lithium Ferro-Phosphate. 7, 66

MILP Mixed Integer Linear Programming. 32, 61

NO1 Electricity Pricing Area in South-East Norway. 77

NTP National Transport Plan. 15

OEFe On-site Energy Fraction. 18

PV Photo Voltaic. 6

SSB Bureau of Statistics (Statistisk Sentralbyrå). 8

TEK17 The Norwegian Building Code (Byggteknisk Forskrift). 3, 35

ZEB Zero Emission Building. 15
ZED Zero Emission Digger. 16
ZEV Zero Emission Vehicle. 15

Abstract

In this Thesis, energy supply solutions for the new Hønefoss neighborhood of Tanberghøgda were studied. The objective of this thesis was to evaluate the use of a solar cell system with a 500 kWp capacity and a 1 MWh capacity battery. The primary objective was to determine if the PV plant and battery could cover the load during and after the construction phase, as well as to evaluate the potential costs of purchasing additional power from the grid. The motivation behind the project was to achieve a nearly zero-emission construction phase and a zero-emission neighborhood with nearly 600 new buildings.

In the first section of the thesis assignment, the construction phase was evaluated in terms of the total cost of purchasing power from the grid when PV production and battery levels were low, and the profit of selling power back to the grid when PV production and battery levels were high. The construction phase was divided into five phases: groundwork, building, facade, internal, and outdoors, each of which required various machines. In the majority of phases, the variable PV production necessitated the procurement of additional electricity from the grid to meet demand. The total costs were calculated using PV production data and spot prices from 2020 and 2021. During the winter months, a higher heating demand is required to achieve the desired indoor temperature of $15°C$. Given that it occurred during the winter, this increases the total demand for the interior phase.

The second model analyzed the PV plant, battery, and interaction with the electrical grid following the completed construction of a particular combined housing stock. The objective was to satisfy the electric demands of the homes and the charging needs of electric vehicles. Additionally, the heating demands of the housing stock were planned to be satisfied by either a local heating system or a district heating system. The model was created in *Python* utilizing the optimization solver *Gurobi* in order to minimize the total cost by optimizing load shifting, battery utilization, and power transactions. The considerable difference in PV production between winter and summer led to a substantial variance in total expenses. The additional power generation from the PV system reduced the external grid's direct emissions by 10% and 88% during the winter and summer seasons.

Both models incorporated multiple variables based on historical data. The enormous disparity between spot prices in prior years had a major impact on total costs. The higher the spot price, the more profitable it is to invest in a high-capacity battery. In addition, the fluctuating PV production made it challenging for the PV plant and battery to always cover the demand. Nonetheless, it provided a respectable level of power and flexibility. To sum up, the combination of battery, photovoltaics, and intelligent charging had a significant impact on total costs and has great potential for future implementation.

Sammendrag

I denne masteroppgaven ble energiforsyningsløsninger for det nye nabolaget Tanberghøgda i Hønefoss studert. Målet med masteroppgaven var å vurdere bruken av et solcellesystem med en kapasitet på 500 kWp og et batteri med en kapasitet på 1 MWh. Det primære målet var å vurdere om solcelle-anlegget og batteriet kunne dekke belastningen under og etter byggefasen, samt å evaluere de potensielle kostnadene ved å kjøpe ekstra strøm fra strømnettet. Motivasjonen for prosjektet var å oppnå en byggefase og et nabolag tilnærmet uten utslipp med nesten 600 nye bygninger.

I den første delen av oppgaven ble byggefasen evaluert med hensyn til totalkostnadene ved å kjøpe strøm fra strømnettet når produksjonen fra solcelle-anlegget og batterinivåene var lave, samt profitten ved å selge strøm tilbake til strømnettet når produksjonen fra solcelle-anlegget og batterinivåene var høye. Byggefasen ble delt inn i fem faser: grunnarbeid, bygging, fasade, intern og utendørs, hvor det var behov for ulike maskiner i hver fase. I de fleste fasene førte varierende produksjon fra solcelle-anlegget til behov for ekstra strøm fra strømnettet for å møte etterspørselen. Totalkostnadene ble beregnet ved hjelp av produksjonsdata fra solcelle-anlegget og spotpriser fra 2020 og 2021. I vintermånedene kreves det en høyere oppvarmingsbehov for å oppnå ønsket innetemperatur på $15°C$. Dette øker den totale etterspørselen i innvendig fase, gitt at den fant sted om vinteren.

Den andre modellen analyserte solcelle-anlegget, batteriet og samspillet med strømnettet etter ferdigstillelsen av en spesifikk kombinert boligmengde. Målet var å dekke de elektriske behovene til hjemmene og ladebehovene til elektriske kjøretøy. I tillegg var planen å tilfredsstille oppvarmingsbehovene til boligmassen enten ved et lokalt oppvarmingssystem eller et fjernvarmesystem. Modellen ble opprettet i *Python* ved hjelp av optimaliseringsløseren *Gurobi* for å minimere totalkostnadene ved å optimalisere lastforskyvning, batteribruk og krafttransaksjoner. Den betydelige forskjellen i solcelle-produksjon mellom vinter og sommer førte til betydelig variasjon i totale utgifter. Den ekstra kraftproduksjonen fra solcelle-anlegget reduserte direkte utslipp fra det eksterne strømnettet med 10% og 88% i henholdsvis vinter- og sommersesongene.

Begge modellene inkluderte flere variabler basert på historiske data. Den enorme forskjellen mellom spotprisene i tidligere år hadde stor innvirkning på totale kostnader. Jo høyere spotprisen var, desto mer lønnsomt var det å investere i et batteri med høy kapasitet. I tillegg gjorde den varierende solcelle-produksjonen det utfordrende for solcelle-anlegget og batteriet å alltid dekke etterspørselen. Likevel ga det en respektabel grad av kraft og fleksibilitet. Oppsummert hadde kombinasjonen av batteri, solceller og intelligent lading en betydelig innvirkning på totale kostnader og har stor potensial for fremtidig implementering.

Contents

Acknowledgment . . . **ii**
Preface . . . **iii**
Glossary . . . **iv**
Abstract . . . **vi**
Sammendrag . . . **vii**
Contents . . . **viii**
1 Introduction . . . **1**
1.1 Background and Motivation . . . 1
1.2 Goal and Structure . . . 1
1.3 Limitations of Work . . . 1
2 Theory . . . **3**
2.1 Technical Requirements for Buildings . . . 3
2.1.1 TEK17 Building Regulations . . . 3
2.1.2 Energy Labeling of Buildings . . . 4
2.1.3 Passive House Requirements . . . 5
2.2 Photovoltaic Cells . . . 6
2.3 Batteries . . . 7
2.4 Heat Pumps . . . 7
2.5 Electricity Price Model . . . 7
2.6 Heat Supply . . . 8
2.6.1 Pump Costs . . . 9
2.6.2 Heating Costs . . . 10
2.7 The Norwegian Construction Industry . . . 12
2.8 Zero-Emission Construction . . . 14
2.8.1 Ambitions . . . 15
2.8.2 Barriers . . . 15
2.9 Literature Review of Construction Projects . . . 16
2.9.1 Project 1: Biri Care Center . . . 16
2.9.2 Project 2: Olav V's Street . . . 17
2.10 Literature Review of Optimized PV Production With a Battery . . . 17
2.11 Literature Review of a Bio-Solar CCHP System . . . 19
2.11.1 Comparing the System With Tanberghøgda . . . 22
3 Description of the Tanberghøgda-project . . . **24**
3.1 Project Introduction . . . 24
3.1.1 Photovoltaic Power and Battery System . . . 24

3.1.2 Systems for Heating Demand . . . 26
3.1.3 Housing Distribution . . . 27
3.2 The Machine Requirements . . . 29
3.3 Time Management . . . 31
4 Methods . . . 32
4.1 Tools . . . 32
4.2 Data Material . . . 33
4.2.1 Cooperation With Master Group . . . 33
4.2.2 PV Production Data . . . 33
4.2.3 Electricity Spot Prices NO1 . . . 34
4.2.4 Housing Stock Load Profile . . . 35
4.2.5 Heating Demand . . . 38
4.2.6 Electric Vehicles and Combined Load . . . 46
4.3 Method to Calculate Energy Needs and Costs During the Construction Period . . . 51
4.3.1 PV and Batteries . . . 51
4.3.2 Costs of Buying Power During the Construction Phase . . . 52
4.3.3 Model Outline of Python Code for Electric Energy Use During Construction . . . 52
4.3.4 Construction Models' Limitations . . . 54
4.4 Method to Calculate Costs Related to the Heating Demand . . . 56
4.4.1 Pump Costs . . . 56
4.4.2 On-Site Heat Production . . . 56
4.4.3 District Heating . . . 56
4.4.4 Boiler Efficiencies . . . 56
4.5 Optimal Electricity Use After Completion of Construction . . . 58
4.5.1 Model description . . . 59
4.5.2 Formulation of the MILP Problem . . . 61
4.5.3 MILP Problem Explanation . . . 64
4.5.4 MILP Problems Limitations . . . 66
4.5.5 Scenario Description . . . 67
5 Results . . . 68
5.1 Energy Requirements and Costs During the Construction Period . . . 68
5.1.1 Simplifications and Assumptions . . . 68
5.1.2 Groundwork Phase . . . 69
5.1.3 Building Phase . . . 70
5.1.4 Facade Phase . . . 71
5.1.5 Internal Phase . . . 72
5.1.6 Outdoor Phase . . . 74
5.1.7 Cost Distribution of Construction . . . 75
5.1.8 Construction Phase Cases . . . 76
5.2 Heating demand . . . 79

5.2.1 Pump Cost . . . 79
5.2.2 Heating Costs . . . 84
5.2.3 Total Costs . . . 84
5.3 Analysis of the PV Plant, Battery and Interaction with the Electrical Grid . . . 87
5.3.1 Battery Level Base Case . . . 90
5.3.2 Load Profile Base Case . . . 92
5.3.3 Peak Reduction Base Case . . . 94
5.3.4 Battery Level Connected Case . . . 96
5.3.5 Load Profile Connected Case . . . 98
5.3.6 Peak Reduction Connected Case . . . 100
5.3.7 Comparison of Base Case and Connection Case . . . 102
5.3.8 Sensitivity Analysis for Transformer Capacity & Battery Constraint . . . 103
5.3.9 Sensitivity Analysis Battery Size . . . 105
5.3.10 Total Cost and Emissions . . . 106
6 Conclusion . . . 109
7 Continuation of Thesis Work . . . 110
Bibliography . . . 111
A Appendices . . . 118
A.1 Python Code for Energy Needs and Costs During Construction Phase . . . 118
A.2 Python Optimization model for Energy Use After Completed Construction . . . 123
A.3 MatLab Heating Code Hønefoss: Eivind W. Roland (Reproduced with permission) . . . 130

1 Introduction

1.1 Background and Motivation

Several industries are electrifying as a result of the increasing emphasis on reducing greenhouse gas emissions. Historically, emissions from traditional fossil-fueled equipment and the vast majority of the public automobile fleet have had a substantial impact on the construction industry. To reduce construction emissions, it is essential to employ zero-emission construction techniques, and the electrification of construction sites is becoming an increasingly common practice. The vast majority of newly purchased vehicles in Norway are electric vehicles, which will inevitably increase the need for charging stations in the coming years. This study aims to investigate these changes and analyze their implementation from a variety of perspectives.

1.2 Goal and Structure

This thesis has two primary objectives that must be fulfilled. The first step is an analysis of the costs associated with operating a zero-emission construction site in Tanberghøgda. This objective requires both the accumulation of data on the local PV generation and the use of the grid's external power supply. The second objective is to calculate the cost of fulfilling the housing stock and vehicle charging electric demand. As well as the cost of meeting the housing stock's heating demand. After introducing background information regarding the project's various characteristics, the project will proceed to describe both the project and its model. To continue, the findings will be presented prior to the project's ultimate conclusion.

1.3 Limitations of Work

The project scope is limited to electricity demands and heating demands during both the construction period, and after the completion of a specific construction stage. The scope does not include all stages of the project's life cycle. This is due to the long time period of which the neighbourhood evolves in regards to energy demands. As these stages also entail upgrading installed energy production capabilities, it was deemed beneficial to analyze the first stage of the areas installed energy production. This would then yield valuable information in regards to the systems viability, and would provide an indication of where future expansions and additions would be necessary.

Various restrictions exist within the models. Both models undergo a number of simplifications. Due to the complexity of the project, this is necessary to develop a viable model. These simplifications include assumptions regarding energy, battery behavior, car and construction equipment

recharge requirements, costs, and model operation. In each model's explication, these simplifications and assumptions are described in detail. In order for the model to function, some computations have been simplified. Due to the difficulty of creating a model that can accommodate a dynamic daily charging schedule, the behavior of the electric vehicle park is also simplified. In turn, these assumptions may result in a simplified conclusion regarding prices and overall emissions, but they are meant to demonstrate the potential for energy savings and economic advantage of using PV generation and a battery to power a construction site, and ultimately the building stock after the construction period.

2 Theory

2.1 Technical Requirements for Buildings

For a structure to be permitted in Norway, it must meet the minimum property standards. This data is compiled in the TEK17 regulations, which are a component of the Norwegian Planning and Building Act [4]. Both new construction and major renovations must comply with the standards. The laws ensure that new buildings are user-friendly, energy-efficient, and compliant with HSE standards.

2.1.1 TEK17 Building Regulations

To conserve energy, maximum limits for the total net energy demand of various building types have been established. For example, the maximum limit for an apartment building is 95 $kWh/(m^2year)$, while the maximum limit for a kindergarten is 135 $kWh/(m^2year)$ and 115 $kWh/(m^2year)$ for office buildings, according to TEK17 regulations [4]. In addition, there are criteria for U-value in various areas of a building to ensure that heat generated within the building stays within the building. The U-value of a building component measures its thermal insulation. Therefore, the U-value requirement for floors is more stringent than that for windows and entrances.

TEK17 specifies the requirements for ventilation systems in relation to the indoor climate. The ventilation system must be able to effectively regulate total air supply, air extraction, air contaminants, and relative humidity. In addition to the standards included in TEK17, a number of recommendations for enhancing the indoor climate are also included. The Norwegian Labor Inspection Authority has prepared a guide on climate and air quality in the workplace [5], which concludes that a temperature below 22 $^\circ C$ reduces the sensation of dry air, a challenge in workplaces with numerous electrical devices that produce heat. In addition, it is recommended to have individual temperature control and window adjustment abilities. Additionally, a clean environment is essential for a wholesome indoor climate. The reference table 1 provides a summary of these requirements and suggestions.

Table 1: Requirements and recommendations for indoor climate in buildings.

Parameters	Description	Requirements
§ 13-2. Ventilation in residential buildings	Housing units must have ventilation that ensures an average supply of fresh air	$\geq 1.2m^3/h$ per m^2 floor area
	Fresh air must be supplied to bedrooms	$\geq 26m^3/h$ per bed
	Fresh air must be supplied to rooms which are not intended for permanent residence	$\geq 0.7m^3/h$
§ 13-2. Extraction volume in the house	Basic ventilation kitchen	$\geq 36m^3/h$
	Basic ventilation bathroom	$\geq 54m^3/h$
	Basic ventilation toilet	$\geq 36m^3/h$
	Basic ventilation washing room	$\geq 36m^3/h$
Recommended temperature	Maximum temperature when heating is required	$< 22°C$
CO_2-concentration level	Recommendation from the Norwegian Labor Inspection Authority	$< 1000ppm$

Due to the pollution generated by the occupants, the table demonstrates that ventilation requirements for multiple rooms are directly proportional to room size. The majority of parameters utilize the unit m^3/h to show the volumetric flow in the room.

2.1.2 Energy Labeling of Buildings

The energy efficiency of homes that will be sold or rented must be labeled by a professional. This policy was enacted in 2010 to raise awareness of energy consumption with the goal of encouraging more individuals to make their homes more energy-efficient. The energy labeling also applies to larger structures, and commercial structures larger than 1 000 square feet are required to possess a valid energy certificate. The energy certificate includes two primary parameters, including a grade spanning from A (best) to G (worst) that reflects the energy efficiency of a building or home under typical energy use conditions. The second parameter specifies the percentage of energy consumption that could be satiated by energy sources other than electricity and oil, and is ranked on a color scale from green to red, with green being the best and red the worst. This is best depicted using a two-dimensional coordinate system, with energy on the y-axis and temperature on the x-axis [6].

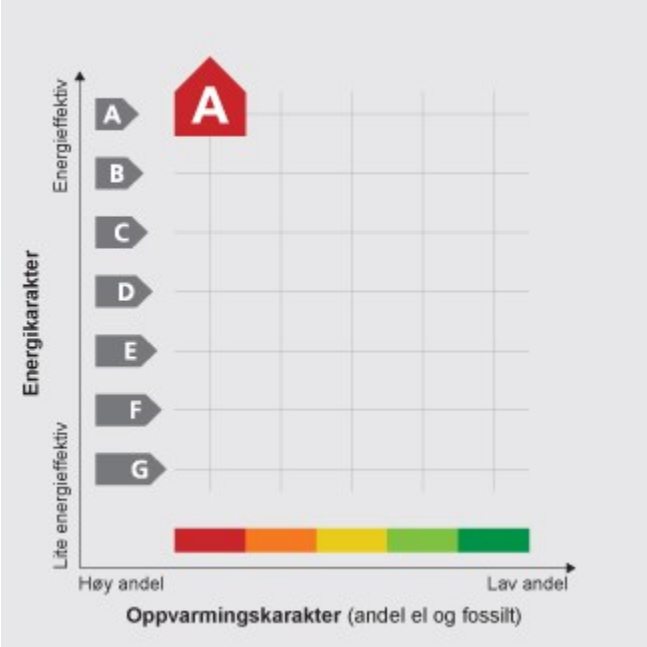

Figure 1: Energy grades and heating grade.

Figure 1 is an example of the energy labeling of a home that is exceptionally energy efficient but uses a significant quantity of electricity and fossil fuels for heating. Table 2 outlines the requirements for achieving the various energy grades. Different requirements apply to numerous categories of structures. Table 2 shows the specific requirements for singe-family homes.

Energy grade	Requirement
A	$\geq 95kWh/m^2$
B	$\geq 120kWh/m^2$
C	$\geq 145kWh/m^2$
D	$\geq 175kWh/m^2$
E	$\geq 205kWh/m^2$
F	$\geq 250kWh/m^2$
G	No limit

Table 2: Energy grade requirements.

2.1.3 Passive House Requirements

The TEK17 requirements for low energy usage in buildings lay the ground for the deployment of passive homes. Passive houses are distinguished by their distinctive construction, which is intended

to reduce energy consumption by adhering to a strict set of requirements [7]. Norway is the only nation in Europe with a unique standard for passive houses. These specifications are NS3700 for residential construction and NS3701 for industrial construction [8].

A passive house must comply with a maximum heat loss coefficient based on its dimensions, a set of requirements for building components and materials, and must meet at least 50% of its water heating demand from sources other than fossil fuels and electricity. There are additional requirements in place to minimize the energy demand for heating buildings [8].

2.2 Photovoltaic Cells

As system costs decrease and the demand for renewable energy rises, solar power is one of the renewable energy sources that is expanding the most rapidly in Norway. Both off-grid and grid-connected PV-systems are growing in viability, with grid-connected systems experiencing the most growth [9]. In addition, because of the high cost of electricity, the payback period of these systems will be shortened even further.

The panels are made using either poly-crystalline or mono-crystalline manufacturing techniques. By fusing together multiple crystalline silicon shards, polycrystalline silicon is produced. Mono-crystalline, on the other hand, utilizes a single silicon crystal; this increases the purity of the crystals and, subsequently, the spectral response. Therefore, the mono-crystalline panel will have an efficiency of approximately 15-20%, as opposed to 13-16% for the poly-crystalline [10].
The complete panel may consist of either full or half cells. The original cell is cut in half to generate a half cell, whose electrical characteristics are greatly enhanced. Due to the squared current in Joule's law, as the current is cut in half for each half cell, the accompanying resistance is reduced by one-fourth of its original amount 2.1.

$$P_{heat} = R \cdot I^2 \tag{2.1}$$

This amounts to a 75% reduction in the electrical losses of the cell. The module will then have double the number of cells. This results in increased electricity generation. In addition, because the modules will have twice as many threads connecting the cells, a solar panel with half-cut cells will be significantly more resistant to the effects of shading on energy production [11]. In addition, as substrings contain only half the current, the temperatures of the associated hot spots will decrease [12].

Introducing bifacial panels is an additional potential PV generation technology. These panels enable light to interact with both sides of the cells by utilizing either a reflective back-film or a piece of transparent glass. This is in contrast to monofacial modules, which have non-transparent backplates. The bifacial shape provides numerous benefits, especially in snowy locations. Firstly, an overall gain of 19% compared to monofacial designs, as well as faster snow shedding and annual snow loss of only 2%, compared to 16% for monofacial designs [13].

2.3 Batteries

The majority of electric vehicles are powered by Lithium-ion batteries, which are optimally charged between 20% and 80% of their capacity. A real-world analysis conducted by *Elsevier* reveals that losses during charging between 80% and 100% are nearly twice as high as during charging between 20% and 80% [14]. In addition, the battery will degrade more rapidly if the 20-80% ranges are violated.

The battery system used in combination with the PV plant is composed of a number of battery modules connected to the circuit system. Utilized battery cells are LFP (lithium ferro-phosphate) cells, which have a high energy density, good rated performance, and are manufactured using high-level automation [15]. The battery management system regulates the battery in terms of monitoring, balancing, and protecting the battery system in order to ensure its steady operation.

Lithium, nickel cadmium, flow batteries and lead-acid batteries are the primary types of batteries used to store solar energy. In terms of durability, maintenance, cost, capacity, and other characteristics, these four components differ from one another.

2.4 Heat Pumps

The most important relationship for heat pumps is described in equation 2.2.

$$COP = \frac{Q}{W} \Rightarrow W = \frac{Q}{COP} \tag{2.2}$$

Where Q denotes the heat supplied by the heat pump, and W denotes the power supplied to the heat pump [16]. There are numerous types of heat pumps, either using different working fluids, or delivering heat for different uses. The air/water heat pump that uses outside air for the evaporator is the most applicable heat pump technology for this project. This system may supply heat for both domestic hot water, and space heating. Also, the operating temperature range is very good, with the ability to operate at $-25°C$.

2.5 Electricity Price Model

The ongoing electrification of all sectors results in a simultaneous increase in power demand, leading to occasionally limited capacity. These modifications are implemented as an initiative to encourage users to spread out their electricity consumption throughout the day in order to avoid high peaks, which are taxing on the transmission grid. A transmission grid fee must be paid in order to buy electricity from the grid. It is one of two elements that the electricity price model consists of, the other being the actual cost of electricity. The fee covers power transmission, planning and installation of new transmission cables, maintenance, surveillance, and transmission line wear [17]. Initially, the grid fee was stated as

$$TGF_{old} = E_{usage} \cdot C_v + C_{fixed,GF} + E_{usage} \cdot C_{variable,GF} \tag{2.3}$$

where E_{usage} is power usage in kWh, C_v is the cost for power usage, $C_{fixed,GF}$ is the fixed cost and $C_{variable,GF}$ is the variable cost of the grid fee. The updated grid fee is presented in equation 2.4 [18].

$$TGF_{new} = C_{fixed,GF} + E_{usage} \cdot C_v + C_{power} \cdot P_{max} \tag{2.4}$$

C_{power} is the cost for the average peak power and P_{max} is the average of the three highest peaks each month. When comparing equation 2.3 and 2.4 the changes in the new model become apparent. The transmission grid fee cost is given in table 3, as presented from Føie [18].

Table 3: Transmission grid cost.

Effect [kW][a]	**Fixed Cost [NOK/year]**	**Effect Cost [NOK/kW]**	**Energy Cost Winter [øre/kWh]**	**Energy Cost Summer [øre/kWh]**
<200	9450	700	19.6	16.9
200-100	9450	536	19.6	16.9
>1000	9450	435	19.6	16.9

[a]Average of 3 highest peaks in winter months on separate days

Previously, the grid fee consisted of a fixed cost and a variable cost based on energy consumption. The new grid fee is more comprehensive and went into effect on 1. July 2022 [19]. The primary distinction is the addition of a fee for peak power usage, calculated as the monthly average of the three highest peaks. The peak value also determines the user's fixed sum category. Another change is that the variable cost associated with power use varies throughout the day, with higher costs between 07:00 and 22:00 and lower costs between 22:00 and 07:00 [18].

2.6 Heat Supply

To cover heating demand a heat source must be utilized. District heating has been a key source of heat of many years as it is dependable, flexible and in many cases utilizes surplus renewable energy [20]. In addition, waterborne heating systems reduce electricity for heating, relieving stress on the transmission net. According to a report presented by Statistisk Sentralbyrå (SSB) there has been an increasing trend of using district heating over the last 20 years [21]. District heating systems are typically designed with heating plants to heat up water using several fuel sources, and transmitted to buildings using pipes. For some buildings and housing areas, on-site heat production may be beneficial. This means the boiler produces heat locally, reducing the heat loss over the line. This however leads to investment costs for installing and maintaining the plant.

The incoming hot water temperature is typically 55 °C [16]. At this temperature adequate hu-

man hygienic needs are met, yet high enough to avoid Legionella growth which typically develops between 20 °C to 50 °C [16, 22]

2.6.1 Pump Costs

To circulate the supply water in the system, a pump must be utilized. The operational costs of the pump are part of the total costs of the system, and must be calculated to obtain accurate results. In order to calculate the pump costs for delivering heated water, some key equations must be presented. Firstly, the overall pump cost is given by equation 2.5,

$$C_{pump} = \sum C_{el} \cdot \dot{W}_{p,i} \tag{2.5}$$

where $\dot{W}_{p,i}$ is the pump power in hour i and C_{el} is the electricity price including the tariffs. The total costs are calculated as the sum of the electrical costs and pump cost in hour i for every hour in a year, 8760 hours. To continue, the pump power is calculated by using equation 2.6.

$$\dot{W}_{p,i} = \frac{\Delta p_i \cdot \dot{V}_i}{\eta_{pump,i}} \tag{2.6}$$

The total pressure drop Δp is presented in equation 2.7,

$$\Delta p = 2RL + \Delta p_W + \Delta p_{AB} \tag{2.7}$$

where R is the specific pressure loss $[Pa/m]$, L is the pipe length $[m]$, Δp_W is the boiler pressure loss and Δp_{AB} is the pressure drop in the consumer substation. However, this results in a constant pressure loss, as all variables are constant. In order to analyze the system using a variable pressure loss, the system characteristic C must be calculated. This may be calculated using equation 2.8

$$C = \frac{\Delta p_{max}}{\dot{V}_{max}^2} \tag{2.8}$$

Furthermore the total pressure loss for each hour may be calculated using equation 2.9 [23] .

$$\Delta p_i = C \cdot \dot{V}_i^2 \tag{2.9}$$

The volume flow in hour *i* is expressed by equation 2.10,

$$\dot{V}_i = \frac{\dot{Q}_i}{\rho \cdot \Delta T \cdot C_p} \tag{2.10}$$

where ΔT is the difference between the inlet temperature T_s and outlet temperature T_r, and ρ is

the density of water $[kg/m^3]$. To continue, the pump efficiency can be calculated as the hydraulic power output produced by the pump, with regards to the power input as displayed in equation 2.11 [16].

$$\eta_{pump} = \frac{P_{out}}{P_{in}} \tag{2.11}$$

To calculate the pump efficiency, the power output is necessary. The power output P_{out} can be calculated using equation 2.12

$$P_{out} = Q \cdot \rho \cdot g \cdot H \tag{2.12}$$

where Q is the flow rate $[m^3/s]$, g is the gravitational constant $9.81\ m/s^2$ and H is the total head $[m]$ [24].

The mentioned variables may effect the efficiency of the pump. An increased flow rate may reduce the efficiencies as the losses from friction and turbulence increase. The head of a pump is the difference in pressure between the inlet and outlet of a pump. A higher head may lead to decreased efficiencies, as the losses over the impeller and other components become higher.

Lastly, the specific pump energy demand can be calculated as:

$$P_{specific} = \frac{P_{p,tot}}{Q_{d,tot}} \tag{2.13}$$

where $P_{p,tot}$ is the total electric energy required to operate the pump for a year and $Q_{d,tot}$ is the total heating demand. This gives an indication of the pump power required in correlation to the heat provided [25].

2.6.2 Heating Costs

The heating costs related to the boiler differ depending on the location. According to the concept report on Tanberghøgda developed by COWI, it is yet to be fully determined if an on-site boiler or district heating is to be utilized [3]. The costs associated with both cases are presented below.

On-site Heat Production

The total costs of the on-site heat production is presented in equation 2.14.

$$C_v = \sum C_{bio} \cdot \frac{\dot{Q}}{\eta_{boiler}} \tag{2.14}$$

where C_{bio} is the price of bio-fuel and $\dot{Q}$ is the heat delivered. Using equation 2.15, the boiler efficiency η_{boiler} can be calculated as

$$\eta_{boiler} = \frac{P_q}{\dot{m}_f \cdot CV} \tag{2.15}$$

where P_q is the useful heat generated, $\dot{m}_f$ is the mass flow rate of fuel and CV is the heating value. The heating value can be determined as Lower Heating Value (LCV) or Higher Heating Value (HCV). In Europe, efficiencies are most commonly based on LCV. Traditional LCV based utility-scale boilers operate in range of 85-95% efficiency [16]. Modern pellet-fueled boilers can achieve combustion efficiencies of 90% or higher due to auto-regulated combustion air blower speed and supply of pellets to achieve an optimal fuel-to-air ratio [26].

District Heating

The other possible heating solution utilizes district heating instead of on-site production. In this case fuel costs are set by *Vardar AS*, the company responsible for district heating in Hønefoss. In the case of utilizing district heating, the total costs are presented in equation 2.16,

$$C_w = \sum_{i=1}^{8760} C_{DH} \cdot \dot{Q}_i \tag{2.16}$$

where C_{DH} is the cost of district heating locally in Hønefoss. The calculations for pump costs are the same as presented in Section 2.6.1. According to *Vardar AS*, the energy price of district heating is set to be 4% lower than spot price provided by *NordPool* [27]. The costs of distribution are set to be equal to electric distribution costs from the grid as presented in Section 2.5, however customers are not charged for peak power usage. The additional public fees are equal to the transmission fees for the electricity distribution [27]. As an additional benefit, all customers recieve full financial support equal to the arrangement in place for electricity. This also applies for usage over 5 000 $kWh/month$, which is the current consumption cap set by the Norwegian Government in regards to electric financial support for private housing [28]. In turn this means large consumers of heat have an extended benefit, making it an economically viable option in comparison to electricity.

Total Costs

The total costs for both heating sources is presented in equation 2.17 and 2.18.

$$C_{Total} = 1.1 \cdot (C_{pump} + C_{on-site}) \tag{2.17}$$

$$C_{Total,DH} = 1.1 \cdot C_{pump} + C_{DH} \tag{2.18}$$

In both cases the pump costs are the same. In turn this means the difference in total costs are due to the costs related to on-site production and district heating. The additional factor of 1.1 is due to the desire of 10% return on investment per year according to consultation with *Fossen Utvikling* to cover boiler, piping and additional costs. For the district heating case, only the pump costs are calculated with a 10% return, as the heating costs from district heating are unrelated to the investments of *Fossen Utvikling*.

2.7 The Norwegian Construction Industry

The increased emphasis on environmental measures has resulted in an industry that is more conscious of reducing emissions. The Norwegian construction sector employs around 261 000 people and has a considerable impact on the economy and environmental standards [29]. According to a survey by *Asplan Viak*, the Norwegian construction industry is responsible for 15.3% of the country's total greenhouse gas emissions. This represents a considerable increase of 31% compared to the 2010 emissions indicated in the same report. In table 4 the distribution of emissions from various sectors of the industry is illustrated. Analyzing the data reveals that the emission linked to 'other sectors' contributes the most to the total emission. In 2017, the construction industry emitted a total of 9 454 000 tons of CO_2e [30].

Table 4: Total emission from construction.

Contribution to emission	2017
Construction	2 076 $ktCO_2e$
Other sectors	4 236 $ktCO_2e$
Energy usage in buildings	1 005 $ktCO_2e$
Export to overseas construction	2 137 $ktCO_2e$
Total	**9 454** $ktCO_2e$

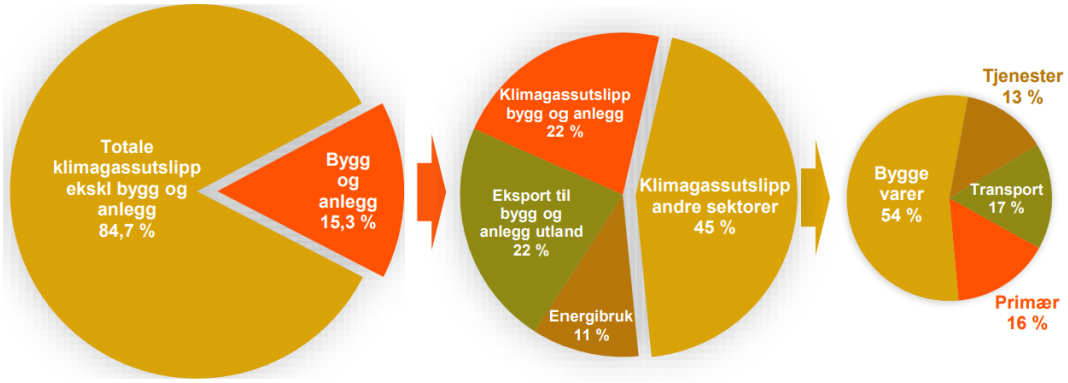

Figure 2: Distribution of emission in the Norwegian construction industry (reproduced from Asplan Viak).

Figure 2 depicts the dispersion of emissions from the construction industry. As a consequence of the construction industry, building materials are the largest contributor to the category 'emission from other sectors,' which refers to emissions associated with other industries. In roughly equal propor-

tions, emissions from services, transportation, and primary commodities account for the remaining 50%. The remaining emissions result from direct construction emissions, international construction exports, and energy consumption in structures. The criteria used to describe the distribution within the 'other sectors' category are specified in table 5.

Table 5: Definitions of terms related to other sectors.

Contribution from other sectors	Definition
Primary	Primary industries, oil and gas, food and clothes
Construction materials	Sectors for typical building materials used in construction
Services	Private and public services
Transport	Transport not included in the construction industry

The annual emissions from the primary, construction, service, and transportation sectors are shown in figure 3. These four categories account for 45% of the construction industry's annual emissions. The construction materials industry has the highest emission intensity, accounting for 54% of the total share, as shown by the figure. The excess amount are distributed fairly evenly among the remaining groups. Despite a fall in 2008, emission rates have remained stable, which may be a result of the economic crisis, during which construction activity declined [31]. Since 2011, the rising trend has caused a 1 088 000-ton increase in CO_2 levels between 2010 and 2017 [30].

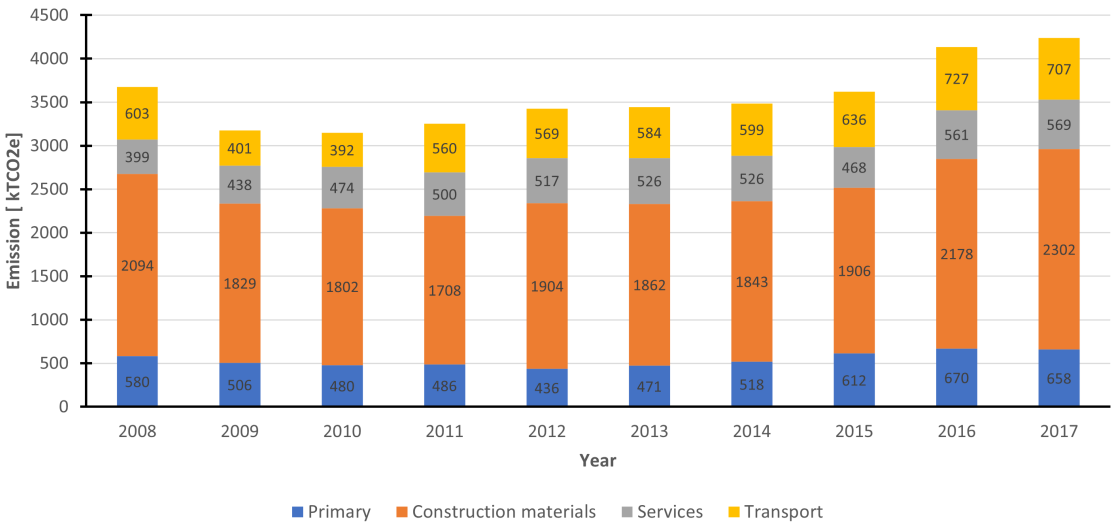

Figure 3: Distribution of emission from other sectors.

According to Asplan Viak, the major sources of greenhouse gas emissions from building energy use are fossil fuels and natural gas. From 2010 to 2017, there has been a distinct declining trend due to a drop in the consumption of fossil fuels. In order to reduce emissions, the use of mineral oil for heat purposes in buildings was outlawed as of January 1, 2020 [32]. The TEK17 construction regulations have resulted in stricter requirements for energy sources and material utilization. Structures greater than 1000 m^2 are required to employ low-temperature water-borne heat, which is more efficient than heat at higher temperatures [33]. It is envisaged that a future modification of the TEK17 laws would impose even stricter requirements on structures, including requirements for low-energy and passive dwellings [3]. The building-related energy emissions will probably continue to decrease in the near future.

2.8 Zero-Emission Construction

For the construction industry to support zero emission sites, all business sectors must undergo reforms. As concerns about global warming rise, the emission restrictions for construction equipment get stricter. Construction equipment has traditionally been powered by fossil fuels with high emission levels due to the heavy workload, the need for adaptability, and the need for dependability. The industrial and the energy sector is crucial for the transition to low-carbon energy, as it accounts for 40% of European emissions [34]. As many businesses seek to reduce emissions in order to reach the zero-net-emissions target established by The European Green Deal, the construction industry needs new technology to replace the emission-intensive machinery [35]. The hybrid and electric power train technology is already widespread in the automobile industry, and its implementation in construction equipment is on the rise. The hybrid technology may increase energy efficiency by 10-30%, but widespread adoption of electric machinery is imminent in order to achieve the objective of net zero emissions by 2050 [36].

The electric drive system for pure electric construction equipment is comprised of an electric drive train and an electric power supply, resulting in the lack of direct emissions. In light of this, the construction equipment generates less noise than conventional machinery and has lower maintenance costs as a result of having fewer moving parts [36]. However, this new technology is accompanied by a variety of obstacles. In an article that examines the evolution and foundational technologies of pure electric construction equipment, reoccurring issues are identified. First, the hydraulic control technology has not yet been adapted for electric machinery, which causes operational difficulties. The second concern relates to energy storage devices, as electric equipment has a reduced operating life, limiting the adaptability of work. Moreover, battery-powered equipment operates at elevated temperatures and voltages and is subject to significant vibrations, all of which compromise safety and dependability. Due to the dearth of widespread adoption, there are high investment costs. The price of pure electric machinery can be two to three times that of conventional machinery; therefore, the price of electric machinery must decrease drastically before it can replace conventional machinery [36].

2.8.1 Ambitions

To reduce GHG (Greenhouse gas) emissions on a national and international scale, ambitious goals through policy initiatives like the European Green Deal are essential. Around 25% of global CO_2 emissions are caused by the construction industry, and the building sector will play a significant role in reducing overall emissions [37, 38]. A study on energy from the construction industry identifies a decarbonized building stock by 2050 as a key pillar for the EU's emission and climate goals. In order to accomplish this, ZEB's (zero emission buildings) are introduced as the new building target by 2030 [38]. The pathway to a decarbonized building stock was designed in accordance with the EPBD (Energy Performance of Building Directive), which established energy requirements for buildings. The initiative includes a plan for the future building stock, with the key points being that all new public buildings will be ZEB by 2027, all new buildings will be ZEB by 2030, and the entire building stock will be ZEB by 2050 [39].

The Norwegian industry has also implemented emission reduction initiatives. In a 2018 report published by the IPCC (International Panel on Climate Change), the importance of limiting global warming to 1.5 degrees Celsius and key measures to achieving climate objectives were outlined [40]. Norway has committed to reducing greenhouse gas emissions by 40% by 2030, relative to 1990 levels, as part of its climate agreement with the European Union. Nonetheless, Norway has presented a revised climate goal of reducing GHG emissions by a minimum of 50% to a maximum of 55% by 2030, relative to 1990 levels [41], which the EU also has increased its goal to. To achieve these grand objectives, national and local measures are being implemented. All new cars and light transport vehicles must be ZEV (Zero Emission Vehicle) by the end of 2025, according to the Norwegian government's NTP (National Transport Plan) for 2018-2019 [42]. Utilizing electric construction equipment in the building sector is also becoming more popular [43].

Several locally enacted policies reflect Oslo's aspiration to be an industry champion in emission reduction and energy conservation. In addition to adhering to national climate policy, Oslo seeks to become a near-zero emission metropolis by reducing emissions by 95% relative to 2009 levels. This necessitates that all urban construction be emission-free. To continue, it was determined that by 2025, all construction projects organized by the municipality of Oslo will be zero-emission [44].

2.8.2 Barriers

There are numerous obstacles in the current industry that may prevent the establishment of zero-emission construction sites. Knowledge and experience are the initial barrier. Information and data from previous or comparable projects are essential for the effective operation of a work site. Since the concept of zero emission building is novel, there is a lack of experience on the topic, which may result in a lack of data for a specific project [45]. This results in decreased productivity, a longer work period, and increased costs. In some cases, the definition of environmental standards is ambiguous, introducing uncertainty into the development of new projects. For the use of new technology that reduces emissions, there are typically no requirements. A law requiring the use of technologies with little to no emission would be effective [45].

Technology and project-related costs present the greatest obstacle to overcome. To accomplish

the objective of zero-emission construction sites, fossil fuel-powered machines must be replaced with electric ones. In certain instances, these machines are less accessible than conventional ones, particularly when it comes to large machinery [46]. This is primarily due to the rapid growth of initiatives employing electrical machines and the sustained expansion of the industry [43]. battery-powered machines have a reduced operating time and, depending on usage, may need to be recharged multiple times per day. To facilitate technological progress, modifications must be made to construction sites. Installing large vehicle batteries and charging stations is one example. Large-scale initiatives require a number of concurrently running machines. This could burden the Internet. Investment costs for the new infrastructure and the new technology will increase the overall project costs [43].

2.9 Literature Review of Construction Projects

Various projects utilizing ZED (Zero Emission Diggers), are presented in this section.The objective of the project is to create excavators suitable for use on construction sites. The goal of the project is to further develop the machinery from a concept to a commercially viable finished product. The ambitious project seeks to be the champion in its category of environmentally responsible construction equipment and to develop innovative solutions for future machinery with zero environmental emissions. In Oslo, the prototypes will be utilized in actual projects. The experiences from the project will aid the further development of the machinery, with an end goal of creating the best suitable machinery for construction work [43].

Nasta's ZERON series is a line of zero emission excavators. Table 6 displays the various machines in the ZERON lineup. To aid in the development of this equipment, it is utilized in various construction projects. The information gleaned from the site's data and comments will be invaluable for future enhancements [43].

Table 6: Zero Emission machinery.

Machinery	Weight [ton]	Battery run time [h]	Specifications
ZERON ZE350LC	38		Cable operated
ZERON ZE85	9,5	3-6	Battery operated
ZERON ZE160LC	18,6	0,5-1	Cable/Battery operated

2.9.1 Project 1: Biri Care Center

The Biri care center is a municipal housing complex in Gjøvik. The project's construction phase began on the fourteenth of May in 2019 and lasted until the end of 2020. The project required compliance with stringent environmental goals, including a 40% reduction in greenhouse gas emis-

sions through the use of wood and low-carbon concrete, the use of renewable heat sources based on heat pumps and a solar PV system, and the use of fossil-free and electrical construction machinery [43]. In addition, the structure had to adhere to the passive house standard and achieve an energy classification of class A. There are specific requirements that must be met in order to qualify as a passive house. These include heat loss, energy supply, heating demand, and construction characteristics [47].

In conjunction with construction equipment powered by bio diesel, the ZE350LC Eldar plug-in excavator was used for this project. The excavator operated for a total of 392 hours. A comparable diesel-powered machine of this size consumes 30 l/h, for a total of 11 760 liters. This is equal to approximately 117 600 kWh. The excavator consumed 28 224 kWh of electricity, which was 24% less than the diesel equipment. This resulted in a **144 000 NOK** savings in energy costs and an anticipated reduction of **35 $\mathbf{tCO_2e}$** in direct emissions [43].

2.9.2 Project 2: Olav V's Street

Olav V's street was reconstructed in the heart of Oslo to create a pedestrian-friendly street with wide sidewalks. The street would also facilitate taxi charging stations. The municipality of Oslo was the first in the world to mandate that a construction site be completely emission-free [48].

In addition to two ZE85 excavators, the ZE160LC was utilized for this project (hereby defined as ZE81 No. 1 and ZE85 No. 2). The ZE160LC excavator ran for 1071 hours, while the ZE85 excavators ran for 1140 and 365 hours, respectively. Unlike the ZE350LC digger from the Biri Care Center, the ZE85 are battery powered, whereas the ZE160LC is both cable and battery powered. The ZE85 has a run time of 3 to 6 hours, depending on the degree of use, according to Nasta, the manufacturer of excavators [49]. The ZE160LC has a significantly shorter run time of 30 to 60 minutes, depending on the degree of use [50]. The battery capacity is further reduced by low temperatures. Due to the limited battery capacity, the equipment required charging throughout the day. This demonstrates that zero-emission construction sites require better charging schedule planning.

Lower emissions and operational costs were achieved by using the ZERON range of diggers instead of conventional diesel equipment.The demand for a comparable machine to the ZE85 excavator is 5.5 l/h, resulting in 18 tCO_2e emission savings for ZE85 No.1 and 6 tCO_2e emission savings for ZE85 No.2. In addition, a comparable machine to the ZE160LC consumes 10 l/h, saving 127 000 NOK and 31 tCO_2e in direct emissions. The operational cost reductions were respectively 77 000 NOK and 25 000 NOK. Using electric machinery resulted in a total savings of **229 000 NOK** and a **55 $\mathbf{tCO_2e}$** reduction in emissions [43].

2.10 Literature Review of Optimized PV Production With a Battery

A case study on a renovated residential building with optimization of photovoltaic panels, batteries and electric vehicles was conducted by VTT Technical Research Centre of Finland [51]. The report aimed to simulate and optimize av PV-based energy system integrated with electric vehicles and an onsite battery. The demo site for the simulation was located in Belgium, in Central European climate

conditions. The main focus of the study was optimizing the electric vehicle and battery charging in order to minimize the need for imported power, and maximize usage of onsite power production. The demo site data was processed in order to create vehicle charging schedules and energy demand profiles for buildings. The data for the models are then used linear and mixed integer programming in order to reduce the cost of imported power. Several cases were analyzed, where different PV panel sizes, battery sizes, and vehicle charging scenarios where utilized.

The different PV nominal capacities and battery capacities for each scenario is presented in table 7.

Table 7: Different cases for the MILP optimization.

Case	PV Nominal Capacity [kWp]	Battery Capacity [kWh] scenario
1	20	B = 64.4, B = 32.2, B = 16.1, B = 0
2	10	B = 64.4, B = 32.2, B = 16.1, B = 0
3	5	B = 64.4, B = 32.2, B = 16.1, B = 0

As presented in table 7, all battery sizes were tested for each PV nominal capacity. The demonstration site had an installed PV nominal capacity of 10 kWp, as well as a battery of 32.2 kWh. In addition, the two electric vehicles had a battery capacity of 18.8 kWh and 83.4 kWh and stood for 26% of the electricity consumption of the property. Furthermore, the optimization model needed to obey a set of constraints including charging and discharging of the battery, charging of electric vehicles and energy balance. Due to the electricity regulations in Belgium, no economic gain nor compensation was given for the export of electricity in the region of the demo site. In turn this meant excess energy was either stored in the onsite batteries, or curtailed.

The results of the simulation displayed the benefits of attaining a battery in combination with the PV power production. When a 64.4 kWh battery was installed, the curtailment in case 1 dropped from 65% to 28%, case 2 saw a reduction from 43% to 2%, and case 3 reduced from 21% to 0%. This displayed an increased flexibility of power, as the property was able to utilize short-term storage of electric power to maximize the use of the PV production, hence avoiding curtailment.

In relation to the drop in curtailment, the utilization of a battery had a substantial impact on imported electricity and energy cost. For case 1, the simulation showed a 50% reduction in both categories. In case 2 import of electricity reduced by 26%, while energy costs reduced by 25%. Lastly, import of electricity and energy costs in case 3 reduced by 6%. The results indicated that a larger PV and battery capacity lead to lower import of electricity from the grid.

To continue, the onsite energy fraction (OEFe) was heavily dependant on PV and battery configuration. For case 1 the OEFe varied between 68% and 44% for the with a 64.4 kWh and 0 kWh

battery size respectively. The OEFe for case 2 varied between 47% and 34% for 64.4 kWh and 0 kWh battery size respectively. Lastly, the OEFe for case 3 varied between 25% and 22% for 64.4 kWh and 0 kWh battery size respectively. The results indicated larger onsite power production for the larger PV configuration. The results also indicated the larger systems were more reliant on battery size in order to achieve the highest OEFe.

Although the possibility of selling surplus energy was not a viable option in this study, the simulation indicated that case 1 was the nearest to the net-zero balance line, which compared the curtailed energy from the simulation to the imported energy need. In other words, the system configuration for case 1 theoretically produced enough power to reach net-zero. Case 2 and 3 were far below the balance line, meaning the OEFe was insufficient to reach net-zero.

2.11 Literature Review of a Bio-Solar CCHP System

This section presents a literature review of a potential bio-solar system for the Andaman Islands in India beginning in 2019 [52]. The case study compared the technological, economic, and socioeconomic benefits of installing the system to a base case consisting of a diesel powered generator and grid consumption. Other renewable systems, such as solar assisting the diesel generator and bio-solar without the recuperative properties of the CCHP, were investigated in the study.

HOMER (Hybrid Optimization of Multiple Energy Resources) was used to solve the model. This tool took in data and optimized renewable energy in terms of economic performance over a given time period. The simulations' load profiles were based on the hotel's electric and heat needs. The model utilized historical occupancy rate data to calculate energy demand from the shower and air conditioning.

The model is executed for four distinct Cases, including baseline, solar-assisted, bio-solar, and bio-solar CCHP. The base Case was representative of the current circumstance, in which the grid met energy demand with a diesel generator as a backup or to cover peak hours. The solar-assisted Case continued to utilize the diesel generator that was backed by PV panels and a battery. In the bio-solar Case, the demand was satisfied by a gas engine powered by syngas and backed by PV panels and a battery. The bio-solar CCHP system had a configuration similar to Case 3, but distinct properties.

Table 8 displays the system configurations that were optimized with regard to NPC. The maximum area permitted for PV panel installation in Cases 3 and 4 was 600 m^2, which corresponded to the available rooftop area. However, there is no assumption of a limit in Case 2.

Table 8: Optimal system configuration for all cases.

Component	Case 1 (Diesel-Grid)	Case 2 (Solar-Assisted)	Case 3 (Bio-Solar)	Case 4 (Bio-Solar CCHP)
Diesel generator	160 kW	90 kW	-	-
Gasifier+Gas engine	-	-	50 kW	40 kW
PV panels	-	200 kW	85 kW	80 kW
Batteries	-	42 kW (7 strings)	84 kW (14 strings)	48 kW (8 strings)
(Nom. Capacity)	-	(319 kWh)	(638 kWh)	(365 kWh)
Converter	-	60 kW	50 kW	45 kW
Boiler	-	-	-	75 kW

The configuration for all Cases behaved as expected. The solar assistance in Case 2 resulted in a substantial reduction in reliance on the diesel generator, but some diesel generation remained. This may have occurred as a result of the benefit of low operating costs being offset by the cost of installing new equipment over a 20-year period. Continuing, it can be seen that the configurations of Cases 3 and 4 were quite similar, with installed capacities that were comparable. However, Case 4 includes a 75 kW boiler that can cover the heat demand if the gas engine is turned off. To continue, the NPC, capital investment costs, and annual CO_2 emission were displayed in the graph 4.

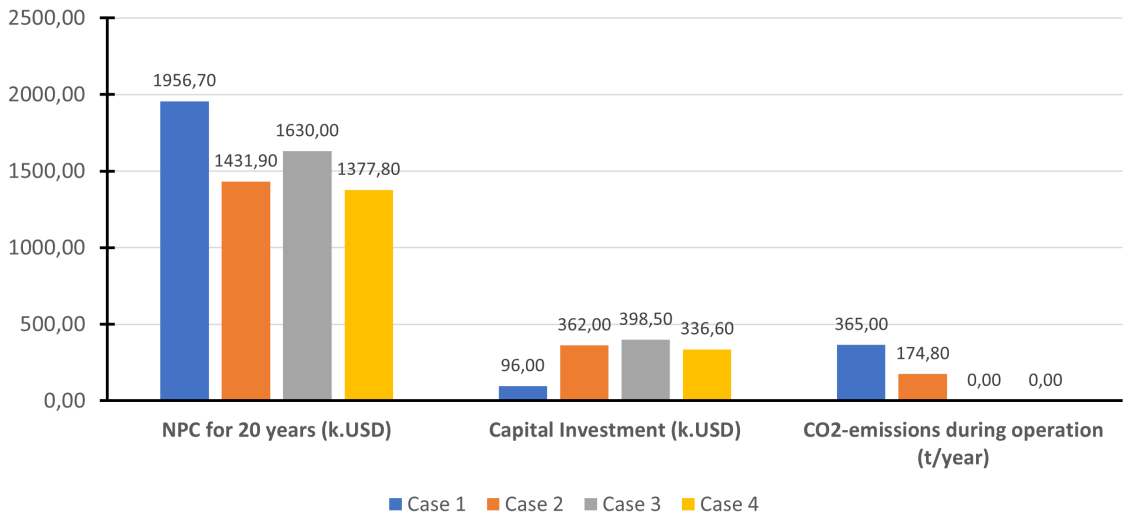

Figure 4: NPC, capital investment and emissions for all cases.

It was evident that Case 1's costs were the highest of the simulation, resulting in a cost of 1 956

700 USD over a 20-year period. Reviewing the results of the other cases revealed potential savings of 326 700 USD for Case 3, 524 800 USD for Case 2, and 589 000 USD for Case 4, respectively. However, Case 1 had a lower cost of investment while Cases 2, 3, and 4 had comparable investment costs. Transporting expensive equipment to the island resulted in high investment costs, whereas a traditional diesel generator was less costly and likely available closer to the island, reducing investment costs. Cases 2, 3, and 4 were all less expensive than the proposed base Case over the course of 20 years because the higher capital investment was offset by lower operational costs. As observed in figure 4, yearly CO_2 emissions vary greatly between the Cases.

The overall fuel consumption and electricity generation is presented in table 9.

Table 9: Consumption and generation for all Cases.

Sub-System	**Case 1 (Diesel-Grid)**	**Case 2 (Solar-assisted)**	**Case 3 (Bio-Solar)**	**Case 4 (Bio-Solar CCHP)**
Diesel consumption	490 511 kWh/year	384 817 kWh/year	-	-
Biomass consumption	-	-	1 526 573 kWh/year	1 142 813 kWh/year
PV generation	-	281 986 kWh/year 58%	119 832 kWh/year 30%	119 832 kWh/year 38%
Diesel engine generation	162 281 kWh/year 41%	134 741 kWh/year 28%	-	-
Gas engine generation	-	-	276 372 kWh/year 70%	194 756 kWh/year 62%
Grid purchases	233 729 kWh/year 59%	71 825 kWh/year 15%	-	-

Beginning with Case 1, it is evident that 59% of the electricity demand was directly met by the grid, while the remainder was met by the diesel generator. The annual consumption of diesel was 490 511 kWh, or 49 849 liters. With the help of the PV-system, reliance on the diesel engine was reduced to 28%, and reliance on grid electricity was reduced to 15%. Diesel consumption decreased by 105 694 kWh/year, or 10 741 liters/year, as the PV-system now meets a significant portion of the demand.

In Case 3, the annual biomass consumption was 1 526 573 kWh. With the PV system limited to 600 m^2, the annual production falls to 119 832 kWh, which now meets 30% of the demand. With the new system configurations added in Case 4, the new biomass consumption was 1 142 813 kWh/year, or 194 775 kWh/year provided by the gas engine. In Case 4, the proportion of the roof covered by the PV-system was greater than in Case 3, despite the production remaining the same. This may suggest that the bio-mass system in Case 4 is more efficient.

To evaluate the system's robustness, two parameters were modified. The first was the price of fuel/syngas for all cases. Due to the volatility of diesel prices and the unpredictability of the island's available biomass, modifying this parameter may cause a new case to be optimal. As expected, Cases 1 and 2, which were the most reliant on fuel prices, showed the greatest decrease in NPC. Cases 3 and 4 experienced a slight decline in NPC, but otherwise remained largely unchanged. On the contrary, it appeared that an increase in fuel costs affected all cases uniformly. Case 4 with 150% fuel prices has a lower NPC than Case 1 with 50% fuel prices, which is an interesting observation. This demonstrates the robustness of the system.

To continue, the lifetime of the generators were increased and decreased by 50%. Reducing the generator lifetime had little effect on Cases 1 and 2, with increases of 6% and 5%, respectively. In case 3, the reduced lifetime had a significant effect on NPC, resulting in the highest NPC of all cases, a 45% increase. The impact was also evident in Case 4, resulting in a 39% increase in NPC. To continue, the values for Case 1 with a longer lifetime were nearly identical to the values for Case 4 with a shorter lifetime. This demonstrates the system's resilience and its superiority even in the face of drastic changes. However, Case 2 is the best option for a shorter generator lifetime in relation to the NPC.

In this case study, the results demonstrated the clear superiority of the CCHP plant over the conventional diesel-based system. The total savings would exceed **578 000 USD**, and the investment costs would be recouped in only four years. A reduction of tCO_2 emissions per year would have a significant impact on the environment if the current situation were to continue. This would amount to **7 300 tons** over the course of 20 years. As described in the previous section, the CCHP plant proved to be a reliable alternative despite drastic changes in fuel prices. Due to the substantial increase in NPC when the generator lifetime is decreased by 50%, it is crucial that the system is well-designed. On the basis of these findings, there should be a willingness to fund the project, primarily due to the substantial emission reduction potential.

2.11.1 Comparing the System With Tanberghøgda

The energy system in the above mentioned case is very similar to the one that is planned for Tanberghøgda. To provide electricity for the zero-emission construction site, a PV system will be installed at the start of the construction period. Furthermore, the site will facilitate the installation of an additional PV system at a later stage in the project's development [3]. A 1 MW battery will also be installed to improve distribution flexibility. This will be advantageous, as the construction phase requires overnight charging of machinery, and later, overnight charging of electric vehicles. To manage the increased output from the new PV system, additional batteries may be installed at a later date. The project in Tanberghøgda plans to install either a local 1.1 MW biomass-powered heat system, with wood pellets as the primary fuel source, or connect to an exisitng district heating system, to meet the majority of the heating demand.

Due to the case study project's similar system configuration to Tanberghøgda, the results can be

compared to gain insight into the advantages and potential benefits of the system configuration. The Neil Island system simulations predict a possible 20-year cost savings of 578 000 USD. This is due to the island's departure from its conventional diesel-powered system, which heavily relied on the volatile diesel price. Even though there are no projected potential savings for the Tanberghøgda project, one could assume there is a potential for savings based on the simulation results. The system is becoming more economically viable as a result of rising electricity prices in the south of Norway, particularly during the winter. However, one must consider alternative energy sources to Tanberghøgda, which are generally much more cost-effective than the diesel-based system for the Neil Island project.

The CO_2 emissions could be reduced by 365 tons annually if the biomass solar assisted CCHP system is used. According to the concept report on Tanberghøgda issued by COWI, the installed solar panels result in an estimated yearly CO_2 reduction of 65 tons. The installed biomass-powered heating system resulted in an estimated 280 tons of CO_2 reduction yearly [3]. As the project develops, the expansion of the energy system will result in even greater emission reductions. The simulations and the COWI report demonstrate a significant potential for reducing CO_2 emissions by selecting a biomass-powered plant with solar assistance. Despite resulting in long-term cost savings, these systems have a higher initial investment cost due to the expense of equipment and the difficulty of installation. This may deter developers, but Tanberghøgda aims to be a pioneer in construction by pursuing low emissions and high energy efficiency. Tanberghøgda receives funding from Enova to support innovation in the ambitious project [3] in order to promote its growth. Both the case project and Tanberghøgda seek to preserve the surrounding biological diversity by reducing emissions and adapting the system to have the least possible impact on the local environment.

In addition to the previously mentioned advantages of the CCHP system, the installation of the system has additional advantages for farmers, hotel owners and local government. The use of biomass provides a reliable source of income for the local farming sector, and in exchange, farmers receive processed charchoal from the gasification process as fertilizer, resulting in sustainable and circular agriculture. Long-term contracts between the parties are also advantageous for hotel owners, as they provide economic predictability from a stable, local fuel source. The proposed plant will improve the island's electric supply network and increase the island's electric reliability. The development of the biomass heating system for Tanberghøgda will encourage the utilization of local biomass derived from forest work. Biomass as a long-term fuel source is a viable option in Ringerike because there are many forests there and a recently constructed wood pellet production facility is 25 kilometers from the project site [53, 54].

3 Description of the Tanberghøgda-project

3.1 Project Introduction

Tanberghøgda is part of a new district in Hønefoss, Krakstadmarka - Hønefoss east, where it is proposed to construct 590 dwelling units, including approximately 17 single-family houses, 250-300 detached houses, and 200-250 low-rise apartments [55]. The project is innovative because it is the first residential neighborhood in Norway to receive CEEQUAL certification. The certification, now known as BREEAM-certification, verifies that the project's execution is sustainable. The CEEQUAL certification requires outstanding indoor air quality, the use of sustainable materials, and the procurement of products in a responsible manner. Life cycle analysis (LCA) are essential to the process, in addition to CEEQUAL certification. The procedure should generate a complete picture of the entire environmental impact of a product's or project's life cycle. The LCA's serve as the foundation for developing environmental product declarations (EPD's) for each individual product. EPD is a similar declaration that describes the environmental impact of a product or service throughout its entire life cycle.

The total construction of the 590 building housing stock is divided into three distinct phases that ends in 2040. Phase 1 is from 2022 to 2028, phase 2 is from 2026 to 2038, and phase 3 is from 2036 to 2040.

As specified in Section 2.8, the energy supply infrastructure must be constructed rapidly in order to establish an emission-free building and construction site. To support the construction efforts, the first energy central for the region will be constructed. For the entirety of phase 1 and the first half of phase 2, this energy center will be the sole energy center. This range corresponds to the years 2022 to 2032. This necessitates the use of the central plant for both the heating and electricity needs of the housing stock and the energy needs of construction.

3.1.1 Photovoltaic Power and Battery System

A 500 kWp solar cell system makes up the energy central for the power supply. The selected panels will be monocrystalline and with half-cell architecture. Furthermore, bi-facial modules will be chosen over mono-facial ones. Alongside the PV-system will be a larger 1 MW battery with a 1 MWh capacity, which should be able to cover a substantial portion of the load and increase the PV system's utilization rate [3].

It will be Norway's largest ground-mounted solar system. According to preliminary studies, this will result in substantial climate reductions; a 60% reduction in greenhouse gas emissions from infrastructure construction in the region [57]. The battery can be used to purchase energy when spot prices are low, reduce peak power, and improve system stability. Peak reduction is also advantageous in terms of lowering the cost of electricity and reducing the frequency of rapid fluctuations

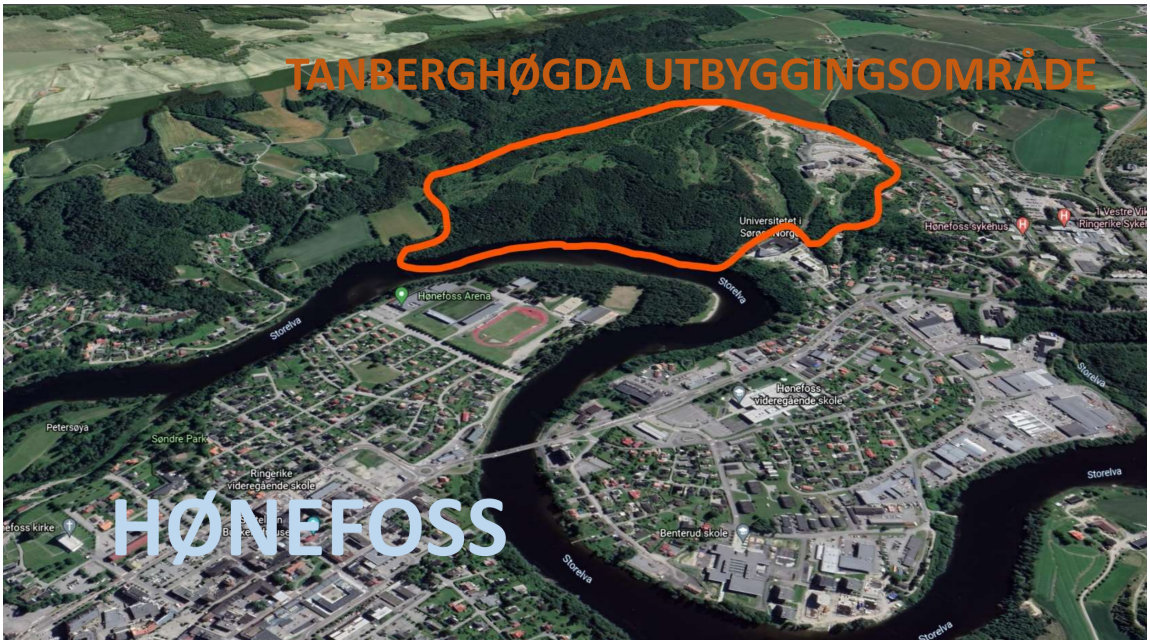

Figure 5: The planned construction area of Tanberghøgda, with reference to Hønefoss [56].

in electricity consumption.

Even when it's cloudy or dark, the battery enables the energy to be used. The local electrical system will receive less power as a result. Through the implementation of a new energy system designed by ENFO, it is intended to coordinate energy production and consumption [57]. Initially, a cloud-based platform architecture for efficient energy management and sales will be developed.

This project is unique among Norwegian housing complexes due to the fact that the ground-mounted solar system and integrated energy production facility are incorporated into the terrain. In a terrain as steep as Tanberghøgda, there is less space for innovative ideas regarding the placement of solar cells; consequently, it is crucial to optimize the location of the cells.

Figure 6: Illustration of the planned PV-system in Tanberghøgda [58].

In addition to serving as grazing land and open space, the area surrounding the PV plant will also receive sunlight due to the bi facial design. This will result in an increase in the area's biological diversity, while the PV plant is aesthetically pleasingly integrated into the landscape. This allows a symbiotic relationship with grazing sheep, as sheep can sustain themselves on the undergrowth, whilst also ensuring the plants do not cover the PV modules. Grazing animals and solar power are a great match, especially sheep. It promotes animal welfare because animals have ready access to rain and sun protection [59]. In addition, a ground-mounted solar system does not permanently occupy the area. The area can be used for agriculture or forestry after the solar cells are removed.

3.1.2 Systems for Heating Demand

The heating demand for Tanberghøgda can be served with either a local boiler system, or a connection to a district heating system from Hønefoss [3]. The return water is assisted by a pump installed in the local area.

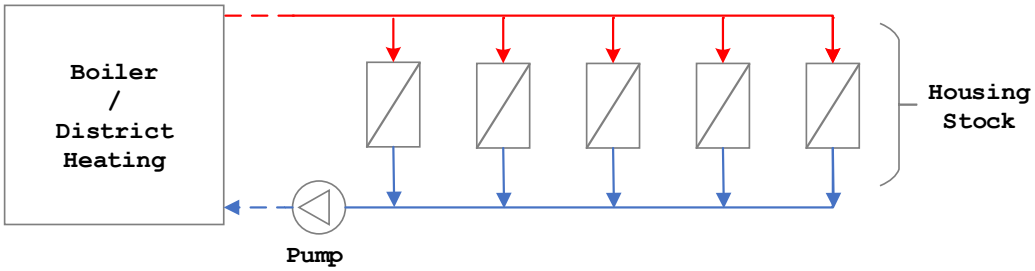

Figure 7: The system sketch for the local boiler or district heating connection.

Figure 7 represents the connection scheme for both heating systems. The piping and pump will be the same for both options, and will be connected either directly to the areas own boiler combination, or to a heat exchanger provided in conjunction with district heating.

For the choice of the local boiler system, two boilers will be installed to supply the heat demand. These pellet-powered systems will be configured as base load and peak load systems. Except for the detached homes in phase 1, these boilers will supply the entire heating demand. The heating system cannot be connected to these homes because they are too far away. According to the concept paper, air/water heat pumps will be considered for all heating needs in these homes. With 300 kW of installed power in phase one, the heating system will also employ an extension strategy. 800 kW is installed in phase two, and these two will meet the entire heating demand until phase three is complete. In the middle of phase two, 1 100 kW will be installed [60].

District heating requires a connection to an external district heating grid. For this solution, a heat exchange is provided to the area, and the piping for the area is installed together with a circulation pump in the same manner as for the local boiler system. Costs for the piping is not covered by the district heating company.

For both system choices, the initial cost for the piping and circulation pump is in essence paid for by the inhabitants as a part of the purchasing sum for the domicilies.

3.1.3 Housing Distribution

The total housing distribution can be seen in table 10.

Table 10: Building distribution for the relevant time period.

Name	Phase	Type	Housing Units	Buildings	Area [m^2]	Common Heat
Teglveien eneboliger	1	Detached House	21	21	3 570	No
Barnehage	1	Kinder Garten	1	1	1 000	Yes
Energisentral	1	Technical	-	1	1 000	Yes
Drivhuset rekkehus	1	Terraced House	36	10	3 240	Yes
Ravinedalen leiligheter	1	Terraced Apartments & Apartments	85	21	5 950	Yes
Ravinedalen	2	Semi-Detached House	17	4	1 530	Yes
Furulunden	2	Semi-Detached House	49	10	4 410	Yes
Konglegate	2	Semi-Detached House	46	9	4 140	Yes
Utsikten	2	Apartment Building	12	2	840	Yes
Skogsveien	2	Apartment Building	64	4	4 480	Yes
Furutre	2	Apartment Building	11	1	770	Yes
SUM			**342**	**84**	**30 930**	

This distribution shows the entirety of phase one and nearly fifty percent of phase two. In addition, the housing stock has been increased by about 22% to accommodate the increase from 481 to 590 total housing units. This modification is described in the concept report [3].

3.2 The Machine Requirements

The project's construction is divided into five phases: groundwork, building, facade, internal and outdoors. There is no longer a need for a demolition phase since there are not any structures in the area to demolish. The construction area for the homes in Tanberghøgda is approximately 40 000 m^2. The project has not yet reached a point where it is possible to determine which and how many machines will be used during the various construction phases. Furthermore, there are not many similar construction projects employing the zero emission principle, as the execution of this idea is still somewhat in its infancy. However, some projects can be analyzed and used to garner information that can be used for comparison. Based on the "Midtbygda Nursing Home" construction project near Bergen, which, like Tanberghøgda, seeks to create an emission-free construction site [61], The construction area at Tanberghøgda is roughly three times that of the nursing home project in Bergen; consequently, the number of machines is increased proportionally. The distribution of machines throughout the different phases of construction is estimated as follows:

Table 11: The machine park for each of the periods.

Groundwork	**Building**	**Facade**	**Internal work**	**Outdoors**
9 x Excavator 3 x Drilling rig 6 x Roller 3 x Wheel loader 3 x Crusher	6 x Excavator 6 x Tower crane 3 x Truck	6 x Excavator 3 x Boom lift 3 x Tower crane 3 x Truck	3 x Tower crane 9 x Scissor lift 3 x Construction elevator	6 x Excavator 3 x Wheel loader

Table 11 makes it clear that the construction phase with the highest energy demand is the groundwork, as excavators are among the machines that require the most energy to operate. The technical specifications of various machine types are shown in the table below. Machines with a single charge cycle are expected to be charged outside of working hours, as the number of charge cycles is determined by the average battery life. The machines with two charging cycles will also be required to charge with fast charging for one hour between 11 a.m. and 12 p.m., during the lunch break of construction site workers.

Table 12: Technical data for the electrical machines.

Machine type	Designation	Wired effect[kW]	Battery size[kWh]	Max charging effect[kW]	Charge cycle [number/day]	Charging effect night[kW]
Excavator	Doosan DX300		390	150	2	44
Scissor lift	Genie GS-4069 DC		15	3.5	1	1.3
Drilling rig	Liebherr LB 16		720	80	1	40
Roller	Dynapac CC900 e		100	75	2	20.5
Wheel loader			40	17	2	3.3
Crusher	Keestrack K7e Zero	86.5				
Truck	Volvo FE electric		265	150	1	22
Tower crane		60				
Boom lift	Manitou 200 ATJE		22	3	1	1.8

For lunchtime-required machines requiring rapid charging, the maximum charging effect is utilized. The maximum charging effect is unnecessary for the others, as the machines can be charged for 15 hours after work hours. Normal charging, or charging overnight, is suitable to completely recharge the battery. The drilling rig is the only machine that cannot be charged from a completely dead battery to a fully charged battery in 15 hours, but it is assumed that fast charging of the drilling rigs can be avoided because only three drilling rigs are required for the duration of the construction process, the drilling rigs have 720 kWh batteries, and the battery level is rarely completely dead or fully charged. The machines' batteries should have a 20% battery at the end of a workday. This buffer prevents machines from losing power during critical work. In addition, it is believed that the battery is charged to 80-90% during the night instead of 100% to prevent battery wear.

3.3 Time Management

The project has not yet advanced sufficiently to schedule the duration of the various construction phases. Therefore, a simplified time estimate is performed and displayed in figure 8 as a *Gantt chart*.

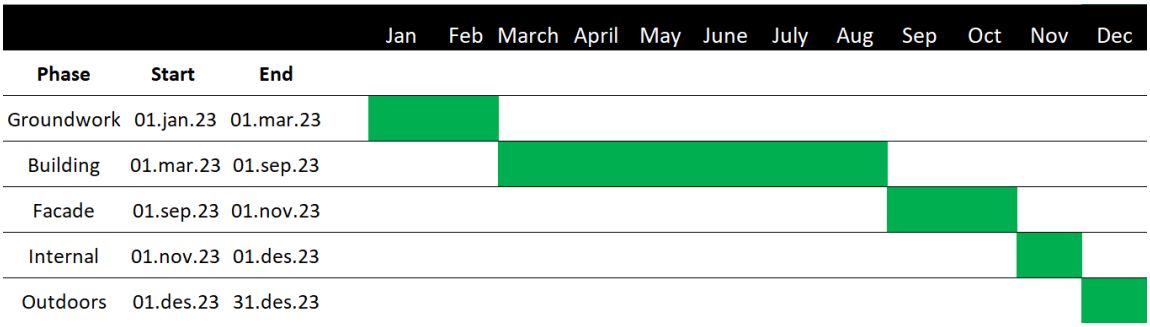

Figure 8: Gantt chart for the assumed time span of the project.

The time perspective in this situation is undoubtedly too limited, but the time connection between the phases is more crucial, the one year horizon was thus chosen as to provide the full range of seasonal data. With nearly 600 buildings to construct, the construction phase is without a doubt the most time-consuming phase. The construction phase will occupy nearly 50% of the total duration. The interior and exterior phases will consume the least amount of time, while the foundation and facade phases will consume the second-most time. The internal phase is anticipated to be less time-consuming than for public buildings because buyers will be able to customize the furnishing of their new home or apartment.

4 Methods

4.1 Tools

IDA Indoor Climate and Energy (IDA ICE) used for simulating internal climate and energy use for buildings. Practical modeling was done in **Python** and **MatLab**. Most of this work took place in Python. To solve the more complex problems, additional software was necessary.

Pyomo is an open-source software suite with a large number of optimization tools. Pyomo can be used to define and structure a wide range of optimization problems. The ability to define *Linear Programming* (LP), and *Mixed Integer Linear Programming* (MILP), was crucial for this project. After a problem is structured with all of its constraints, Pyomo can import third-party solvers to perform the necessary calculations and present an optimal solution.

Gurobi is a *Solver*, and is used alongside Pyomo's model to solve the defined problem. Gurobi is one of the fastest and most powerful commercial solvers available. Additionally, a license can be acquired for free through NTNU. As such, it was a good choice for this project.

Excel is used in combination with Python and MatLab. Scripts can import data stored in Excel sheets, and subsequently store it as arrays or dictionaries inside Python / MatLab.

4.2 Data Material

4.2.1 Cooperation With Master Group

In order to obtain data regarding electric demand, heating demand and other crucial elements for building an optimization model, cooperation with another Master group was initiated (hereby referred to as **Group 2**). The goal of Group 2's thesis was to define appropriate types of building constructions together with heating solutions for three different building types in order to achieve minimal energy consumption. Group 2 also conducted its research on Tanberghøgda, making the result very relevant for further research in this project.

In order to create and simulate the different building types Group 2 utilized IDA-ICE, a powerful simulation tool used to construct building models and simulate different parameters in the software. The three building types created was an apartment, a terraced house and a detached house. In addition, all building models were constructed to meet the requirements set by TEK17 and the passive house standard NS3700. Furthermore different heating solutions were considered, resulting in three different space heating scenarios.

To utilize the data properly, a suitable heating source and standard was chosen for all building types. For this project the TEK17 regulations were opted as the standard for all houses. For the apartments and terraced houses, space heating with radiators were chosen as heating source. As described in Section 2.1.1, these were the current building regulations for construction and therefore the most relevant. Radiators were chosen as heating source as this is a commonly used in the housing market. The detached houses however are not connected to the district heating network. Therefore heat pumps are utilized, and the heating needs for detached houses were part of the electric demand, not the heating demand.

4.2.2 PV Production Data

In connection with their preliminary work on Tanberghøgda, COWI provided data on photovoltaic production. The data was collected using the software *PVSyst*. The program simulates production for each hour of the year. To accurately represent these numbers, numerous parameters must be taken into account. Climate data and panel orientation are also investigated in addition to panel varieties. Therefore, these should serve as a reasonable starting point for production values, even if they may be somewhat optimistic compared to actual values. Figure 9 depicts four production profiles, one for a day in each season. The profiles display a typical average day for January, March, June, and October.

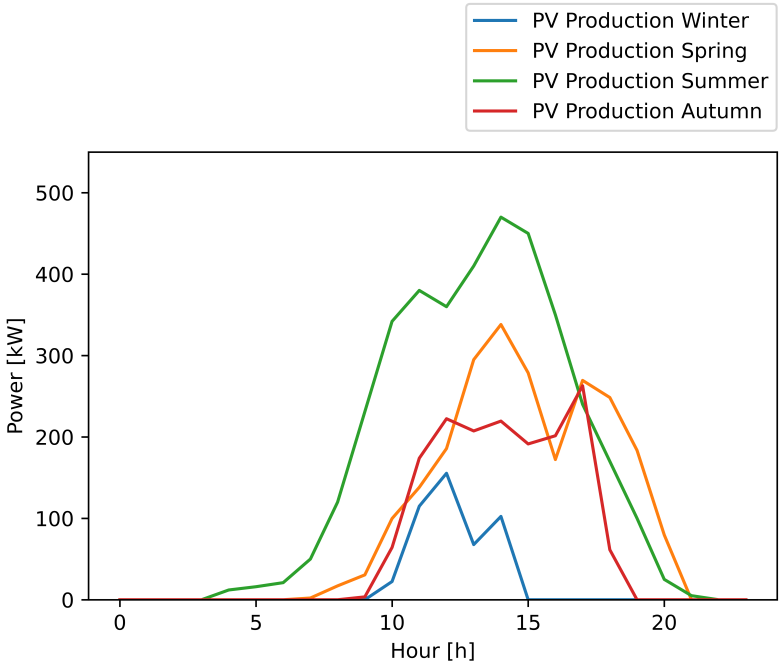

Figure 9: PV production profiles for a 24 hour period for spring, summer, autumn and winter.

The total production during spring is as follows:

- Spring: 2 338 kWh
- Summer: 3 752 kWh
- Autumn: 1 608 kWh
- Winter: 463 kWh

Examining figure 9 reveals that the production profiles differ greatly. This is to be expected, as there are fewer daylight hours and less intensity during the winter. The total output of a winter day is 87 % less than that of a summer day. Despite this, significant amounts of power are still produced during the winter. This may be due to the use of bifacial modules, as discussed in Section 2.2 on page 6.

4.2.3 Electricity Spot Prices NO1

Through Nord Pools *Free Transfer Protocol* (FTP), it is possible to obtain more detailed data for longer time periods than is available online. After reaching an agreement with Nord Pool, it was possible to obtain hourly data for an entire year for the corresponding bidding zone. The data of interest was the 2020 and 2021 spot prices in zone NO1, which covers Tanberghøgda. The spot prices are later used in combination with PV production, battery level and energy consumption to evaluate when to buy and sell power.

4.2.4 Housing Stock Load Profile

Through the use of Group 2's simulation work on the Tanberghøgda building stock, relevant load data may be obtained. Group 2 is another group working on the Tanberghøgda project. This information was produced through simulations in IDA ICE. Detached, terraced homes, and apartments were simulated. The building models were simulated as either TEK17 or passive house. For further use in this thesis, TEK17 data was chosen, as it is more representative of the buildings at Tanberghøgda. Energy requirements were collected as hourly data for each dwelling, which could then be translated into energy requirements per W/m^2 for each building type. Table 13 contains this information.

Table 13: Sample data for energy demand for both detached houses and terraced houses. Note that the total electricity demand for the detached houses is for both heating(*HP , assuming a COP = 4*) and electricity for both appliances and lighting.

Type	Hourly Average Heating Demand [W/m^2]	Hourly Average Electricity Demand [W/m^2]	Area [m^2]	Heat Supplied by Boiler [kWh/day]	Total Electricity Demand [kWh/day]
Terraced House	3.68	2.81	13 320	1 176.42	898.30
Terraced House (Winter)	12.05	2.78	"	3 852.14	888.71
Detached House	3.89	2.82	3 570	-	574.98
Detached House (Winter)	11.56	2.79	"	-	1 229.51
Apartment Building	3.27	3.40	12 040	944.89	982.46
Apartment Building (Winter)	6.79	3.36	"	1 962.04	970.91
Kindergarten and Energy Central	3.89	2.82	2000	186.72	135.36
Kindergarten and Energy Central (Winter)	11.56	2.79	"	554.88	133.92

As the Tanberghøgda neighborhood contains more than three types of structures, some small simplifications were required. The kindergarten and energy central is assumed to have the same characteristics as the detached houses in regards to thermal profile and electric demands, while the terraced apartments are assigned the apartment characteristics.

Using the data from table 10 the total areas were calculated and the total heat and electric demands were then reached. The electric demand consists of all appliances and lights. However, as mentioned previously, detached houses are not connected to a central heating system; therefore, all heat must be supplied by electric air/water heat pumps. Using equation 2.2 and assuming a *COP* of 4, the total electricity demand for the heat pumps can be calculated by multiplying the heat demand by a factor of 1/4. The electric load profile for the area could then be calculated.

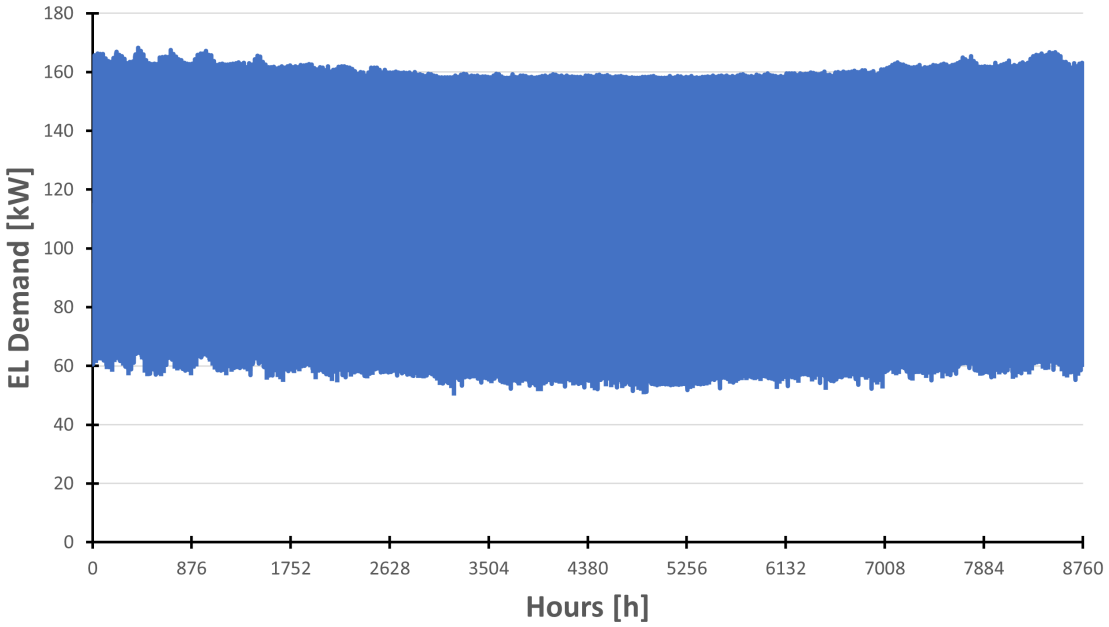

Figure 10: Total El demand for the housing stock for one year.

Figure 10 displays the electric demand ranging from around 60 kW to 160 kW, with a total demand of 878.2 MWh for the entire year. A minute dip towards the summer hours can be observed. This is to be expected, due to the reduced electric demand for the heat pumps in the detached houses. The remaining electric demand remains relatively unchanged through the year, there of the stable demand for the entire housing stock. The distribution of the electric demand for the housing stock is presented in figure 11.

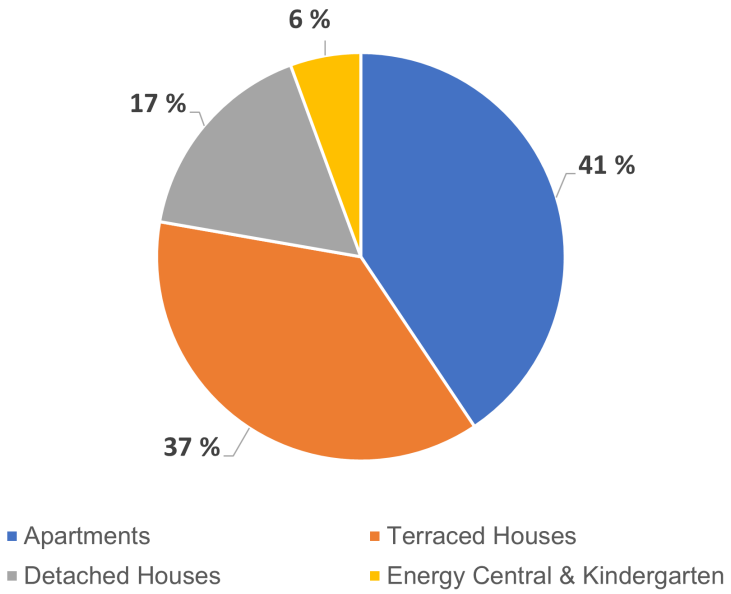

Figure 11: Housing stock distribution for the total electric demand during one year.

As expected, the detached houses can be seen to have a proportionately larger share of the el demand compared to their actual size. This is due to the fact that all heat to the detached houses is delivered from heat pumps, which need power.

Furthermore, average data sets for the electric demand for the entire housing stock could be gathered for all four seasons. These data sets had to be representative of the entire month and contain consistent, outlier-free data. January, March, June, and October were chosen. Figure 12 shows these outcomes.

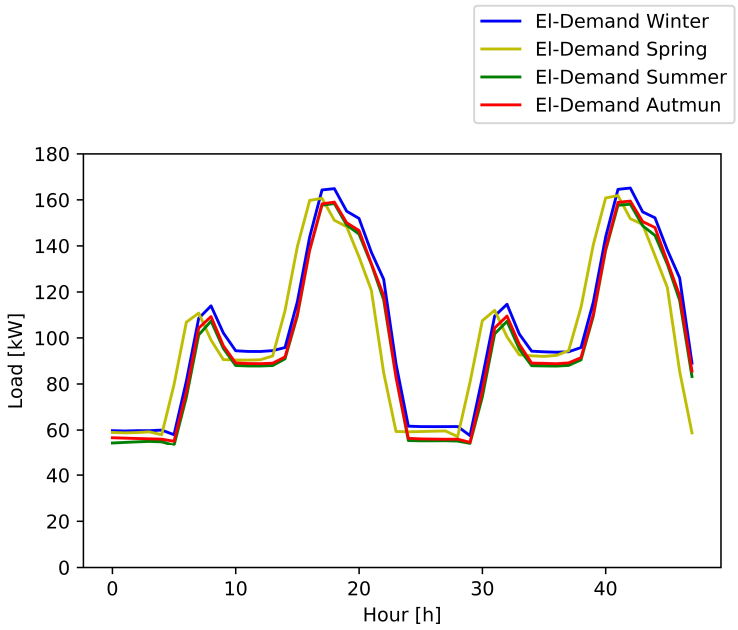

Figure 12: Total El-demand for a 48 hour period during winter, spring, summer, and autumn.

As shown in figure 12, the combined el-demand follows the same general trend and varies slightly. The results for winter are as anticipated, slightly higher than those for summer. During the winter months, the heating supplied by heat pumps to detached houses will be the most significant difference.

4.2.5 Heating Demand

A heating demand load profile could be determined using Group 2 IDA-ICE simulation data. A total of 27 360 m^2 was used because all structures, with the exception of detached homes, are linked to the heating system. The total distribution of these three building categories in regards to the total heat demand is shown in figure 13.

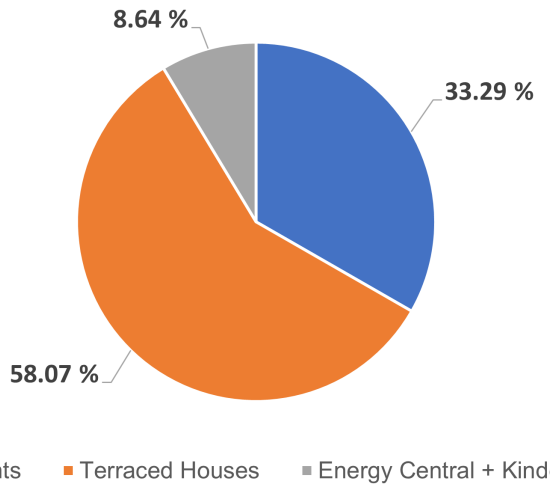

Figure 13: Distribution of the yearly heat demand for the area. Total demand = 1516 MWh.

The yearly profile is presented in figure 14, this therefore shows the yearly heating demand curve for the terraced houses, apartment buildings, kindergarten, and the energy central. As expected the terraced houses have the highest share of demand, followed by the apartments when taking into account the area distribution presented in table 13.

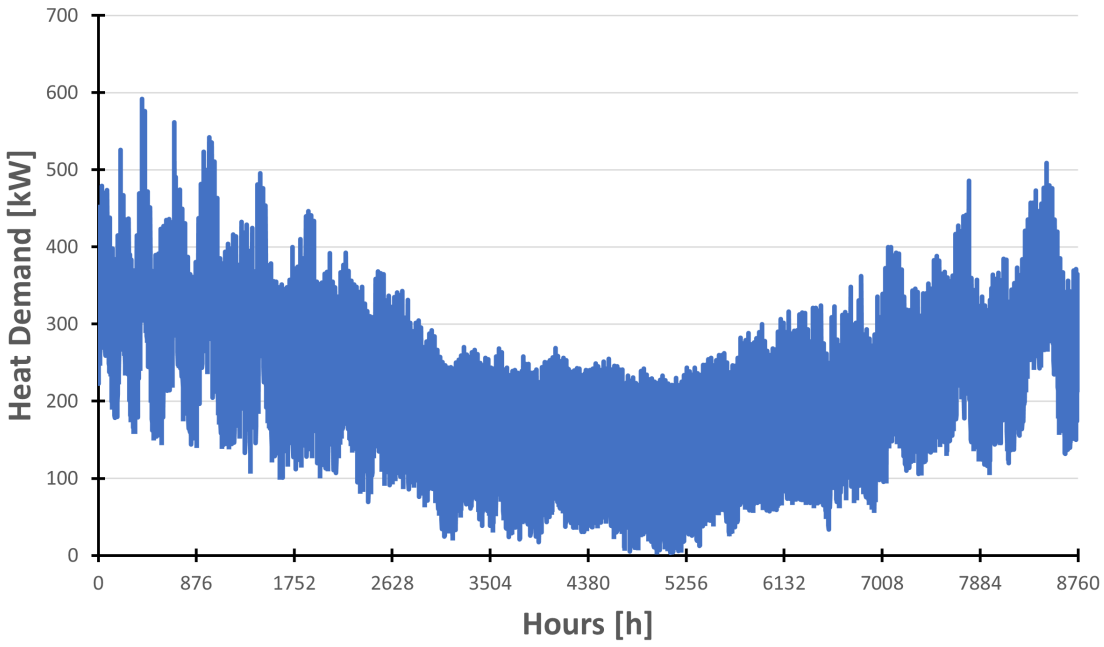

Figure 14: Yearly heat demand for buildings connected to the heating system in Tanberghøgda.

The winter peaks in figure 14 reach almost 600 kW in the coldest period of the year. This relates to the current dimensioning of the phases at this time. As expected the heating demand drops significantly towards the summer months which in some periods drops to zero during the warmest days for the year. The middle of phase two would require an installed power of 1 100 kW, as shown in Section 3.1.2. Consequently, it is reasonable to assume that the entire load is covered.

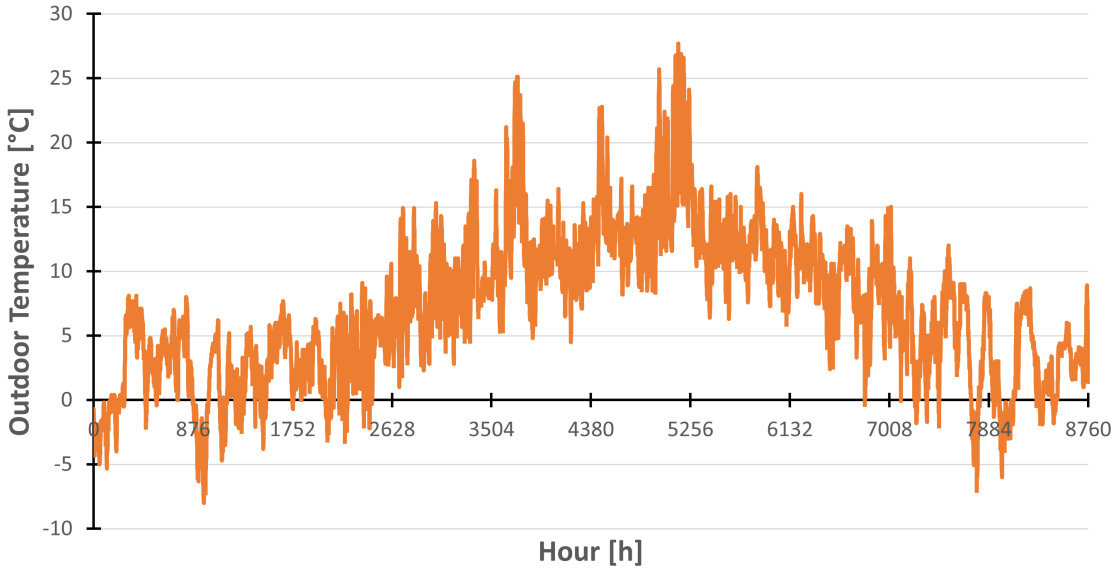

Figure 15: Yearly outdoor temperatures in Tanberghøgda.

The outdoor temperatures varies between -8 $°C$ during winter and 27.7 $°C$ during summer. The temperatures displayed in figure 15 correlates with the heat demand values in figure 14. The correlation is displayed in figure 16.

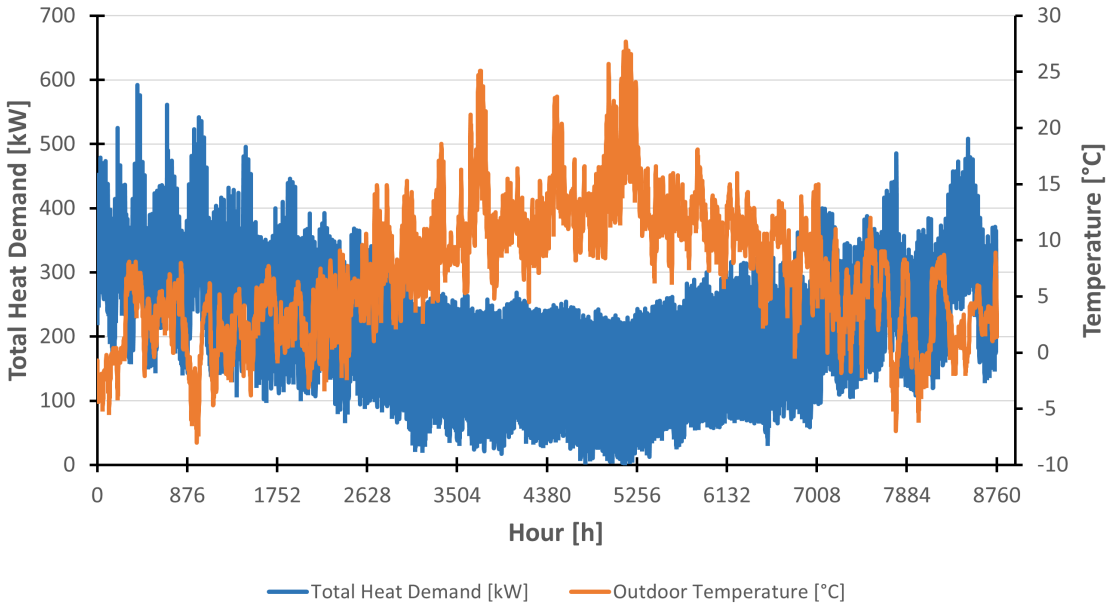

Figure 16: Yearly total heat demand and outdoor temperatures in Tanberghøgda.

The heat demand is at its peak when the temperatures are at the lowest. The outside temperatures exceed standard indoor temperatures a few days during the year, and during these hours the heat demand is approximately equal to zero.

Additionally, the boiler supply and return temperature were made available by Group 2. These data sets were made for terraced houses, apartment buildings, and detached houses. The supply temperature for the different housing types were almost identical, as displayed in figure 17 where the deviation of temperature is presented through a simple numerical difference between the return temperatures for apartment buildings and terraced houses.

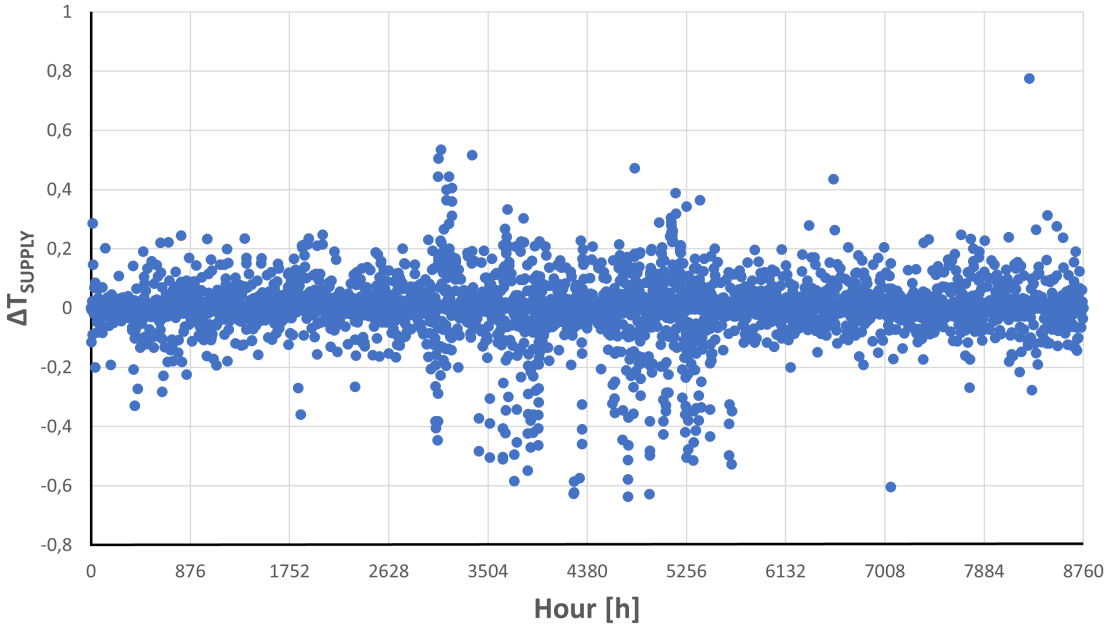

Figure 17: Difference in supply temperatures for the apartment building and the terraced houses. Note that the difference is less than one degree Celsius year round.

The difference can be seen to be minute, as such, the decision was made to use one supply temperature model for all heat demand. The broad range of deviation is between -0.2 and 0.2 °C with a few isolated instances ranging from -0.7°C to 0.8°C. For further calculations the apartment building data for supply temperature was used.

The return temperature however was not as similar, as can be expected as the different building types have different heating demands. To compensate for this, and still produce one single temperature model for the heating delivery, figure 13 was used to make a weighted return temperature for all hours of the year. Each building types share of the total heat demand was multiplied by the corresponding return temperature, after which all these results could be summed up to make the weighted return temperature. The aforementioned supply and return temperatures are shown in figure 18.

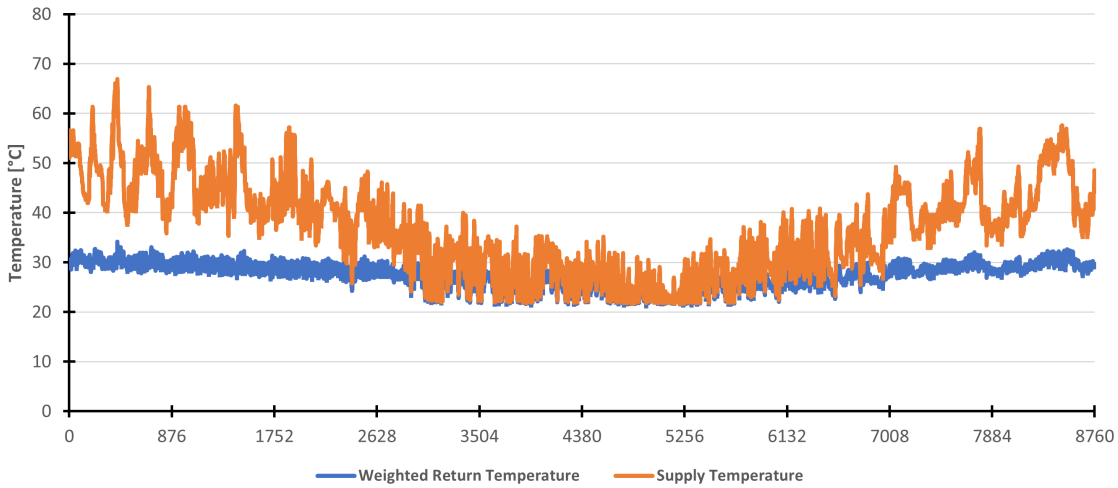

Figure 18: Yearly weighted return temperatures with the boiler supply temperature.

The data shows a trend of higher supply temperatures during the winter months, along with lower supply temperatures during the warmer summer months. This is to be expected, together with a return temperature which remains lower and has a lot less variance. During the warmest months, the difference in temperatures are very small as the heating demand is very low.

These correlations can be further examined when assessing the ΔT of the system, the difference between the supply and return temperatures.

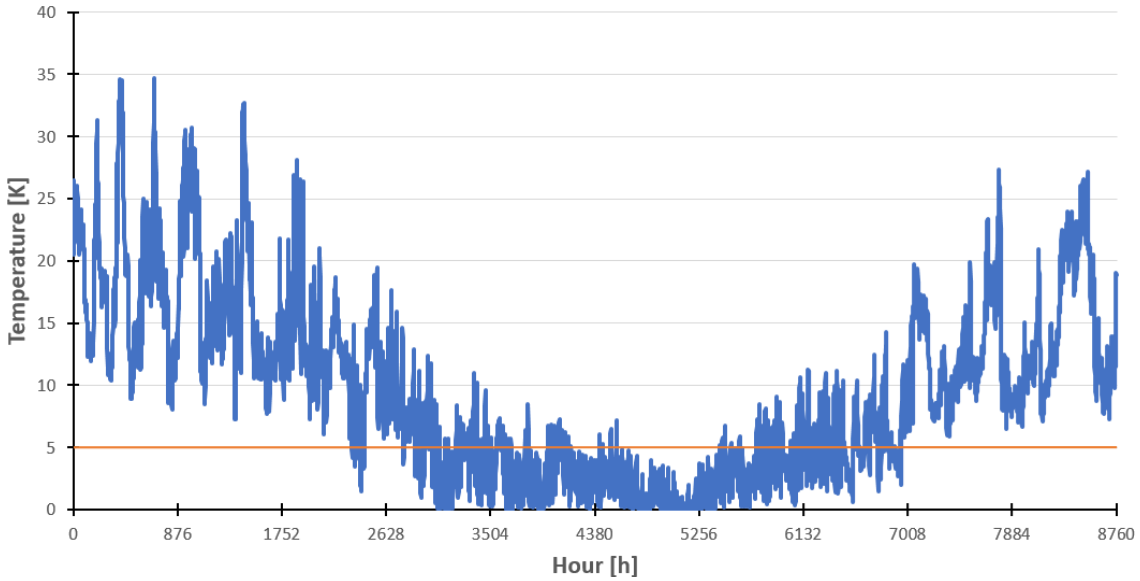

Figure 19: Yearly weighted ΔT.

Figure 19 displays the difference between the supply and return temperature. During the warmer summer months, the ΔT is low, due to the low heat demand and subsequent low supply temperature. When the temperature drops below 5 $^{\circ}C$, the pump closes [62].

The opposite can be observed for the colder months. This corresponds to the outside temperatures shown in figure 15. In addition, there is a clear correlation between the temperature difference between supply and return, compared to the heating demand presented in figure 14 which is to be expected.

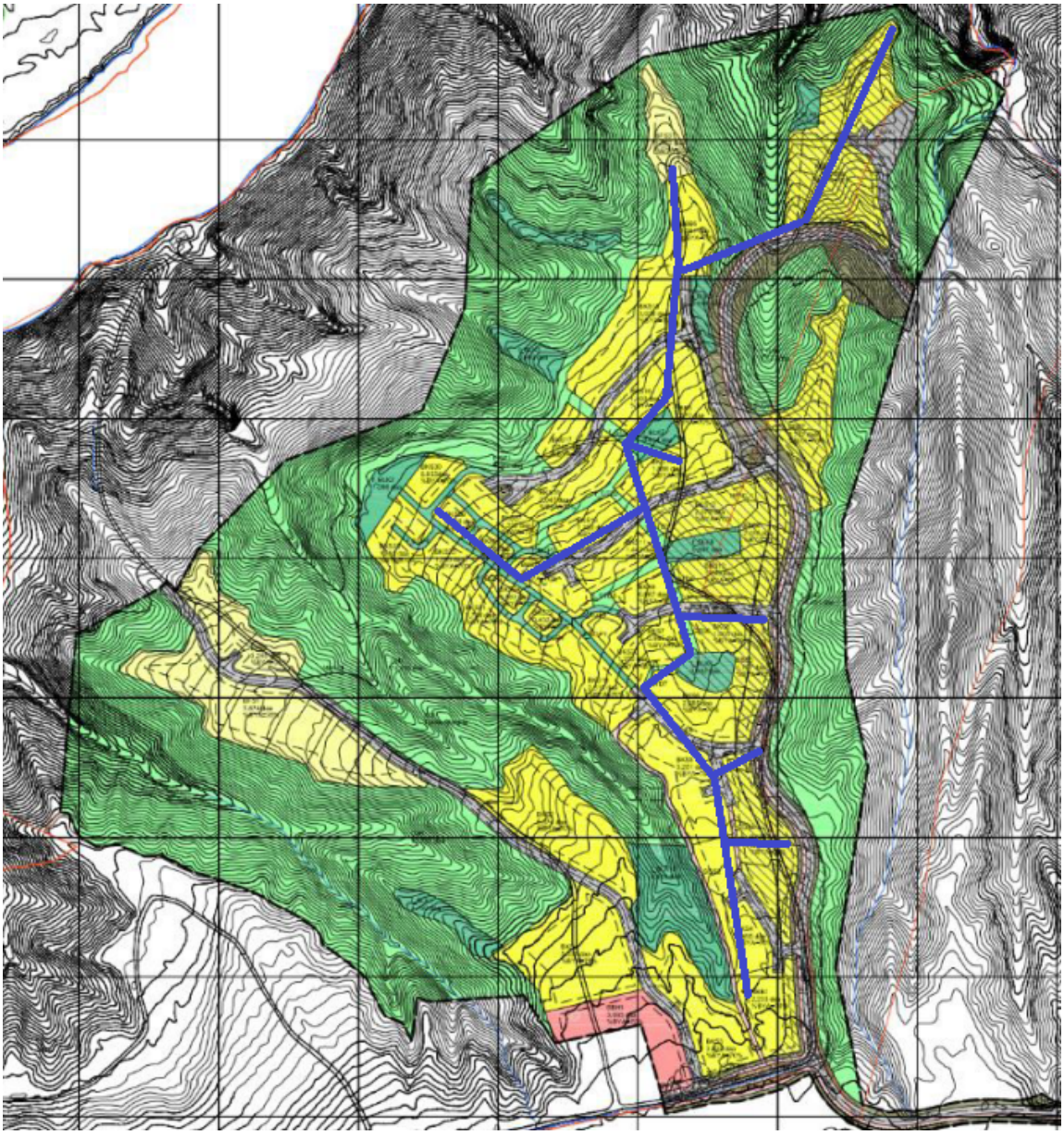

Figure 20: Heating network in Tanberghøgda.

Figure 20 shows a possible heating network in Tanberghøgda, with a total length of approximately 2 000 meters. The ΔT will be used in equation 2.10 together with the heat demand, $\rho = 1\,000\,kg/m^3$, and $c_p = 4.2\ kJ/kgK$ to calculate the volume flow for each hour.

The total pressure drop can be calculated using equation 2.7, assuming $R = 200\ Pa/m$, $\Delta p_{AB} = 50\,000\ Pa$, $\Delta p_W = 75\,000\ Pa$ and $L = 2\,000\ m$.

The pressure loss and volume flow can be used to calculate the pump power with equation 2.6. Finally, the cost of electricity, together with the pump power, dictates the cost of using the circulation pump, as described in equation 2.5.

The costs for the heat production for district heating and on-site heat production is calculated using the heat delivered, with the distinct costs. For the on-site heat production, the cost of bio fuel must be used. For the district heating, the cost is 4% lower than the spot price of electricity. These equations are described in equations 2.14 and 2.16.

4.2.6 Electric Vehicles and Combined Load

There are 342 homes in Tanberghøgda in phase two, as shown in figure 10. 2032 pertains to the examined time frame. All new passenger vehicle production after 2025 must be emission-free. The majority of automobiles at Tanberghøgda are therefore electric vehicles. According to the report *Reisevaner I Ringeriksregionen 2013/14*, the average number of cars per household in Ringerike municipality is 1.64 [63]. Combined with the anticipated 70% EV participation, this resulted in a total of 390 electric vehicles. According to SSB data from March 25. 2022, approximately 16% of all passenger cars in Norway are electric vehicles [64]. However, the new law will increase the proportion of electric vehicles in the coming years. The EV connection schedule depicted in figure 21 is based on EV distribution, as a part of the NTNU course "TET4135 Energy Planning". The data represents the number of EV's connecting at each hour for a 24 hour period.

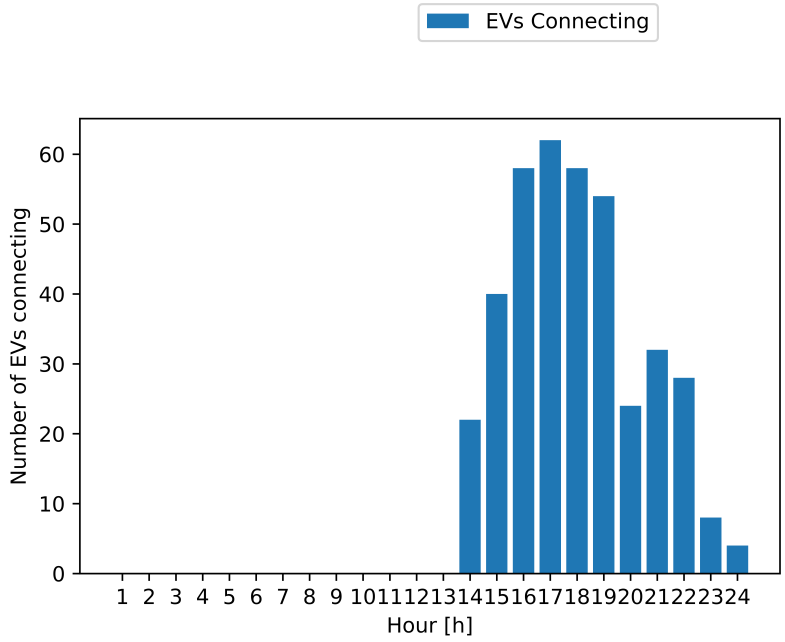

Figure 21: Connection schedule for the 390 electric vehicles at Tanberghøgda.

When examining the figure above, it is clear that the vehicles begin to connect at 14:00. After that, a peak occurs at 17:00, when the majority of people with normal hours return from work. There is a second, smaller peak at 21:00, which corresponds to residents possibly returning from late errands. The daily total of new connections equals the number of EVs in the area.

The charging demand could be calculated using the connection schedule. Using data from the report *Reisevaner I Ringeriksregionen 2013/14*, and assuming slightly more than two average trips per car between charging sessions, a use of 47 km could be used [63]. In addition, an average consumption of 0.215 kWh/km [65] could be used to calculate an energy requirement of 10 kWh per car, This amounts to 3 900 kWh. The cars are assumed to connect every other day. Any additional charging is assumed to occur at commercial chargers or at the residents' place of employment.

The EV schedule and subsequent load of 3 900 kWh can be compared to the housing electric load during the winter of 4 977 kWh in figure 22 . Figure 23 shows spot prices for all four seasons, for both 2020 and 2021.

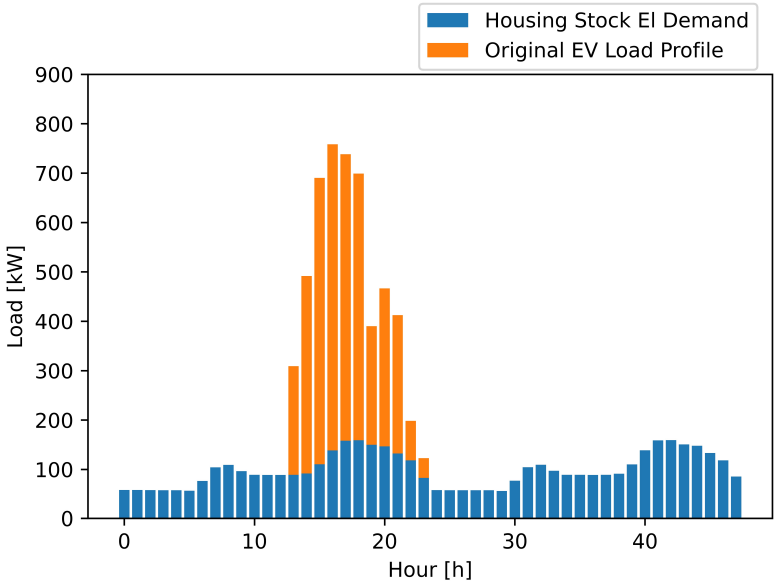

Figure 22: Housing stock and EV-demand.

The EV and housing stock load profile can be seen in figure 22. Evidently, the connection of the EVs produce a significant peak of approximately 800 kW. EVs account for 3 900 kWh of the yearly total. The large share of EV-charging is reasonable given that the electric demand for the homes is for appliances, lights and other miscellaneous demands, and not heating (except for the detached homes).

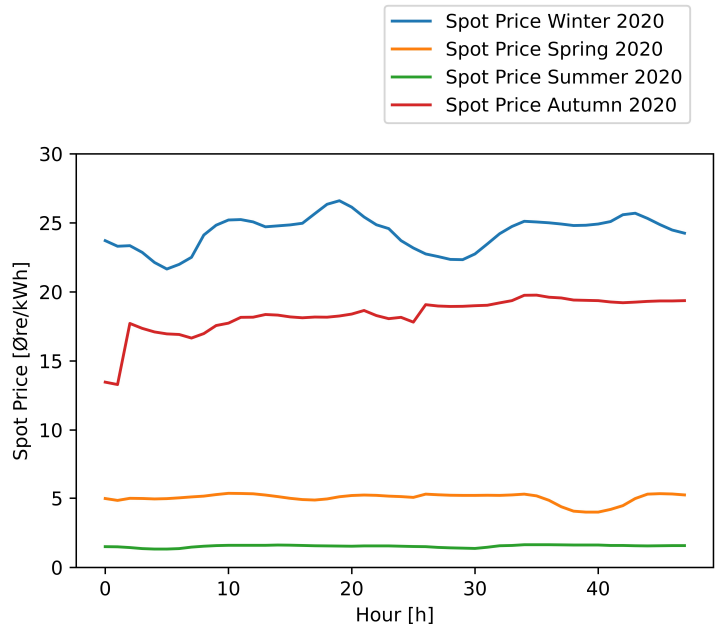

(a) Spot prices for 2020

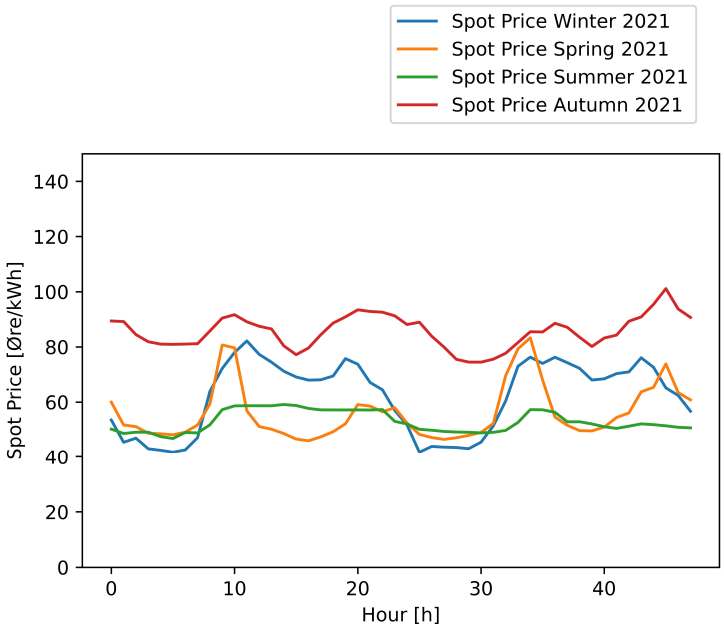

(b) Spot prices for 2021

Figure 23: Spot prices for all four seasons during 2020 and 2021.

Figure 23 displays the spot prices for a 48 hour period for all four seasons for 2020 and 2021. The 2020 data expectedly shows increased price levels for the winter and autumn periods, while the summer and spring periods have a much lower price level. The 2021 data holds a much higher price for all seasons, with the autumn set having the highest price of all. This can be seen in figure 24

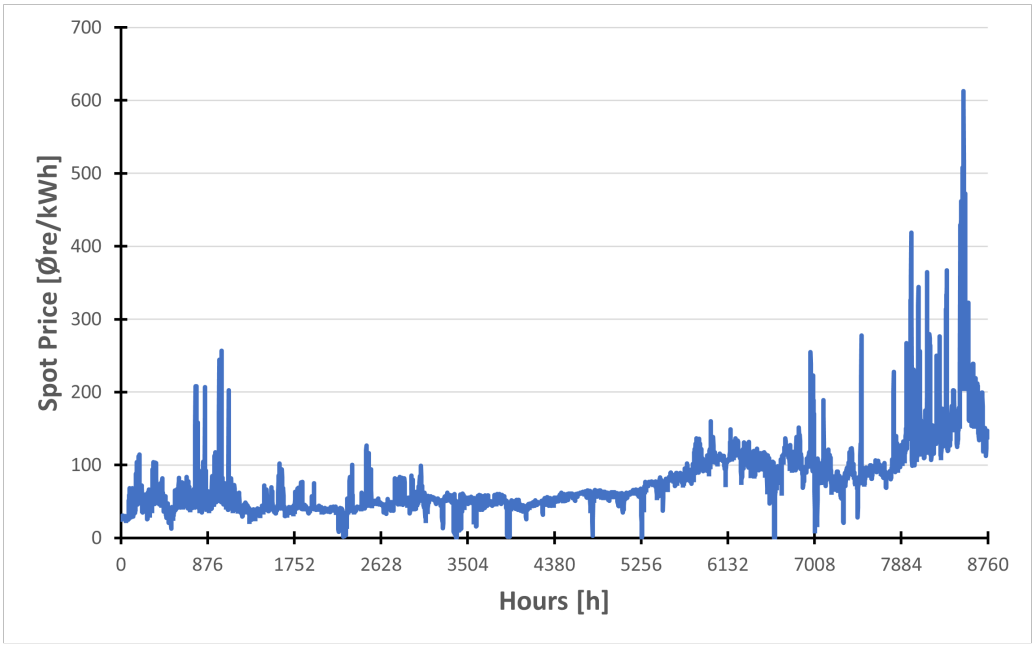

Figure 24: Spot price data for the entire year of 2021.

The increasing price levels in 2021 was caused mainly by increased gas and coal prices in Europe, along with increased prices for emission allowances in the EU emissions trading system [66].

4.3 Method to Calculate Energy Needs and Costs During the Construction Period

4.3.1 PV and Batteries

During construction, it is optimal for the PV system and battery to supply as much of the total capacity as possible. The capacity of the PV system is 500 kWp, while the maximum capacity of the battery is 1 MWh. This combination enables solar energy to be stored in the battery so that excess energy can be utilized on days when the construction site generates more solar energy than it requires. This model prohibits the use of batteries for flexibility sales/purchases, but permits the direct sale of excess PV system power. This model is focused on serving the construction's own load at all times, and as a result, the interaction with the external grid is limited to ensure that power is always available for the heavy construction equipment, as well as significantly reducing the strain on the external grid through decreased peak power demand and decreased purchasing/selling based on spot price. The battery is described as follows in the code for the inspection of emission-free construction sites:

$$\mathbf{AB[t] = AB[t\text{-}1] + (PV\ \ prod[t\text{-}1] - EC[t\text{-}1])} \tag{4.1}$$

- `AB` : Available Battery
- `EC` : Energy Consumption

Where **AB[t]** is the available battery at the start of hour t. The battery has a maximum capacity of 1 MWh and a minimum capacity of 0 MWh. Equation 4.1 shows that the battery will be fully charged if the PV production is greater than the energy consumption in hour t, and vice versa if the energy consumption is less than the PV production. Therefore, the battery level at any given time depends on the amount of available solar energy and the stage of construction. As shown in table 11, the energy consumption during the internal work phase will be significantly lower than that of the foundation phase.

The energy consumption in equation 4.1 is entirely based on the charging of the machines utilized during the present construction phase. Therefore there is no energy consumption when the machines are in operation. During lunch, energy consumption equals the sum of maximum charging power for machines with two daily charging cycles. In addition, it is presumed that employees have every weekend off, so the energy consumption is zero from the time the machines are fully charged at the end of business hours on Friday until lunch on Monday. This estimate does not account for the energy required to heat barracks and offices, charge electric tools, and perform other electricity-dependent activities on a construction site. The user-friendliness of the designed model is one of its characteristics. Due to the model's simplicity, it is easily adaptable to a year's worth of iterations. As a result, it may take advantage of the easily accessible vast quantities of data regarding PV production and spot pricing.

4.3.2 Costs of Buying Power During the Construction Phase

Throughout the hours of the year when the PV production and battery level are less than the energy consumption, it is necessary to purchase electricity in order to maintain operation. Alternatively, it will be possible to sell excess energy during hours of the year when PV production and battery demand are so high that you have excess energy even after the battery's maximum capacity has been reached and your energy needs have been met. The costs vary based on the hourly spot price and the amount of electricity required. During the winter groundwork phase, for instance, costs will be high due to high demand and limited solar production.

Under specific conditions, surplus energy can be sold back to the grid. The price at which the power suppliers purchase electricity is less than the hourly spot price. This is accounted for in the model by multiplying the spot price by 0.5 when selling electricity. The model [67] also takes into account the 100 kW per hour transmission limit to the electricity grid. This means you risk having surplus energy that you cannot use to cover loads or sell back to the grid. Considered are only the costs associated with the procurement and sale of electricity. Materials, transportation, equipment rental, etc. are not included.

The heating demand to achieve the desired internal temperature in the buildings is based on a MatLab script from an NTNU Master Thesis addressing energy supply for zero emission construction site (reproduced with permission) [61]. Local weather data for Hønefoss are retrieved from the Norwegian Climate Service Center and exported to Excel [68]. The MatLab script analyzes the Excel file data and calculates the heating demand required to achieve the desired interior temperature of $15°C$. The building envelope area and building volume are scaled up with regards to the total area of the total building area of the housing stock. All remaining parameters are unchanged. As a biomass boiler powered by pellets is intended to be installed in the early phases of construction, it is anticipated that the boiler will meet the heating requirements during the internal phase.

4.3.3 Model Outline of Python Code for Electric Energy Use During Construction

A Python model was created to determine the total cost of electric energy use during the construction phase. The model employs PV-production data, spot price, and energy demand for the various construction phases. A yearly load profile could be created using this information. Figure 25 illustrates the general outline of the model's decision-making process.

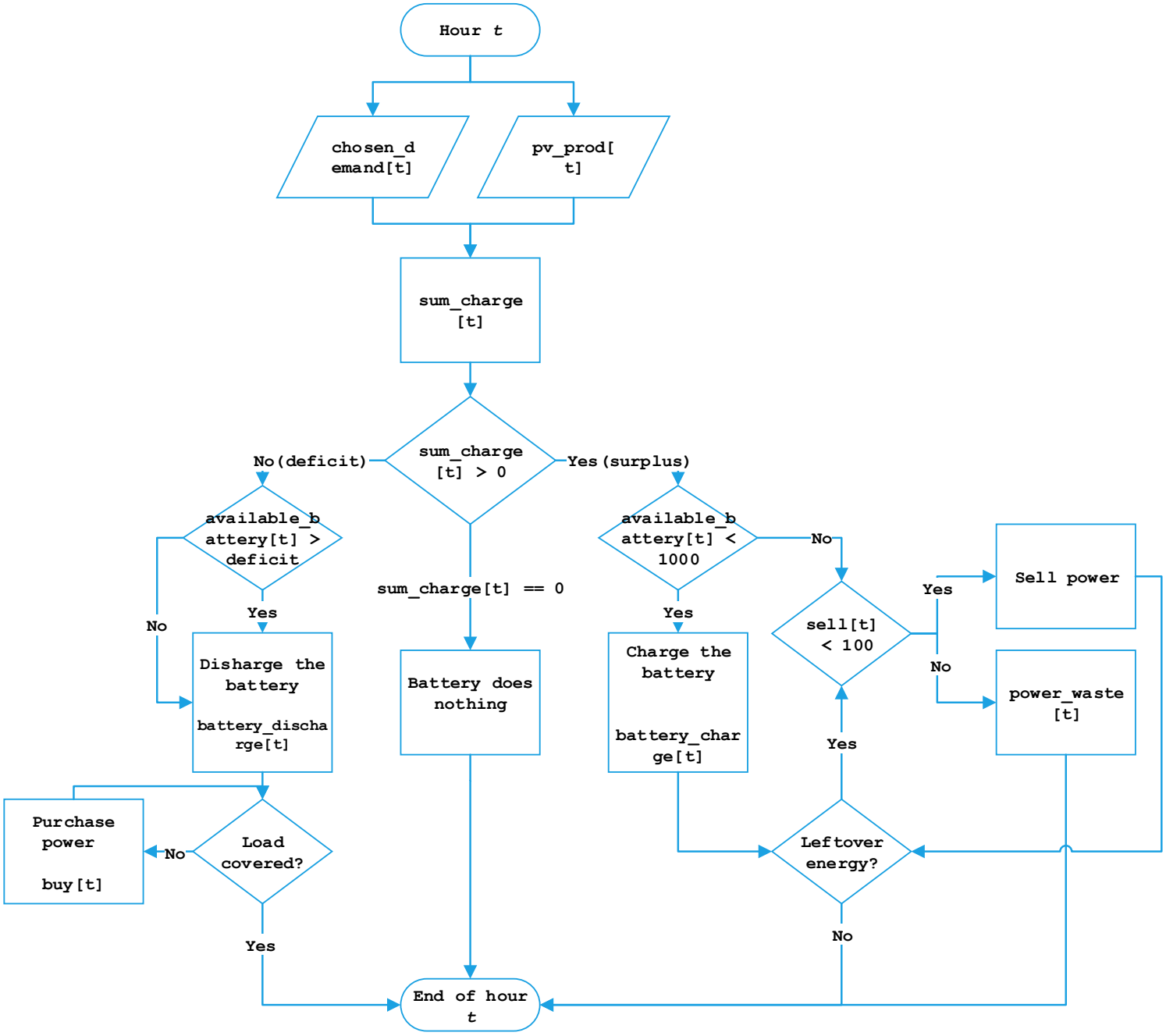

Figure 25: Flowchart of the model for construction phase energy use.

Parameters

- `chosen_demand[t]` : The chosen demand model of the different phases of construction.
- `pv_prod[t]` : Hourly PV production for the area.
- `sum_charge[t] =pv_prod[t]-chosen_demand[t]`
- `deficit[t]` : All negative values of `sum_charge[t]`, denotes a power deficit.
- `surplus[t]` : All positive values of `sum_charge[t]`, denotes a power surplus.
- `available_battery[t]` : Available battery in beginning of hour *t*.
- `battery_charge[t]` : Amount charged each hour.
- `battery_discharge[t]` : Amount discharged each hour.
- `buy[t]` : Amount bought for each hour.
- `sell[t]` : Amount sold for each hour.
- `power_waste[t]` : Amount of power gone to waste each hour, i.e leftover power after the battery has been charged, and the transmission cap is reached in regards to selling.

As previously stated, the model's decision-making starting point is `sum charge[t]`. Every hour, this variable is evaluated to determine whether the system is in deficit or surplus. If a surplus is discovered, demand has already been satisfied; therefore, the battery has priority. If there is excess power, the next step is to sell it to the external grid. Limitations apply to both the battery and power sales to the external grid. Any remaining energy after this point is therefore useless and will be wasted. The end of the hour *t* is reached after the charging, selling, and power waste phases.

In contrast, if a battery shortage is detected, the first action is to maximize battery usage. If capacity exceeds demand, no additional action is necessary. Alternatively, power will be purchased from the external grid at the spot price if the battery is unable to meet all of the demand.

If `sum charge[t] = 0`, then all demands have been satisfied and no further action is necessary. The remaining battery capacity will be carried over to the next hour.

4.3.4 Construction Models' Limitations

Several limitations apply to the model. The region's demand is the model's top priority. Consequently, the algorithm is not cost-optimized. The battery will not delay using stored energy regardless of future spot pricing; as a result, the associated cost will be greater than if a cost-minimization algorithm had been implemented. In addition, the battery only receives power from PV production and does not sell energy to the grid; all sales are directly derived from an excess of PV production in the same hour it is created. Due to its ability to sell during periods of high spot price, a battery that sells to the grid could further reduce costs.

In addition, if the battery could import energy from the grid, it would be possible to acquire and store energy at a low cost for later use or sale. The simplifications regarding other areas of energy consumption, such as the barracks, and the lack of energy consumption on weekends contribute to a likely reduction in the total energy consumption estimate. The model does not account for grid-imposed transmission costs. A portion of the battery's behavior is irrational due to the low spot price for surplus power. Taking into account the transmission grid fee, the model would not sell

power if grid costs exceeded selling profit.

Other battery-related considerations also apply, as explained in greater detail on page 66 in Section 4.5.4. The general limitations of the presumed known data, as described in the same section, also apply.

4.4 Method to Calculate Costs Related to the Heating Demand

4.4.1 Pump Costs

The pump costs calculations are based on the main equation 2.5, where all the remaining variables are obtained using equations 2.6 - 2.12. As further explained in Section 4.4.4, the calculations are completed with variable efficiencies. The total pump costs for each case is presented in table 17. The investment cost for parts, installment of the piping network and bio-fueled boiler is estimated to be around 40-50 øre/kWh, according to consultation with *Fossen Utvikling* .

4.4.2 On-Site Heat Production

On-site heat production meets the heating demand using a pellet fueled boiler operated by *Fossen Utvikling*. As explained in the concept investigation conducted by *COWI*, a possible solution is implementing a 300 kW boiler for the first stage of development, followed by a 800 kW boiler for the second stage of development. In turn this means the housing area will have a 1100 kW heating capacity when completed [3]. Looking at the boiler as an investment, *Fossen Utvikling AS* desires a 10% yearly return on the investment. The investment and operational costs related to the boiler must therefore be taken into account.

4.4.3 District Heating

Another option to meet the heating demand in Tanberghøgda is connecting to the existing district heating network in Hønefoss. By opting for this solution, *Fossen Utvikling AS* is no longer responsible for the deliverance of heat to the housing area. Regardless of which heating source is chosen, the developers must implement a piping system locally in the housing area in order to distribute the heat to each housing unit. In addition, the developer will install a heat exchanger to transfer heat from the district heating network to the local piping network. By utilizing the existing district heating system, *Fossen Utvikling AS* avoid investment and operational costs related to the boiler. In turn this also means the loss of potential revenue selling self-produced heat to the housing area.

4.4.4 Boiler Efficiencies

Equation 2.14 can be utilized to calculate the total costs associated with on-site heat production. The efficiency of the boiler is variable, subject to pressure losses due to friction and turbulence. Though the make and model of the pellet fueled bio-boiler is unclear, literature and industry standards provide a foundation for further calculations. Variable efficiencies are analyzed, and a set of cases is created in order to observe trends and changes in total cost depending on the efficiencies. According to the Norwegian Standard NS-EN303-5:2022, the minimum requirement for efficiency for boilers over 300 kW is 82% [69]. This forms the lower limit for the efficiencies that are to be tested.

To continue, the upper limit is determined by analyzing literature on pellet fueled boilers. According to research conducted on boiler efficiencies and emissions for different types of pellets as fuel, an upper limit of 93.8% efficiency was achieved [70]. As presented in Section 2.6.2, additional literature suggest a possible combustion efficiency of 90% or higher in modern pellet-fueled boilers.

As *Fossen Utvikling* is aiming for Tanberghøgda to be a pioneer in regards to low energy consumption and modern solutions, it can be assumed that the installed boilers are modern and are able to achieve high efficiencies. Therefore an upper limit of 94% efficiency is set. With a lower and upper limit to the boiler efficiency in place, a cost analysis using different efficiencies in the defined range can be conducted. The broad span of efficiencies enables room for reflection on the impact on total costs for the on-site heat production. The cost calculations with variable efficiency is presented in Section 5.2.1.

4.5 Optimal Electricity Use After Completion of Construction

As the construction phase comes to a close, the area's load profile will separate into two distinct areas. From simulations, an assumed inelastic electric load profile will be assigned to the housing mass. The housing stock will be referred to as area 2. Area 1 will be comprised of the PV system, the circulation pump, and EV charging. The latter of these is adjustable, however all vehicles must have completed charging by 08:00 the day after being connected. These areas are separate, and for the base case, can not exchange power. This is explained by the fact that, at the time of writing, electricity can not be shared between two different energy meters. However, this can change in the future [71]. Therefore, the decision was made to separate into two cases, one for the current situation of no power sharing between the meters, and one case including power sharing. The relationship between the two areas, and their potential power exchange, can be seen in figure 26:

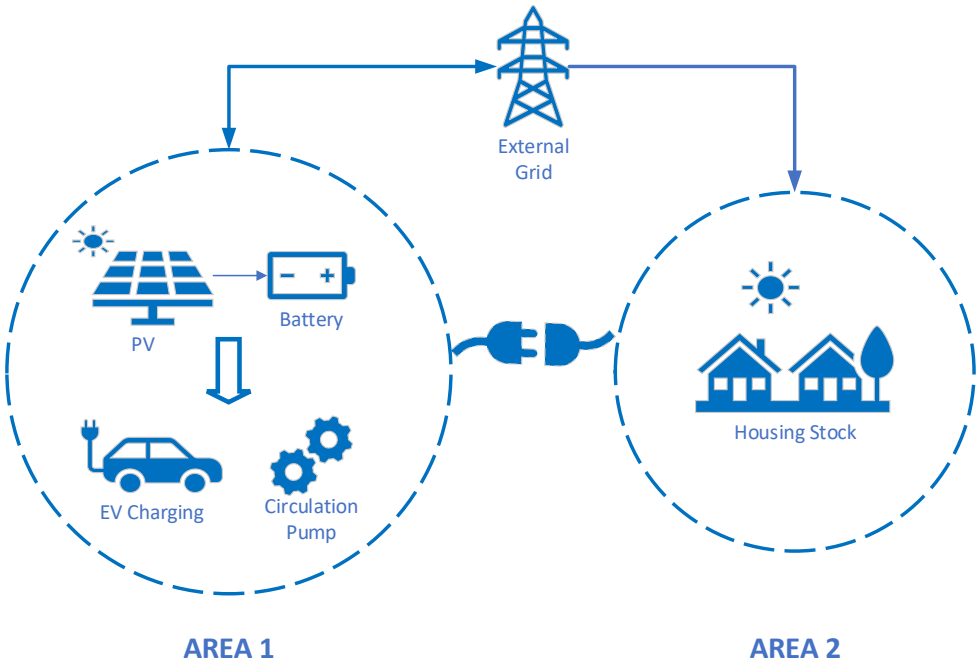

Figure 26: The relationship between the two separate areas and their potential connection.

In area 1, the number of electric vehicles is assumed to be 390, with an energy demand of 10 kWh per vehicle per charge. The load for area 1 can be served by power purchased from the grid at spot price. The data on spot prices is taken from *NordPool* [72]. Additionally, the PV-system combined with the battery can serve the load. This system can also sell power back to the grid, at a certain fraction of the spot price. However this transmission capacity is limited to 100 kW. Figure 27 is

relevant for comprehending the model's overall structure.

4.5.1 Model description

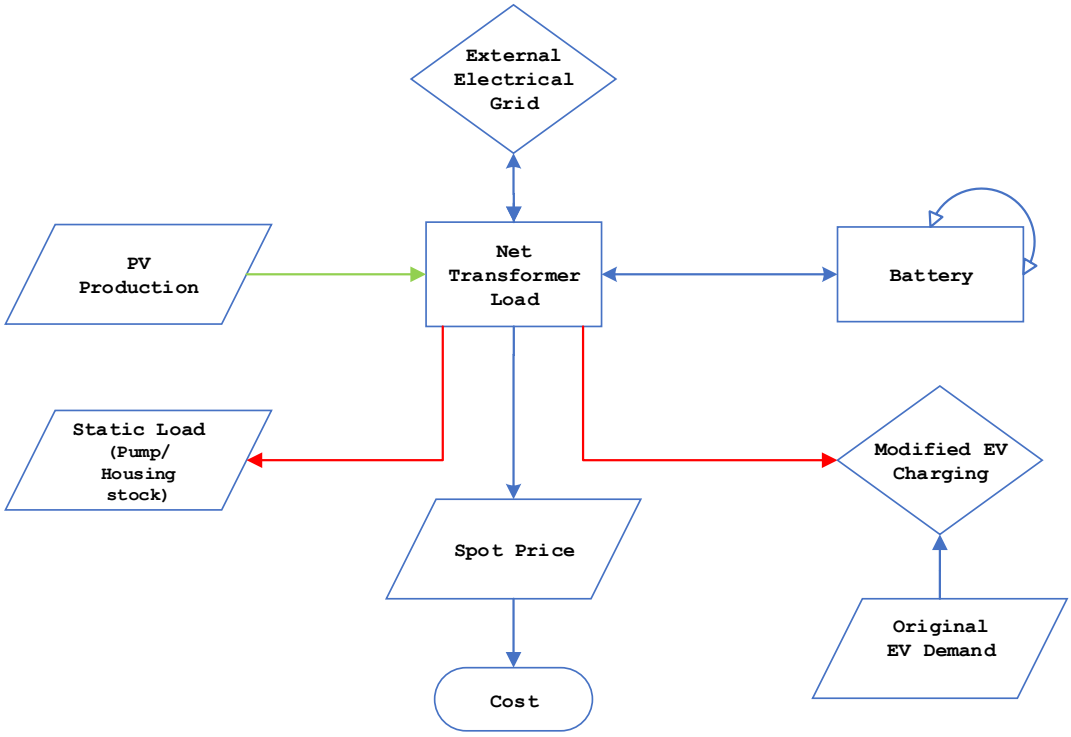

Figure 27: Flow chart visualizing the basic ideas of the model. note that variables are presented with the diamond shape, constants with the parallelogram, and balance equations with the square. All connections are direction-specific, and are highlighted as such with the arrows.

The net transformer load is crucial to the model. As the cost is determined by multiplying the net transformer load by various spot prices, any algorithm will effectively minimize the net transformer load because the spot price is a collection of fixed numbers that cannot be influenced by the decision variable. In addition, the net transformer load is constrained by a positive capacity constraint that can be set to any power level. This constraint is essential because it determines the intended peak power reduction level. Applying the capacity constraint to the net transformer load model allows for unrestricted power levels within the model as long as the ultimate value connected to the external grid falls within the acceptable range. As PV-to-battery power is exempt from net transformer load in equation 4.2 and discharge is a negative term, this is advantageous as it encourages active battery

utilization. Since there are no transmission efficiencies, the battery is subject to a capacity constraint imposed by the grid. This is to ensure that the battery cannot be entirely charged and discharged every hour and a half in order to generate marginal profits from selling power to the grid. This term will be discussed in greater depth in the result section.

The connectivity between nodes is represented by their connection to the net transformer load; this is possible because each node is connected to the node in issue. Similarly, the battery is an essential component of the model; in fact, the battery and the net transformer load are the two balance equations for the model.

$$\textbf{NTL = Load + Mod EV Charging - PVTG - BD + GTB} \tag{4.2}$$

$$\textbf{Battery[t] = Battery[t-1] + BC[t-1] - BD[t-1]} \tag{4.3}$$

Where:

- `Net Transformer Load : NTL`
- `Modified EV Charging : Mod EV Charging`
- `PV to Grid : PVTG`
- `Battery Discharge : BD`
- `Battery Charge : BC`
- `Grid to Battery : GTB`

As can bee seen in equation 4.3, the battery can be charged by the external power grid and the PV system. The charge is subsequently carried forward from one time phase to the next. As with the previous model used to calculate energy demands and costs during the construction period as described in Section 4.3 on page 51, the state of the battery at time step t signifies the start of hour t. According to the equation 4.2, the discharge contributes to the net transformer load and can therefore serve any load by reducing the total sum. The loads in this model is the EV charging, together with the circulation pump. For the case analysis allowing the exchange of power between area 1 and area 2, the housing stock will be added as an inflexible load. The latter load, together with the pump load are both static loads, denoted as such in both figure 27 and 28. As they are both constant, they are treated the same inside the model.

If the net transformer load becomes negative, the battery, or the PV system, can sell power back to the external grid at 50% of the current spot price. This is possible through the creation of two separate `net_transformer_load` variables, one containing only positive values, and one containing only negative values.

To further illustrate the individual connections between the nodes, figure 28 can be studied.

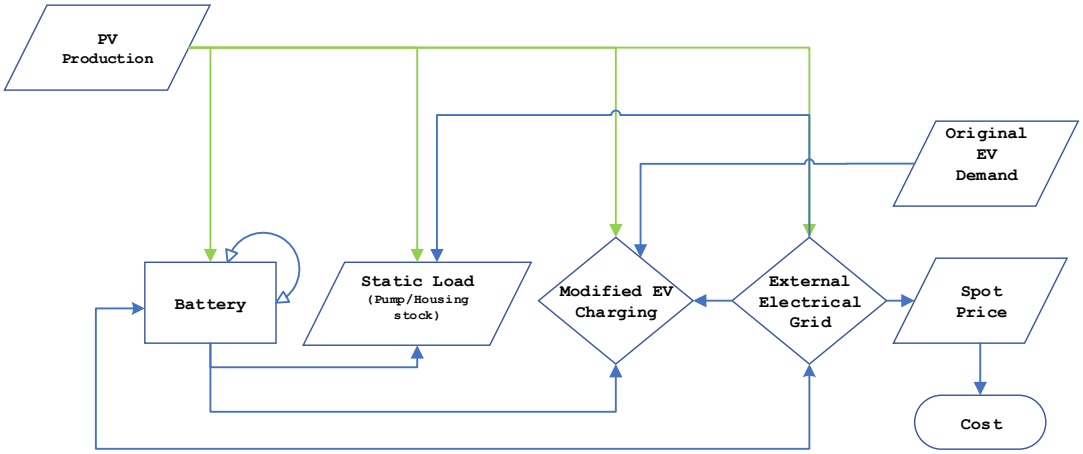

Figure 28: Flow chart visualizing the individual connections between the nodes in the system.

Despite their complexity, the diagrams represent every component of the system. The most valuable lessons are how PV and batteries can supply system loads and sell power to the grid. In addition, the cost function is essentially a product of the external grid. As previously stated, a deficit necessitates the procurement of power, while a surplus may under certain conditions be sold back to the grid.

To accommodate the increased number of factors, it was determined that external software would be used to model the system. This issue can be formulated as a MILP problem with a cost-minimization objective function. To resolve this issue, it was determined to use a combination of two software applications. *Pyomo* is used to structure the functions and constraints, while *Gurobi* determines the optimal solution.

4.5.2 Formulation of the MILP Problem

The model starts with defining three separate models concerning the time-steps:

$$t \epsilon \{0, 48\}$$
$$t_1 \epsilon \{1, 48\}$$
$$c \epsilon \{0, 32\}$$

Due to the system's complexity and the various time-binding models, this model is optimized for a period of 48 hours. Consequently, model *t* covers the entire time frame for which the issue will be resolved. Model t_1 covers the same time period, but its index begins at one rather than zero. This is necessary because several of the constraints use *t-1* indexing, so the following would happen: $t = 0 \Rightarrow [0 - 1]$, this is an error because *Gurobi* and *Pyomo* prohibits indexing element -1 of a model or variable. The final model, *c*, indicates the period of time during which all EV charging must be completed; 32 hours corresponds to 08:00 on the second day. The electric vehicles were added as

connecting only during the initial 24 hours. As discussed in Section 4.2.6 on page 46, the electric vehicles can be assumed to connect every other day. This is also beneficial for the model, as it can operate with a single endpoint for all charging, which significantly simplifies the operation.

Constants

- `Load` : Hourly load profile [kW] for the buildings and/or circulation pump in time period t. Assumed to be completely inelastic.
- `Number_of_EVs_connecting` : Data showing number of EVs connecting in every hour of time period t.
- `Original_EV_demand` : Hourly data of EV charging demand[kW] corresponding to the original EV connection schedule
- `Spot_price` : Spot price [NOK/kWh] for every hour in time period t.
- `PV_Prod` : Hourly production data [kW] for the PV system in time period t.
- `Total_charge_need` : Sum of EVs that connect through the entirety of the time period t, multiplied by the assumed level of charge
- `Transformer_capacity` : Constant capacity constraint of 400 kW to ensure that the grid does not get overloaded.

Variables

- `net_transformer_load` : Net sum of power [kW] demand for the system for each hour in time period *t*. A positive value denotes the need to purchase power from the grid, conversely, a negative value signifies the opportunity to sell power to the grid.
- `positive_transformer_load` : All positive values from the `net_transformer_load` variable, all other values are zero. Used for calculating cost of buying power.
- `negative_transformer_load` : All negative values from the `net_transformer_load` variable, all other values are zero. Used for calculating gain of selling power.
- `pvtogrid` : Amount of power [kW] from the PV-system that is dispatched for direct consumption for each hour in time period *t*.
- `charged` : Load profile for EV-charging after the allowed delays have been implemented in accordance to the optimal solution. Given as [kW] for each hour in time period *c* .
- `batteryCharge` : Power [kW] dispatched to the battery for each hour of time period *t*.
- `batteryDischarge` : Power [kW] dispatched from the battery for each hour of time period *t*.
- `batteryLevel` : Available power in [kWh] for the battery. Values are assigned for the beginning of each hour in time period.
- `gridToBattery` : Power [kW] dispatched to the battery from the external grid, purchased at spot price for every hour in time period *t*. Set to 500kW.
- `pvtowaste` : Power [kW] that can not be utilized due to constraints on selling and consumption.
- $x_d :\in \{0, 1\}$: Binary decision variable for discharging the battery, for time period t_1. If discharging takes place, the corresponding $x_d = 1$, for all other cases $x_d = 0$.
- $x_c :\in \{0, 1\}$: Binary decision variable for charging the battery, for time period t_1. If charging takes place, the corresponding $x_c = 1$, for all other cases $x_c = 0$.

Abbreviations

- `net_transformer_load : NTL`
- `positive_transformer_load : PTL`
- `negative_transformer_load : NeTL`
- `pvtogrid : PVTG`
- `charged : C`
- `batteryCharge : BC`
- `batteryDischarge : BD`
- `batteryLevel : BL`
- `Load : L`
- `Original_EV_demand : OEVD`
- `Spot_price : SP`
- `PV_Prod : PV`
- `pvtogrid : PVTG`
- `pvtowaste : PVTW`

- gridToBattery : GTB
- Total_charge_need : TCN
- Transformer_capacity : TC

Mathematical Formulation

$$\text{minimize} \quad \sum_{i=0}^{t} \texttt{PTL[i]} \cdot \texttt{SP[i]} + \sum_{i=0}^{t} \texttt{0.5} \cdot \texttt{NeTL[i]} \cdot \texttt{SP[i]}$$

subject to:

(**1**)	TCN	$= \sum_{i=0}^{c} \texttt{C}$	$i = 0, \ldots, c$
(**2**)	TCN	$= \sum_{i=0}^{t} \texttt{C}$	$i = 0, \ldots, t$
(**3**)	C[i]	$\leq \sum_{i=0}^{i} \texttt{OEVD} - \sum_{i=0}^{i} \texttt{C}$	$i = 0, \ldots, c$
(**4**)	NTL[i]	$\leq$ TC	$i = 0, \ldots, t$
(**5**)	BD[i]	$\leq$ BL[i]	$i = 0, \ldots, t_1$
(**6**)	x_d[i] + x_c[i]	≤ 1	$i = 0, \ldots, t_1$
(**7**)	BL[i]	= BL[i-1] +BC[i-1] - BD[i-1] + GTB[i-1]	$i = 1, \ldots, t_1$
(**8**)	NTL[i]	= L[i] + C[i] - PVTG[i] - BD[i] + GTB[i]	$i = 0, \ldots, t$
(**9**)	PTL[i] + NeTL[i]	= NTL[i]	$i = 0, \ldots, t$
(**10**)	PTL[i] $\cdot$ NeTL[i]	= 0	$i = 0, \ldots, t$
(**11**)	BC[i] + PVTG[i] +PVTW[i]	= PV[i]	$i = 0, \ldots, t$
(**12**)	BL[0]	$= 1000$	
(**13**)	TC	$= 400$	
(**14**)	BL[i]	≤ 1000	$i = 0, \ldots, t_1$
(**15**)	GTB[i]	≤ 500	$i = 0, \ldots, t_1$
(**16**)	NTL[i]	≥ -100	$i = 0, \ldots, t$
(**17**)	PTL[i]	$\geq$ 0	$i = 0, \ldots, t$
(**18**)	NeTL[i]	$\leq$ 0	$i = 0, \ldots, t$
(**19**)	BL[i]	$\in \{0, 1000\}$	
(**20**)	x_d,x_c	$\in \{0, 1\}$	
(**21**)	C[i], PVTG[i]	≥ 0	$i = 0, \ldots, t$
(**21**)	BC[i], BD[i]	≥ 0	$i = 0, \ldots, t$
(**21**)	GTB[i], PVTW[i]	≥ 0	$i = 0, \ldots, t$

4.5.3 MILP Problem Explanation

Presented below is a brief explanation of the objective function and constraints from the mathematical formulation of the problem.

- **Objective function**: As previously described in Section 4.5.1, the cost function is a product of the external grid. As such, the sum of the power that is purchased is multiplied by the spot price, to obtain the cost of purchased power. After which the gain of selling power, obtained by multiplying the spot price, the surplus power, and a factor of one half, is added. The data

set containing the sale of power is negative, thereof the addition in the objective function.

- **Constraint (1)**: Ensures that the sum of the amount charged during time period *c* equals the total charge need.
- **Constraint (2)**: Ensures that the sum of the amount charged during time period *t* equals the total charge need.
- **Constraint (3)**: The amount of charging per hour must be less than the total charge needed for all connected vehicles through hour t, minus the total amount already charged.
- **Constraint (4)**: Ensures the integrity of the transformer capacity.
- **Constraint (5)**: The battery can not discharge more power than it already has in the beginning of hour *t*
- **Constraint (6)**: The sum of binary decision variables for the act of charging or discharging the battery must be less than or equal to one. Ensuring that the battery can not both charge and discharge at the same time.
- **Constraint (7)**: As previously discussed in equation 4.3 the battery level in the current hour must be equal to the battery level of the previous hour, plus the charge from both the PV system and the external grid, minus the battery discharge.
- **Constraint (8)**: As discussed in equation 4.2, the net transformer load equals the sum of the load, EV charging, and battery charging from the external grid, minus the battery discharge, and spare power from the PV system.
- **Constraint (9)**: Ensures that the positive and negative subvariables of the net transformer load equal the net transformer load.
- **Constraint (10)**: Makes sure that one of the elements from either positive or negative transformer load must be equal to zero. Therefore the product of the two must be equal to zero. Combined with the previous constraint, the net transformer load is split into two variables that are negative and positive, and only one of them can hold a value at each time step.
- **Constraint (11)**: Balance equation for the PV system. Power produced from the system must be used for either battery charging, sold to the grid, or wasted.
- **Constraint (12)**: Initial condition for the battery. With this value it starts fully charged.
- **Constraint (13)**: Sets the transformer capacity to whatever value is wanted. As previously discussed this value is paramount for reducing power peaks in the system.
- **Constraint (14)**: Battery level limit for all time steps, as the battery is 1000 MWh, the value is set to 1000.
- **Constraint (15)**: Limit for the allowed charge amount per hour from the grid to the battery. The value is set to 500 MWh.
- **Constraint (16)**:Limit for the negative transformer load. The value is set to 100 MW, which means sales from the combined system to the external grid can not exceed 100 MW.
- **Constraint (17)**: Positive transformer load can only be positive or zero.
- **Constraint (18)**:Negative transformer load can only be negative or zero.
- **Constraint (19)**: The battery level is between zero and 1000 MWh.
- **Constraint (20)**: Binary decision variables for the charging and discharging of the battery

can be one or zero.

- **Constraint (21)**: Variables set to be equal to or greater than zero.

4.5.4 MILP Problems Limitations

Despite its complexity, this model has limitations. The algorithm initially minimizes cost. Consequently, despite the application of a number of constraints, this model disregards a number of advantageous operational aspects. These characteristics are prevalent and present in every component of our combined system.

Battery

All discharge and charge efficiencies are disregarded, beginning with the battery; consequently, the battery is utilized more frequently. Especially when it provides a negligible benefit and would not otherwise be utilized in an efficient context. Additionally, as described in Section 2.3 on page 7, various battery technologies necessitate distinct usage patterns to ensure battery life. In this model, a LFP battery is assumed to be used. The usage pattern does not take into account the optimal discharge of this battery. Therefore, the battery can be thoroughly discharged multiple times in under 48 hours. This is optimal from a short-term cost standpoint, but not a long-term cost standpoint, as the battery would need to be replaced more frequently. Consequently, it may be advantageous for a more advanced model to include parameters indicating the battery's optimal operation.

EV-Model

Focusing on the EV-model reveals a number of limitations. The model initially has a fixed charging endpoint. This means that none of the respective vehicle users may expect their vehicle to be finished before 08:00 the morning following their connection. Some vehicles may be completed well ahead of schedule, but this cannot be anticipated. It would be preferable if the vehicles completed their charging by different set points, as not all usage patterns can be expected to be comparable. This applies to both individual consumers and various periods of the week, as the weekend charging pattern may vary. As indicated in Section 4.2.6, it is presumed that the amount of charge for all vehicles is identical. Obviously, this is an oversimplification, as the variety of electric vehicles and utilization patterns will dictate anything but a constant charge quantity. Therefore, it would be advantageous to implement a more advanced model in which individual vehicles possess characteristics such as required charge and acceptable charging window.

General Limitations

For the general model limits, it is assumed that all information is known before the best solution is discovered. For any real-world scenario where the model should be used to make decisions, this can be a challenge. The housing stock demand model can likely be based with a degree of accuracy using historical data. The EV-model is also somewhat predictable, though possibly not to the same degree as the demand for the housing stock. Day-ahead prices can be used to estimate the cost of electricity, and meteorological data can be used to predict PV production. Eventually, the model may employ predicted data, but then it would be susceptible to data fluctuations.

4.5.5 Scenario Description

Construction Phase Cases

In recent years, the spot prices have fluctuated significantly. Both spot prices for 2020 and 2021, as well as battery sizes for spot prices for 2020 and 2021, have been analyzed. Batteries with capacities of 0.5 MW, 1 MW, and 2 MW were tested in various scenarios. Originally, the size of the battery was 1 MW. Total cost for the entire construction phase was tested for the different scenarios.

Operational Phase Cases

In the operational phase base case, the PV system and battery will provide power for the circulation pump along with the EV-charging. On the flip side, the housing stock will need to purchase power from the external grid. This is due to the fact that electricity can not be shared between two different meters, as described in Section 4.5 and illustrated in figure 26. However, as there is a chance this may change in the future, an interconnection case will also be considered. In this scenario, the two areas will have an interconnection which will allow for unlimited power exchange, and thus allow the optimization algorithm to work with all loads. In this way, there are two scenarios, base case and the interconnection case. Both cases will be run for four seasons, winter, spring, summer, and autumn. Both cases need to have good grounds for comparison, both between them, and in between themselves for the different seasons. This is especially important as the optimization code only runs for a 48 hour period. Therefore it is paramount to choose an appropriate data set for spot prices. As can be seen in figure 23 on page 49, the spot prices for 2020 present more typical seasonal price patterns. Therefore it was chosen as the data set for all scenarios for the operational phase. To summarize, the base case and the connection case will be run for four seasons in 2020. Initial values for parameters are presented in Section 4.5.2.

5 Results

The results were based on three separate models: one for the construction phase, one for the operational phase that followed the construction phase, and one for heat supply. Various cases were analyzed using the methods described in chapter 4. The results are provided on an annual, weekly, and daily basis to illustrate how the numerous parameters and variables interacted.

5.1 Energy Requirements and Costs During the Construction Period

Based on the method presented in Section 4.3, a **Python** code was developed using technical data about electrical machinery, PV production data, and spot price data as inputs. The code generated diagrams of the battery level, PV production, and demand profile for the duration of the specified construction phase, as well as the cost or benefit of purchasing or selling electricity to the grid. Power was purchased and sold during the majority of the construction phases due to fluctuating demand and PV production. PV production was typically lower in the winter, and construction costs increase proportionally.

5.1.1 Simplifications and Assumptions

The most significant limitations are described in Section 4.3.4. Typically, some phases can be executed concurrently, but this code analyzed each phase individually and calculated the cost or gain for that specific time period. The duration of each phase varied, as shown in the Gantt chart in Section 3.3.

The number of charging hours must be an integer, as the model only considers complete hours. As stated in Section 3.2, it was assumed that the machines had a 20% battery level at the end of a workday. This buffer prevented machines from running out of power while performing crucial tasks and reduced battery wear. In addition, it was assumed that the battery was charged to 80-90% overnight instead of 100% to prevent battery wear, as described in the theory section of 2.3. It was assumed that construction workers have every weekend off, but holidays and vacations were considered work days.

As discussed in Section 3.2, the project has not progressed far enough to determine which machines will be used and how many machines will be needed for each construction phase. The technical information was based on a project that envisions an emission-free construction site [61]. The number of machines from this project was scaled up to match Tanberghøgda's larger development area.

The main calculations were based on spot prices from 2021. This was chosen as the main data set to produce the most relevant costs for the long periods which were present in this simulation.

Spot price data from 2020 was also used for comparison.

5.1.2 Groundwork Phase

The groundwork phase was the most machine-intensive phase, requiring a total of 15 excavators simultaneously, which resulted in a higher demand than other phases. Figure 29 showed the demand, available battery, and PV production.

The groundwork phase took place in January and February, as displayed in the *Gantt chart* in figure 8. The values on the x-axis in figure 29, ranging from 0 to 1 440, corresponded to the number of hours in January and February.

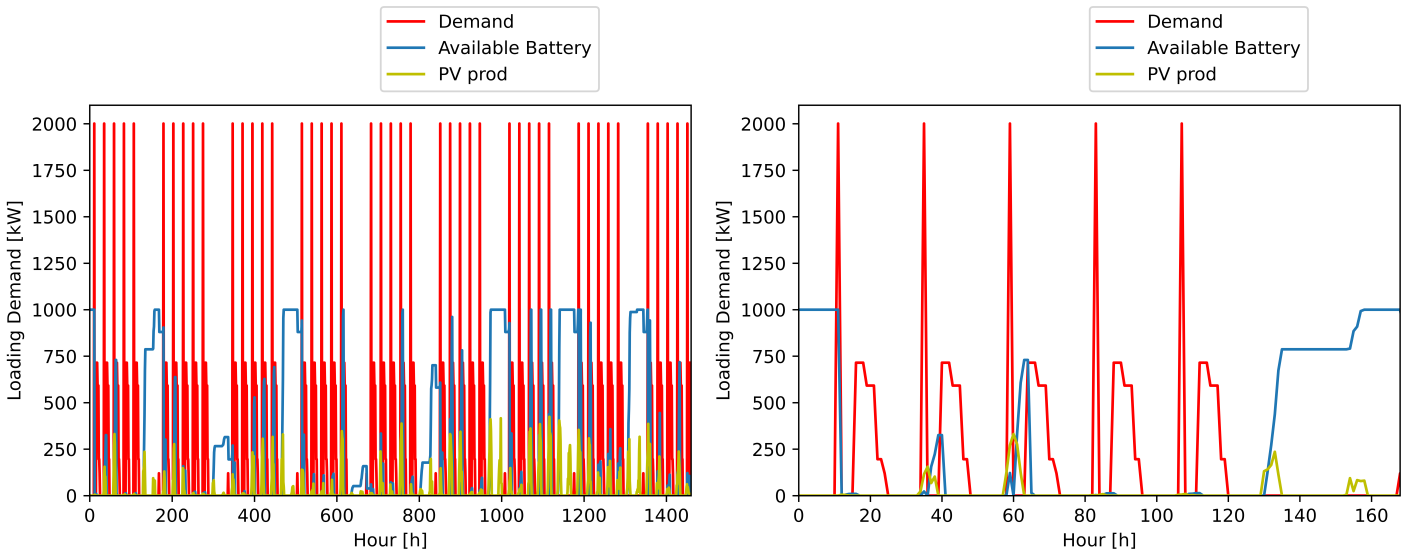

(a) 2 month period, winter

(b) 1 week

Figure 29: Groundwork in two different time frames.

As shown in figure 29, the demand reached 2 000 kW during each lunch break due to the construction equipment's high charging demand. The PV and battery had a maximum combined capacity of 1 500 kW, which resulted in inadequate coverage. Consequently, the system purchased power from the grid. The groundwork phase had a net cost of 134 728 NOK, which was comprised of a gain of 1 218 NOK from selling power to the grid and a cost of 135 946 NOK from purchasing power. The periods with no demand and 1 000 kW of available battery capacity occurred on weekends, when there was no activity. During the groundwork phase, there were a total of eight weekends, as represented in the graph. The available battery, which corresponded to the battery level at the

beginning of each hour, peaked on weekends when there was sufficient time to completely charge. This was evident when investigating one week of groundwork, as shown in the figure 29.

Since different machines had different charging requirements, as shown in figure 29, the demand gradually decreased as the evening progressed. Due to the limited hours of sunlight in Norway during the winter, PV production was zero for the majority of the day, and the first week of 2021 was particularly unlucky in terms of PV production. As this phase of construction was scheduled for January and February, the PV system was unable to sufficiently charge the battery, resulting in periods with no stored power available. This necessitated the purchase of power from the grid to meet charging demand at the end of the day. Nevertheless, the available battery was able to reach its 1 MW capacity over the weekend, when there was no demand and the PV generated 364.3 kWh over six hours of sunlight. This enabled the system to sell excess PV power back to the grid. As shown in figure 29, PV production over the weekend was especially low, which was reflected in the amount of power sold to the grid.

5.1.3 Building Phase

With a total duration of six months, the construction phase was the most time consuming phase. The demand curve is depicted alongside the battery and PV production that is available in figure 30.

The building phase lasted from the beginning of March to the end of August, which correlates to hour number 1 440 to hour number 5 760 in the year.

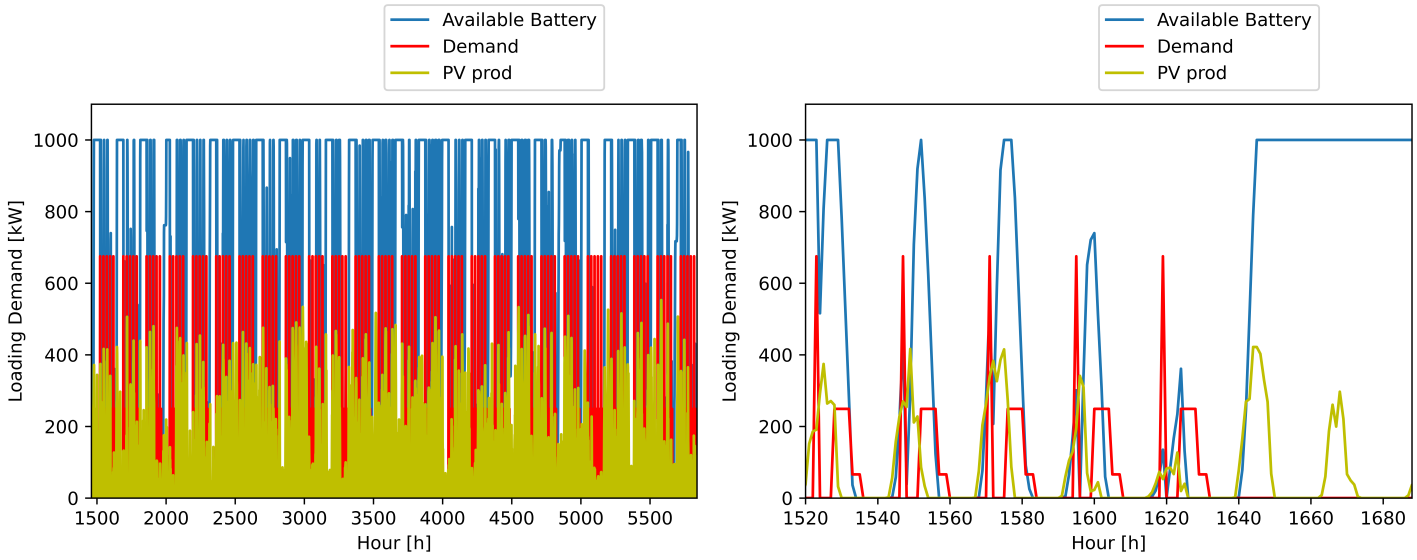

(a) 6 month period, spring and summer

(b) 1 week

Figure 30: Building phase in two different time frames.

PV production ranged from 50 to 500 kW over a period of six months. The battery was accessible for weekly charging and discharging. During periods of high demand, the system relied on PV production to keep battery levels acceptable. Clearly, when PV production was insufficient, the system drew power from the battery to satisfy demand. Although the construction process took six months, the total cost of acquiring electricity was only 6 167 NOK. This was due to the fact that the majority of PV generation occurs during spring and summer. Total PV production was 400 493 kWh, according to table 14. This resulted in a monthly average output of 66 748 kWh, a 52% increase from the groundwork phase. In addition, the building phase had a significantly lower maximum demand of 675 kW than the groundwork phase's maximum demand of 2 000 kW.

It was evident that solar energy generation satisfied the majority of demand on a weekly basis. When initiating equipment charging, the available battery power was observed to decrease. This was set to 16:00, signifying that PV production to charge equipment during the initial phases of the phase would be limited due to insufficient solar exposure. Solar energy was used to charge the batteries before lunch since all equipment had been fully charged overnight. Lunchtime demand was met by PV generation and battery storage. When demand was low on weekends, the battery was quickly charged to its maximum capacity and any excess energy was sold to the grid. Rarely did the system purchase electricity from the grid, resulting in exceptionally low purchase prices.

5.1.4 Facade Phase

The facade period took place in September and October. In figure 31, both the demand curve and the battery level are presented.

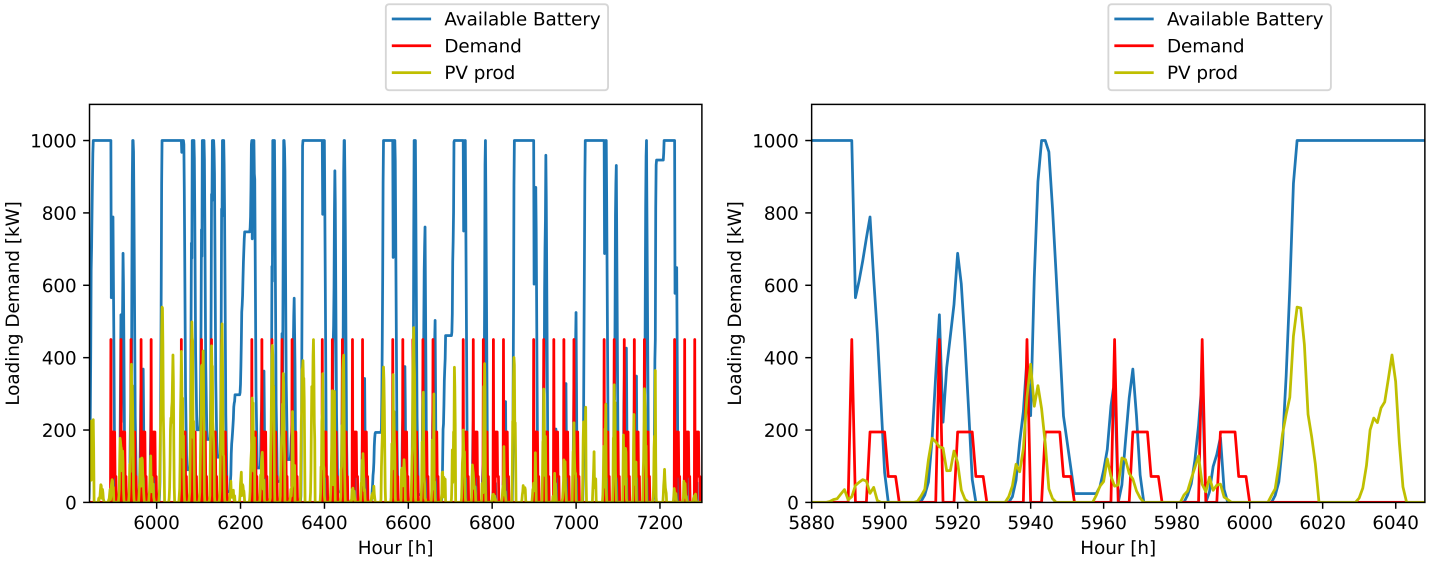

(a) 2 month period, summer and autumn

(b) 1 week

Figure 31: Facade phase in two different time frames.

Monday's PV production peaked at 62 kW, while Saturday's PV production peaked at 539 kW. PV production and battery capacity were sufficient to meet demand on days with the most sunlight. In September and October, a total of 78 485 KWh of electricity was produced, with a demand peak of 450 kW occurring during lunch breaks. In some cases, as shown in Figure 31(b), the relatively high PV production allowed the battery to be fully charged throughout the day. The peak PV production on Wednesday was 381 kW, so the PV production after lunch was sufficient to completely charge the battery before the machinery required charging at the end of the workday. It was interesting to discover that the facade phase generates 7 058 NOK by selling power to the grid. In comparison to the remainder of the phase, this portion was relatively long-lasting. This suggested that the system was incapable of maximizing solar utilization. With a larger battery, the system would be able to store more power from PV production and purchase less power from the grid, thereby reducing acquisition costs.

5.1.5 Internal Phase

The results from the internal phase of the project is presented in figure 32. In this phase, the shell construction was completed, and the interior workings were begun. In this period, there was a heating demand in order to ensure proper drying of materials.

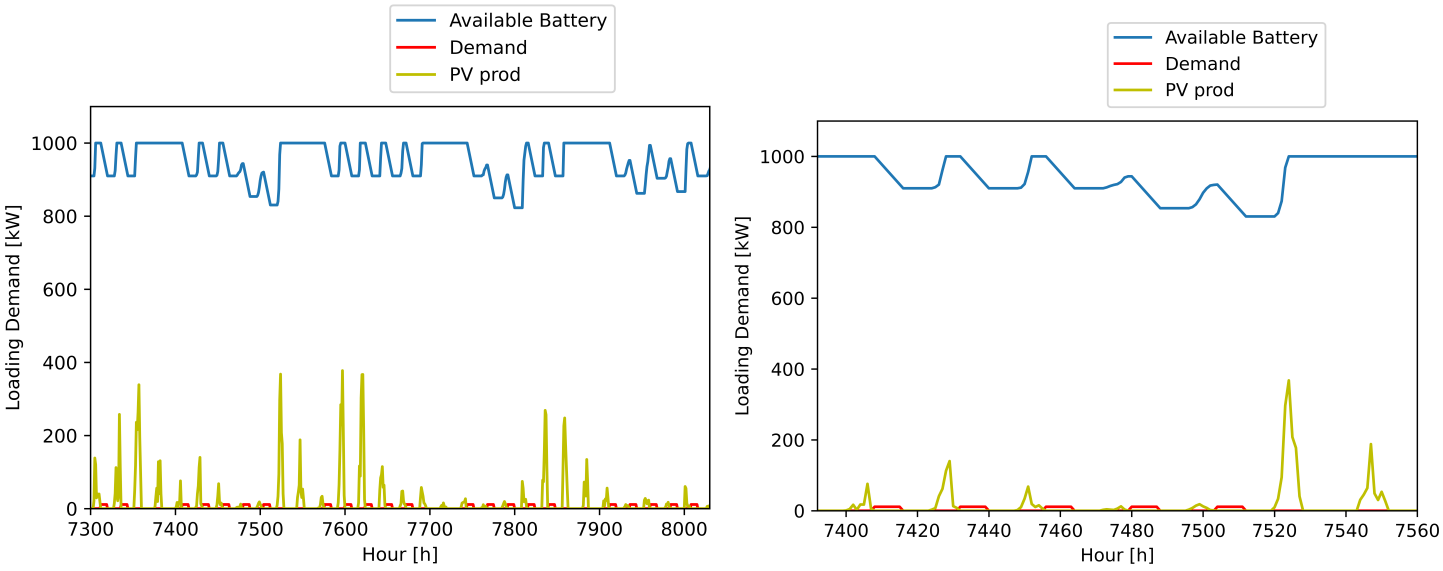

(a) 1 month period, autumn

(b) 1 week

Figure 32: Internal phase in two different time frames.

In comparison to the other phases, the electric demand was relatively low, according to the results. In general PV production was quite low, but the system was capable of producing up to 400 kW at certain peaks. As a consequence, the battery was never entirely depleted and there was always a capacity surplus to meet demand. Consequently, the system did not require grid power and was able to sell excess power back to the grid. This phase's total solar production was 12 627 kWh, a decrease of 81% compared to the average solar production during the construction phase. After meeting its own demand, the profit from selling power back to the grid was only 3 204 NOK. Notable was the fact that periods without solar demand were effectively supplied by the battery, whose capacity never dropped below 80% for the duration of the phase. This indicates that, if the project were to be delayed, the battery and solar production may be sufficient to last through the winter.

As described in Section 4.3.2, the internal phase of construction required internal heating of the building to reach the intended indoor temperature. The heating demand is presented in figure 33.

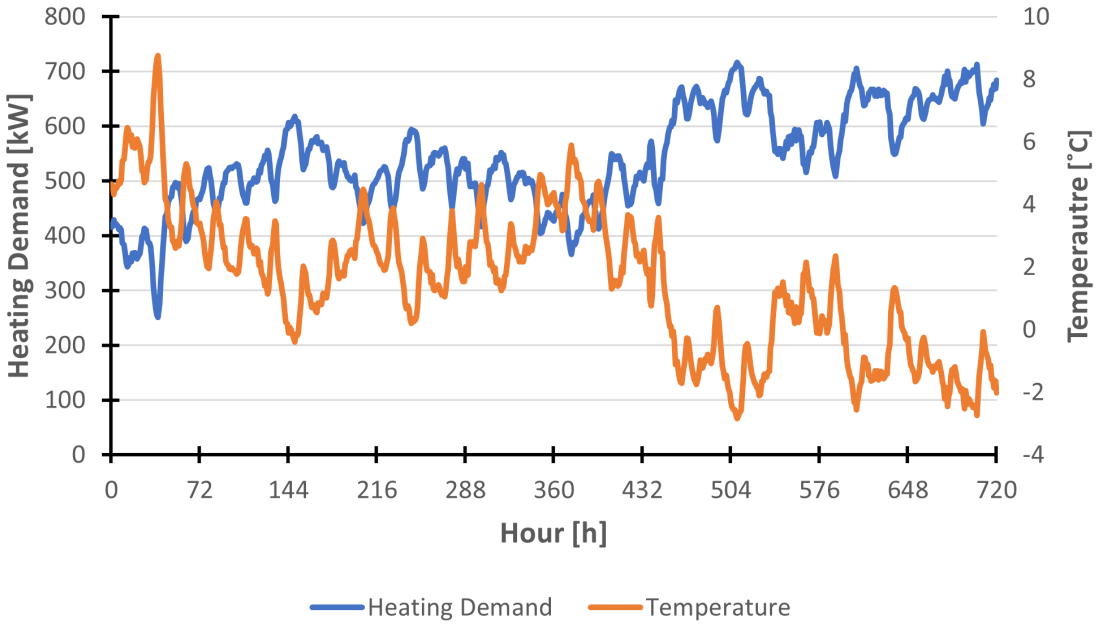

Figure 33: Heating demand for indoor building temperature.

To calculate the heating requirements for the internal phase, a Matlab script from an NTNU Master's thesis on zero-emission construction sites was reproduced with permission [61]. The script took the total facade area , desired temperatures, and the outside temperatures into account when calculating heating requirements. Using the outdoor temperatures at Hønefoss during this period and modifying some input variables provided a heating demand for the entire area.

The heating demand for the internal phase in November was **388 989** kWh, with a minimum power peak of 251 kW and a maximum power peak of 716 kW, according to the MatLab script ran with building data. The average monthly heat demand was 541 kW, well within the capacity of the biomass boiler specified in Section 3.1.2 on page 26. There was a strong correlation between the anticipated demand for heating and the ambient temperature. As the interiors of the structures were incomplete, they were vulnerable to external temperatures at this stage of construction. This reflected the heating demand. As shown in hours 585 and 595, the temperature and heating demand were nearly exactly inverse, which indicated that a significant decline in temperature caused an instant increase in heating demand.

5.1.6 Outdoor Phase

The results from the outdoor phase is presented in figure 34.

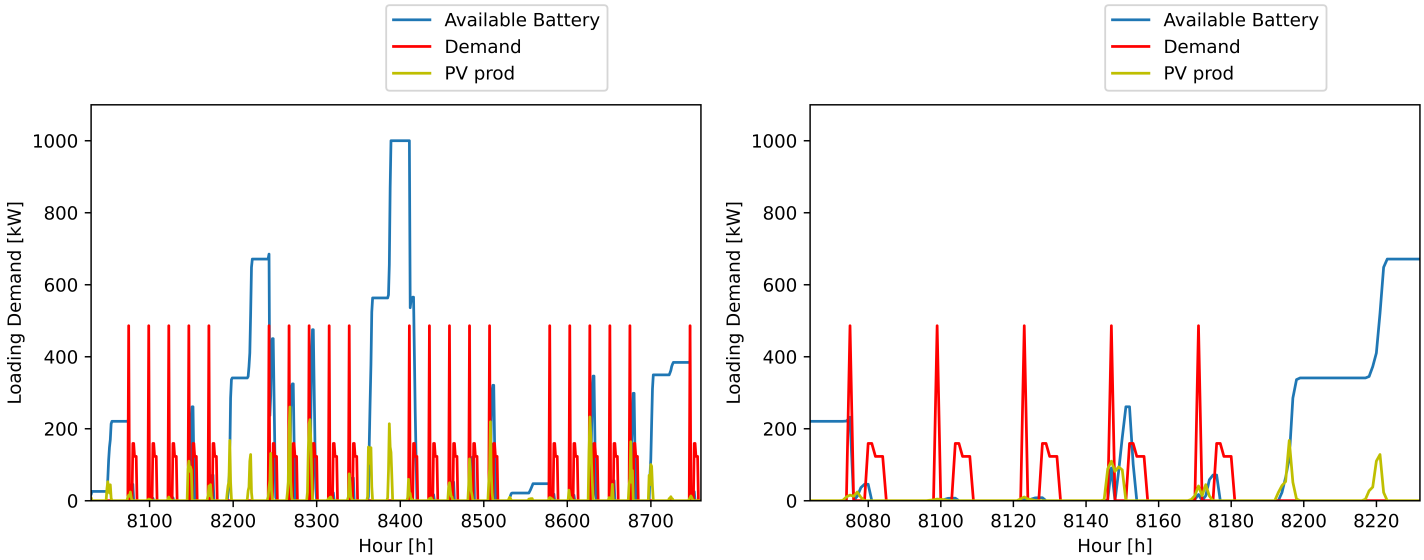

(a) 1 month period, winter

(b) 1 week

Figure 34: Outdoor phase in two different time frames.

The outdoor phase occurred in December, 2021's lowest solar production month. Consequently, this resulted in major costs. The peak PV production for the entire month was just over 250 kW, and on majority of days it did not exceed 50 kWh. This resulted in a total cost of 34 846 NOK and a modest profit of 217 NOK from the sale of excess power to the grid. The available battery did not reach 1 MWh even over the weekend, as shown in 34 (b).

5.1.7 Cost Distribution of Construction

The total gain/cost and power production in the various phases is displayed in table 14, where cost of purchasing power is presented as negative.

Table 14: Cost distribution and power production

	Groundwork	Building	Facade	Internal	Outdoors
Power production [kWh]	43 965	400 493	78 485	12 627	7 477
Gain of selling power [NOK]	1 218	20 140	7 058	3 204	217
Cost of buying power [NOK]	135 946	26 306	22 622	0	35 063
Total gain/cost [NOK]	**- 134 728**	**- 6 166**	**- 15 564**	**3 204**	**- 34 846**

More than 70% of the total cost was incurred during the groundwork phase, as shown in table 14. During the internal phase, the increase in selling power was greater than the decrease in purchasing power, resulting in a net gain of 3 204 NOK. Due to the low PV production during the winter, there was a negligible increase in selling power. The increase in selling power was 20 140 NOK during the construction phase, which lasted from the beginning of March to the beginning of September. During the months of June, July, and August, when PV production peaked, the majority of the increase occurred. Due to the extended duration of the power phase relative to the other phases, the power production clearly peaked during the power phase.

Given that the residential area has not yet been constructed, determining the accuracy of the results was complicated. In addition, there were very few examples of zero-emission construction initiatives, making it challenging to compare results to those of the past. Determining if the total cost of 185 806 NOK for the groundwork phase was reasonable or not was challenging. As indicated in the theoretical Section 2.9.2, the use of zero-emission excavators rather than conventional diesel excavators decreases operational outcomes.

To calculate the total costs for heating using pellets, the data for the construction phase presented in table 14 was utilized. With a demand of 388 989 kWh for the heating in November, the total costs can be calculated by multiplying the price of pellets. In turn, a total cost of **175 045** NOK was achieved. This includes the price of pellets and variable price presented in Section 5.2.2.

Utilizing the new transmission costs, the transmission grid tariff was determined. Tanberghøgda is located in Ringerike, where grid transmission is managed by *Føie* [18]. The cost of the new grid tariff was determined using the guidelines outlined in Section 2.5. As the model did not account for a limitation on the power imported from the external grid, the average of the three highest peaks each month was high, especially during the winter months, when the average was 868 kW from November to April. Significant portions of the construction phase fell within the category of 200 - 1 000 kW average peak power. According to *Føie's* grid tariff, this had a fixed cost of 536 NOK/kW, a winter power cost of 0.196 NOK/kWh, and a summer power cost of 0.169 NOK/kWh.

As a result of the model's constraints, the transmission tariff calculations were illogical. According to Section 4.3.4, the transmission grid charge was not considered. During periods of surplus power production, the model sold power to the grid regardless of the current market price. This would result in a net loss in certain circumstances due to the new tariff model, and the calculations were therefore not viable for our model. The electricity transmission charge alone exceeded 90 000 NOK based on the amount of power sold and purchased. The system's primary objective was to satisfy its own demand; it was not optimized for cost reduction. According to these results, the additional cost per kW of transmitted power was excessively high.

5.1.8 Construction Phase Cases

Different scenarios has been tested with regards to the total cost for the entire construction phase. Different spot prices and battery sizes has been tested, as described in Section 4.5.5. Spot prices for 2020 and 2021 as well as battery capacities of respectively 0.5 MW, 1 MW, and 2 MW were tested

in various scenarios, resulting in six scenarios shown in table 15. Originally, the battery size was 1 MW.

Table 15: Different Spot Prices and Battery Size.

Spot price year	Battery size	Total cost
Spot prices 2020	Battery size of 0.5 MWh	62 057 NOK
	Battery size of 1 MWh	57 904 NOK
	Battery size of 2 MWh	55 024 NOK
Spot prices 2021	Battery size of 0.5 MWh	222 116 NOK
	Battery size of 1 MWh	188 101 NOK
	Battery size of 2 MWh	165 151 NOK

In 2020, spot prices for NO1 were significantly less expensive than in 2021. The dry weather in southern Norway, along with increased gas and coal prices in Europe, and increased prices for emission allowances in the EU emissions trading system [66], contributed to the atypically high prices. In fact, the average spot price in 2020 was nearly eight times lower than the average spot price in 2021, according to [72]. Using spot prices from 2021, the total cost was roughly four times more expensive. As the spot prices rise, selling power increases, but the cost difference exceeds the gain difference, resulting in a higher total cost. When selling power back to the grid, the price was also below the spot price. The *python-code* employs a selling factor equal to 50% of the spot price.

When sizing the battery, the total cost was reduced proportionally to the spot pricing. In 2020, the price gap between 1 MW and 2 MW batteries was only 2 880 NOK, but by 2021, it had increased to 22 950 NOK. As stated in Section 5.1.7, it was challenging to determine whether or not the results are acceptable; nevertheless, the connection between the various scenarios is interesting.

The 2 MWh battery contributed to a decrease in cost. In 2021, the total cost decreased by 12.2%. Therefore, if the construction period is extended, the actual cost savings of introducing a 2 MW battery will be greater. During the weekends, when the machines were fully charged and not in use, the 2 MW battery was able to fully charge when the PV production was sufficient and supplied a larger portion of the week's charging demand. In 2021, the battery size of 500 kW increased the total price by 18%. During the weekends, the battery would fully charge and sell power to the grid, but during the week, it had little power to supply to the machines. As seen in Section 5.1.7, the cost of purchasing power was greater than the profit from selling power, resulting in a 500 kWh increase in total cost.

To determine the optimal battery size, the cost of various batteries, their lifespan, and the anticipated spot price had to be evaluated. It is difficult to predict and impossible to control the spot price. As described in Section 5.1.8, the spot price was substantially higher in 2021 than in 2020 and has continued to rise in 2022, indicating that it may be profitable to increase the battery size

of [72]. The initial average spot price for 2022 was significantly higher than that of 2021. Due to the high spot price, it was financially advantageous to purchase as little power from the grid as possible, which could be accomplished by supplying as much load as possible with PV and battery. Assuming PV production was constant, the only variable that could be assumed was battery price.

The lifespan of an energy storage battery ranges from 5 to 15 years, while the lifespan of a PV plant is between 20 and 30 years [73]. This implies that the battery must be replaced at least once during the lifespan of the PV plant, which must be accounted for when calculating the battery investment cost.

Total Cost

All phases' total costs could be compared based on the diesel used to fuel all construction equipment. Using the conversion presented in Section 2.9.1 to calculate diesel consumption, a total of 65 278 liters of diesel was required to meet the machine requirements of 652 788 kWh. Using the average diesel price in 2021, 15.51 NOK/l [74], it was possible to compare the simplified costs for the base case to the results of the various segments. These results are shown in table 16.

Table 16: Total cost with and without PV and battery. Based on 2021 spot prices.

Phase	Total Cost [NOK] Using diesel	Total Cost [NOK] With PV and battery	Cost Reduction [%]
Groundwork	442 726	134 728	69.57
Building	148 371	6 166	95.84
Facade	75 003	15 564	79.25
Internal	2 334	- 3 204	237.27
Outdoors	50 478	34 846	30.97
Total	**718 912**	**188 100**	**83.6**

Emission from Construction Phase

Using the phase division depicted in the 8 figure, the total demand for all phases was 652,788 kWh. Using the diesel consumption calculation presented in Section 2.9.1, this totals approximately 65 278 litres of diesel. According to Michelin, the total emission was **175 $\mathbf{tCO_2e}$** at a CO_2 concentration of 2.68 kg/l [75]. The climate declaration allowed the use of 11 g CO_2e/kWh for power delivered in Norway in 2021. The corresponding emissions were **3.673 $\mathbf{tCO_2e}$**, as the total quantity of electricity purchased from the grid throughout all phases was 333 827 kWh. This represented a reduction in emissions of 98%.

As demonstrated in Section 2.9.1, there was a significant opportunity to reduce emissions by using electric construction equipment, and the Tanberghøgda project was no exception. If the project duration lengthens, potential emission reductions will follow. Comparing the results with the construction projects presented in Section 2.9.1 and 2.9.2 in terms of project size and equipment suggested that the results were plausible and within the acceptable emission range.

5.2 Heating demand

In this section, calculations regarding the delivered heat to Tanberghøgda was conducted and analyzed. It was yet to be determined if an on-site pellet fueled boiler or the local district heating network was to be utilized. The following section provides an overview of relevant costs and power demands related to meeting the heating demand.

5.2.1 Pump Cost

Firstly, the total pressure loss per hour, Δp_i, was calculated using equation 2.7, 2.8 and 2.9. The maximum total pressure loss is:

$$\Delta p_{max} = 2 \cdot 200\, Pa/m \cdot 2\,000\, m + 50\,000\, Pa + 75\,000\, Pa = 925\,000\, Pa$$

and the maximum volume flow during the year was $48.17\ m^3/h$ which gave a system characteristics C:

$$C = 925\,000/48.17^2 = 398.48\, Pa/(m^3/h)$$

The system characteristics C together with the volume flow was used to calculate the total pressure drop per hour, Δp_i.

To calculate the pump power, the pump efficiency per hour had to be calculated. To do so, a function with the volume flow per hour, $\dot{V}_i$, was estimated and presented in figure 35.

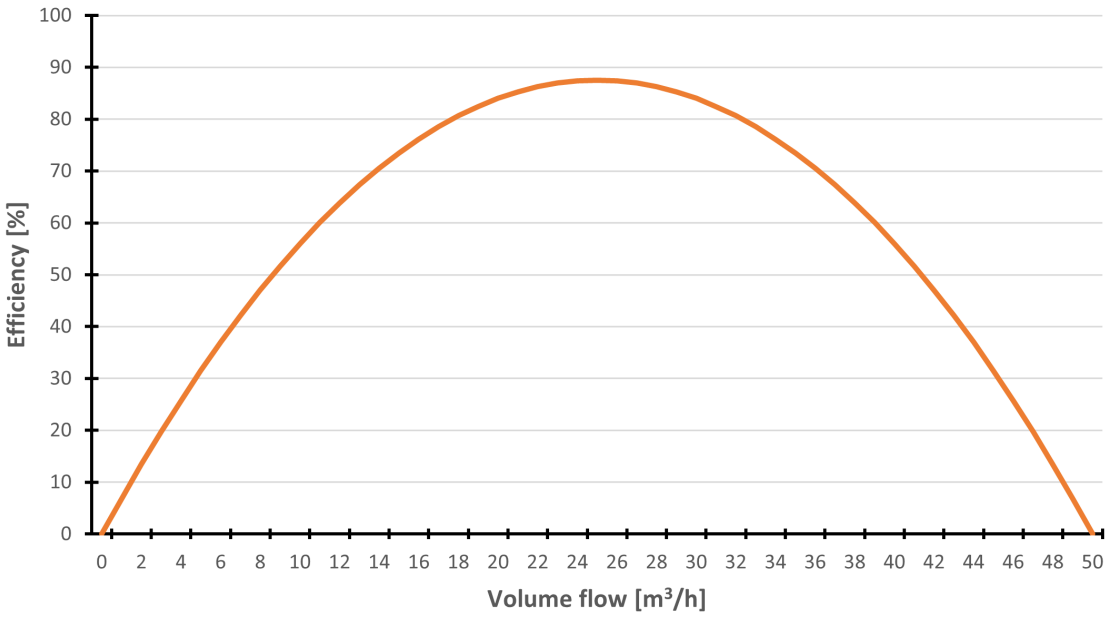

Figure 35: Pump efficiency as a function of volume flow.

This graph displayed the pump efficiency on the y-axis and the volume flow[m^3/h] on the x-axis. The function that described the different pump efficiencies with respect to the volume flow was:

$$\eta_{pump,i} = -0.14\dot{V}_i^2 + 7\dot{V}_i$$

This function fitted well, given that the average volume flow throughout the year was $9.4\,m^3/h$ and the maximum volume flow of $48.2\,m^3/h$. To continue, the pump efficiency over the entire year was calculated and presented in figure 36.

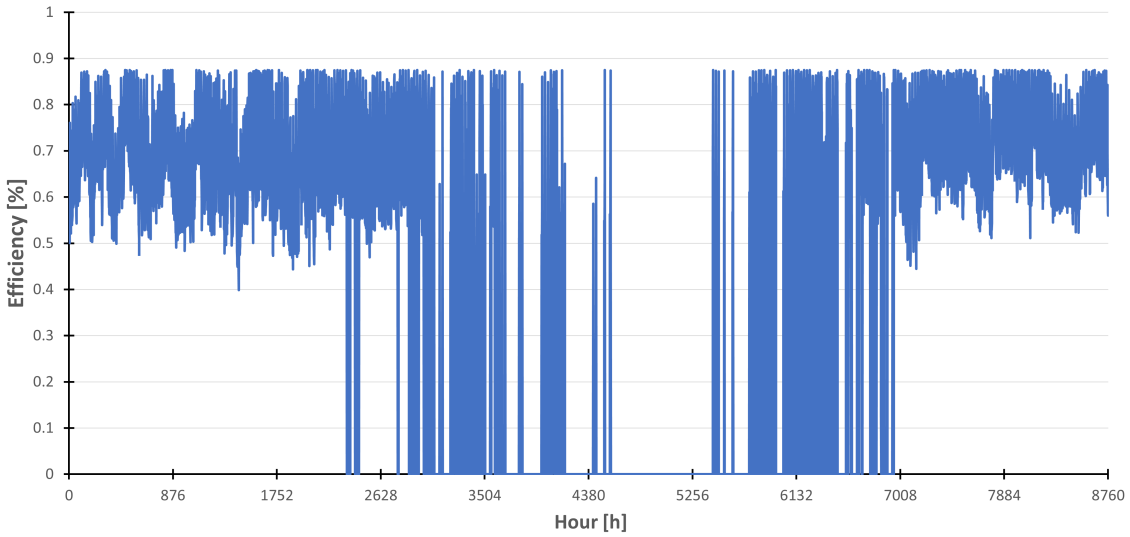

Figure 36: Pump efficiency in 2020.

The figure demonstrated that the efficiency of the pump varied greatly in correlation to the volume flow for each season. During the winter periods, the efficiency was high due to higher volume flow of water. This tended to give a better efficiency, as can be seen by analyzing figure 35. During the seasons with lower heating demand, the pump efficiency dropped vastly and behaved quite volatile. An observation to be made was that the efficiency was equal to zero during the summer months, as the system was not operating.

Consequently, the Δp_i was calculated using equation 2.9 and illustrated in figure 37 and 38.

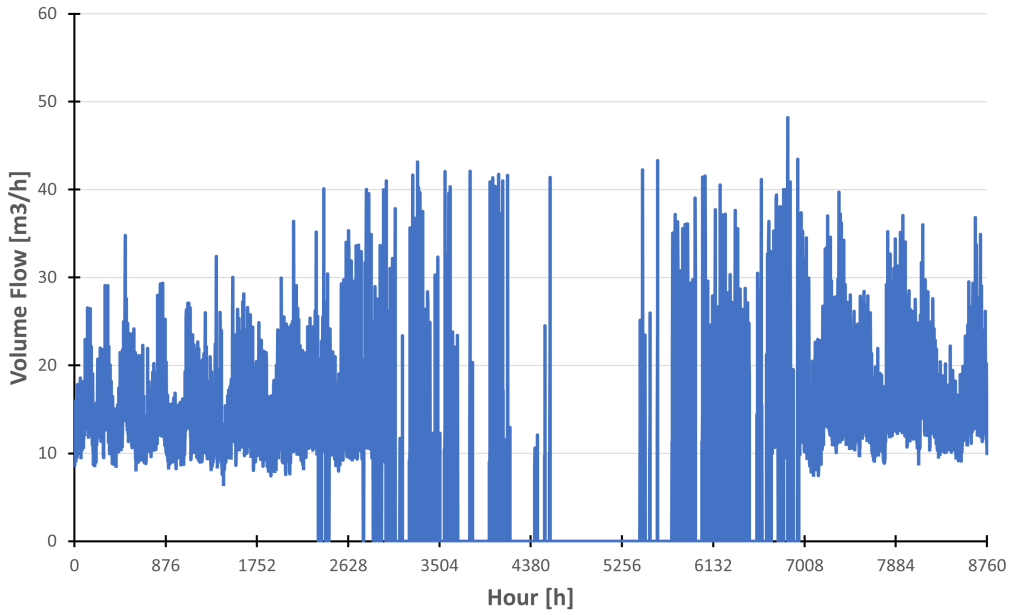

Figure 37: Volume flow per hour over a year.

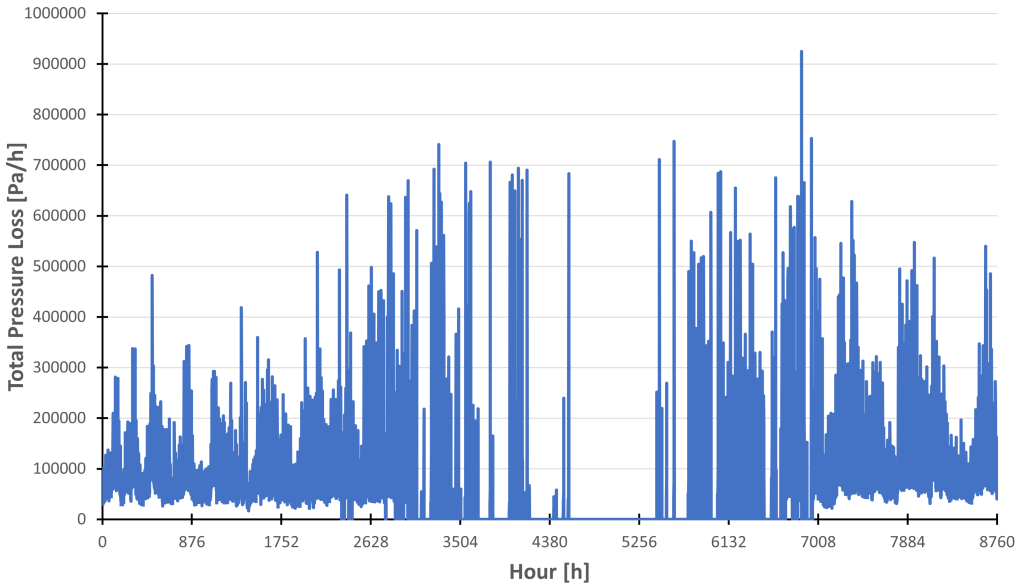

Figure 38: Total pressure loss per hour over a year.

The Δp_i corresponded directly to the $\dot{V}_i$, because of the constant system characteristics C. During several hours in June, July, and August, both the volume flow and the total pressure loss were equal to zero because the pump was closed when the ΔT fell below 5 K, as described in Section 4.2.5.

The pump power was computed utilizing equation 2.6, with the variables volume flow, total pressure loss, and efficiency, which gave the following pump power throughout 2020:

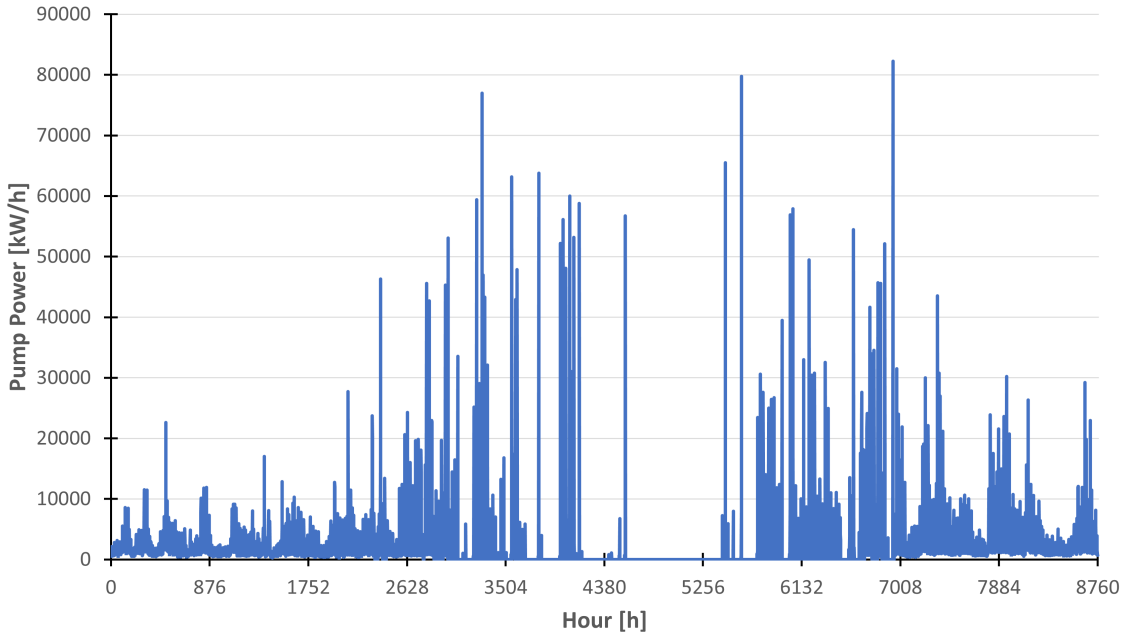

Figure 39: Pump power per hour over a year.

When comparing the pump power to the yearly efficiency, some observations can be made. As the pump efficiency decreases, the pump power increases. This correlation was reasonable, as the low efficiency meant the system must compensate with a high volume flow. In turn this led to a high pump energy demand.

Due to the low volume flow during the summer, the efficiency dropped below 0.5. This resulted in a peak pump power during the summer, which in turn resulted in a peak pump cost during the summer, as shown in figure 40.

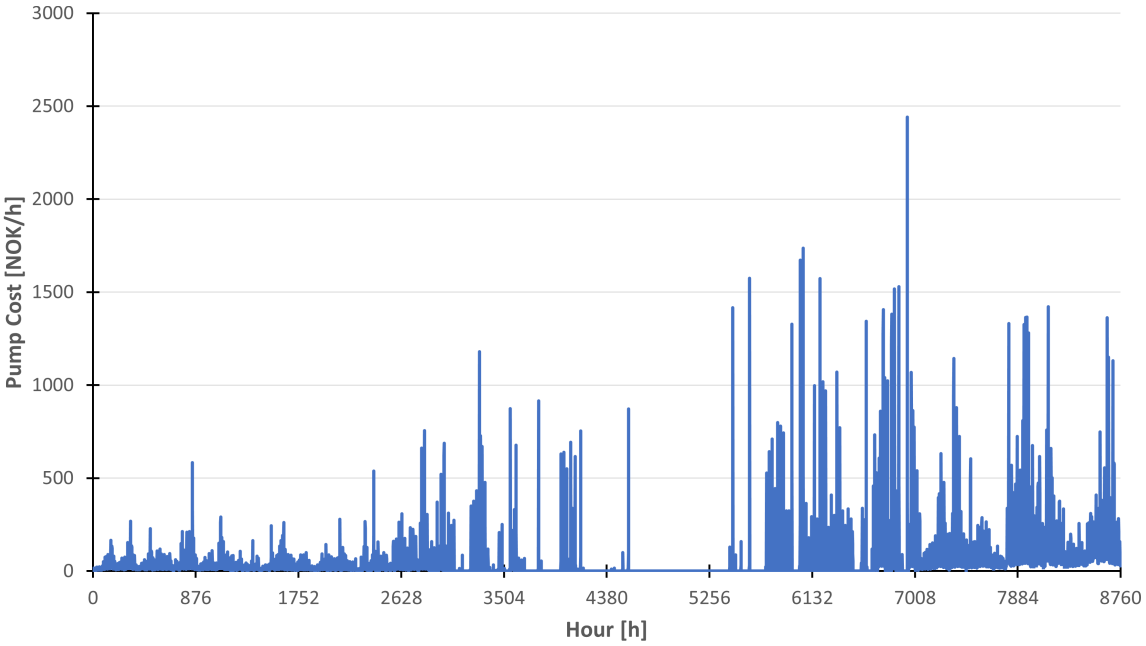

Figure 40: Pump cost per hour [NOK/h].

Using equation 2.5 gave a total pump cost for 2021 of **356 802 NOK/year**. The pump cost was drastically more expensive the last 4 months. The pump cost from the start of September until the end of December was 251 375 NOK, which was more than 70% of the total cost, as a result of an increase in pump power, in addition to a peak in the spot prices during the end of 2021.

To decrease the overall pump cost, a few different measures could be implemented. The most influencing variable was the spot price, which was high in 2021. The impact of the spot price became evident in a brief sensitivity analysis conducted. Calculating the total pump cost, using the spot prices from 2020, the total pump cost decreased to 46 828 NOK, which was nearly a 87% decrease compared to the original 2021 spot price. To continue, an increase in the efficiency would also decrease the pump costs. Given a scenario where the efficiency was kept constant at 0.9, the total pump cost would be decreased to 292 317 NOK with the 2021 spot price values.

Lastly, the specific pump energy demand was calculated using equation 2.13. The results provided information on the electricity demand of the pump relative to the delivered heat. The specific pump energy demand was 2.72 kWh/MWh.

From relevant literature, the specific pump energy demand ranged from 5-10 kWh/MWh for district heating plants, and 20-50 kWh/MWh for larger plants. Though the results calculated are slightly lower than to be expected, it was still in a reasonable range compared to the values from literature [25]. The distribution net for the area was relatively small which may led to a lower

pump energy demand in contrary to to larger plants.

5.2.2 Heating Costs

The chosen efficiencies are based on the literature presented in Section 4.4.4. The total costs for on-site heat production are calculated using equation 2.14, and the results are presented in table 17.

Table 17: Production costs for different boiler efficiencies.

Efficiency [%]	Production Costs [NOK]
82	831 835
84	812 029
86	793 145
88	775 119
90	757 893
92	741 418
94	725 643

The table displays a decrease in total costs in relation to increasing efficiency. This is to be expected, as the other variables in the cost function remain the same. The cost difference between the lowest and highest efficiency was 106 192 NOK, displaying a potential saving by opting for a boiler with higher efficiency.

A pellet price of 42 øre/kWh together with a variable cost of 3 øre/kWh was utilized in the production cost calculations. The values originate from fuel cost estimations provided by *COWI* in internal documents [60]. The fixed operating costs can also be added as 2% of the investment cost, or 116 000 NOK, for a total investment cost of 5 800 000 NOK, as described in *Kostnadsberegninger varmesentral Tanberghøgda* [60].

As described in Section 2.6.2, the price heating cost for district heating provided by *Vardar Energy* was 4% lower than the spot price from *NordPool*, and was calculated directly in the total costs for district heating.

5.2.3 Total Costs

The total costs was calculated as presented in equation 2.17 and 2.18, depending on which heating source is chosen. The results from Section 5.2.1 and 5.2.2 give a total cost of **1 569 944 NOK/year** when utilizing district heating and a price 4% lower than the spot price as explained in Section 2.6.2. Additionally the specific costs for district heating utilizing a heating demand of 1 516 MWh is **1.036 NOK/kWh**.

Compared to the fixed price provided by *Vardar Energy* for 2023, which was at 1.35 NOK/kWh for a 1 year period or 1.3 NOK/kWh for a 3 year period, the results were reasonable [27]. The fixed price will generally be higher due to the uncertainty of change in spot prices. The last years have

especially displayed the volatility of the electricity market. Predictions from *Statnett* also indicate a volatile electricity price in the next 10-15 years [76]. The correlation between delivered heat from *Vardar Energy* and spot prices led to a higher price, which in some cases make it sensible to opt for the fixed price.

To continue, the total costs and specific costs for on-site production is presented in table 18. As displayed the efficiency of the boiler has a direct impact on the total costs.

Table 18: Total costs of on-site production.

Efficiency [%]	Total Costs [NOK]	Specific Cost [NOK/kWh]
82	1 307 507	0.862
84	1 285 714	0.848
86	1 264 942	0.834
88	1 245 113	0.821
90	1 226 165	0.809
92	1 208 042	0.797
94	1 190 690	0.785

The results display that the total costs for on-site production is substantially lower compared to district heating for 2021 data , even with the return requirements of the on-site boiler. For the consumer this entails a lower costs for purchasing heat.

Discussion and Sensitivity Analysis

Though the results may indicated a lower specific costs for the on-site production, the results presented were only for 2021 spot prices. When calculating the total costs using 2020 data, the total cost for district heating was 229 322 NOK due to substantially lower electricity prices. In comparison, the total cost for on-site production with the highest efficiency would be 849 718 NOK. The large contrast in price was due to low electricity costs, leading to low district heating costs. To continue, the fuel costs for the boiler were considered to be 0.45 NOK/kWh including variable costs, which was in many periods higher than the electricity costs. In turn this led to a much higher cost for on-site production compared to district heating. Lastly, an increased fuel price may effect the price of on-site production greater, as larger buyers such as *Vardar Energy* may negotiate better prices due to higher purchasing volumes over a longer time frame.

According to a long term electricity market analysis conducted by *Statnett*, there was expected to be high price volatility over the next 10-15 years [76]. Therefore it may be difficult to assess which heating source was the best option for this specific case. The difference in price would presumably be closer to the 2021 data presented in the results.

A sensitivity analysis of the impact of pellet price on total cost was conducted. A bench mark boiler efficiency of 90% was set, as the analysis is focused on the varying pellet price. The total costs are presented in table 19.

Table 19: Total costs of on-site production with variable pellet price.

Pellet Price [NOK/kWh]	Total Costs [NOK]	Specific Cost [NOK/kWh]
0.45	1 226 165	0.809
0.55	1 411 427	0.931
0.65	1 596 690	1.05
0.75	1 781 953	1.175
0.90	2 059 847	1.359

As displayed, the increased pellet price led to higher total costs making it less lucrative for *Vardar Energy*, and more costly for the residents of the area. With an efficiency set at 90%, the specific costs increase 68% when the pellet price doubled. This demonstrated the dependency of pellet price with regards to total costs of on-site production. Though a doubling of price is unlikely in the near future, the increase electricity prices may shift the heating demand to sources that are not electricity reliant. The abrupt increase in demand will likely effect the price of pellets. It will be crucial for *Vardar Energy* to obtain long term contracts for deliverance of pellets in order to have predictable heat deliverance.

Due to the volatile electricity prices observed in 2021 compared to 2020, concluding which heating source is preferable for *Vardar Energy* to opt for was difficult. As stated by *Statnett*, the electricity prices are predicted to experience volatility over the next decade. Assuming that the spot-prices would be similar to the 2021 data, on-site production would be the best option as even the lowest boiler efficiency yields a lower specific cost of energy than district heating. As presented in table 19, the price of pellet may also see a slight increase before becoming a less viable option. However a large increase in pellet price would lead to the on-site production becoming less profitable. As mentioned above, long term contracts for pellet deliverance may be a possible solution to this issue.

The profitability of the on-site production when compared to the district heating system is based heavily on electricity prices. When analyzing 2020 spot price data, this becomes apparent. The heating cost using district heating was 229 322 NOK, while heating costs for on-site production were 849 718 NOK. This proves a clear superiority to the district heating, and the on-site production simply cannot compete. However it is highly unlikely electricity prices in the near future will be as low as 2020. Therefore on-site heat production will likely be a profitable and viable option for Tanberghøgda.

5.3 Analysis of the PV Plant, Battery and Interaction with the Electrical Grid

To reduce the cost of purchasing power from the grid over a 48-hour period, a **Python** optimization code was created based on the strategy explained in Section 4.5. The model was based on the mathematical model described in Section 4.5.2, with parameters including transformer load, spot prices, PV production, and the number of electric vehicles connecting to the system. The output was the minimal total cost and a graph of the variables and parameters specified. In every instance below, the battery was initially fully charged.

To fully analyze such a complex system, many cases was analyzed. Initially, the system was divided into two areas, as described in the Section 4.5. Area 1 comprised the PV & battery, EV-charging, and circulation pump, whereas Area 2 consisted of the housing stock and its inelastic electricity demand. Due to the impossibility of their interconnection at the time of writing, the base case did not allow any power exchange between area 1 and area 2. The remaining cases concerned the interconnection between the regions and the effects on costs and system parameters when power could be freely exchanged between region 1 and region 2. The housing stock el-demand is displayed in Section 4.2.4 in figure 12. This data thus corresponds to area 2's electric load. For area 1, the unmodified EV-load is exhibited in Section 4.2.6 in figure 22. Together with the EV's, the circulation pump was served by electricity in area 1. The circulation pump data from Section 5.2 is presented for the relevant 48 hour periods below.

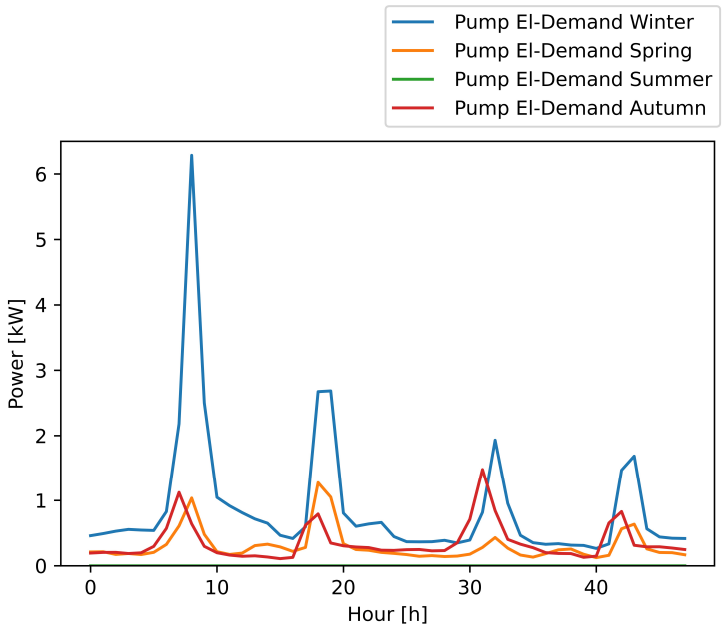

Figure 41: Pump el-demand for 48-hour periods for each season.

Figure 41 shows how the winter period has the highest pump power demand, followed by the autumn, spring, and finally the summer period where the pump is not operating due to low demand. The demands can be summed to the following values:

- Winter : 42.66 kWh
- Spring : 14.51 kWh
- Summer : 0 kWh
- Autumn : 17.10 kWh

Considering the interconnection case, all electric loads were connected together, and could be studied.

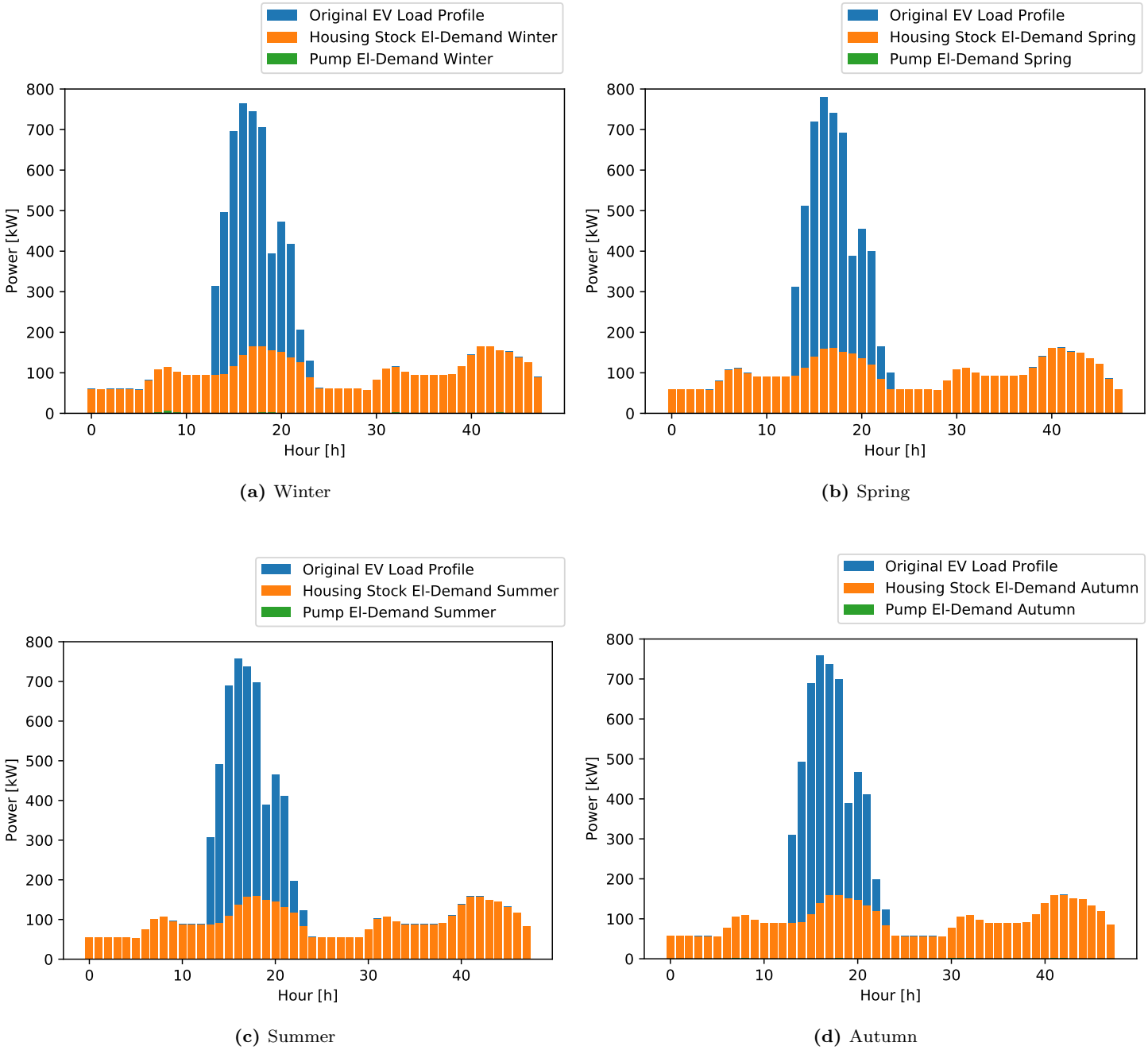

(a) Winter

(b) Spring

(c) Summer

(d) Autumn

Figure 42: Electric load profiles for area 1 & 2 connected together. Note that pump el-demand for the summer period is zero.

Figure 42 depicts how the different seasons affected the load profiles. As previously discussed, the housing stock el-demand was not affected to a large degree according to seasons, and the pump power was mostly very small compared to the other loads. This resulted in almost indistinguishable load profiles, with the following loads:

- Winter : 8 919.9 kWh
- Spring : 8 768.4 kWh
- Summer : 8 575.7 kWh
- Autumn : 8 657.8 kWh

Both the base case and the interconnection case were simulated for all four seasons of 2020 in order to gain a complete understanding of the system's impact. The 2020 data set were selected for the primary simulations to ensure sufficient grounds for comparing seasonal cases. As previously discussed in the Section 4.2.6 on page 49, the 2021 data, despite being more current and representative in terms of total cost, did not exhibit the typical seasonal price pattern within the one-year period. Therefore, choosing the 2020 data was considered a better choice, as these simulations were run for a 48 hour period, and the comparison between them was paramount.

5.3.1 Battery Level Base Case

Depending on PV production, demand, and spot price, the battery level ranged from 0 to 1 000 kWh. The objective function of the model was to minimize total cost, necessitating the use of the battery to cover the load, especially when the spot price was high. Figure 43 depicts the battery level for the four different cases, as well as PV production and spot price.

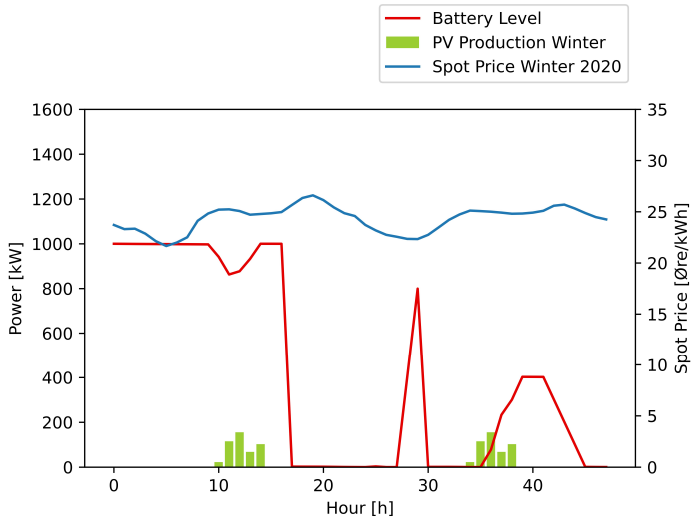

(a) 2020 Winter

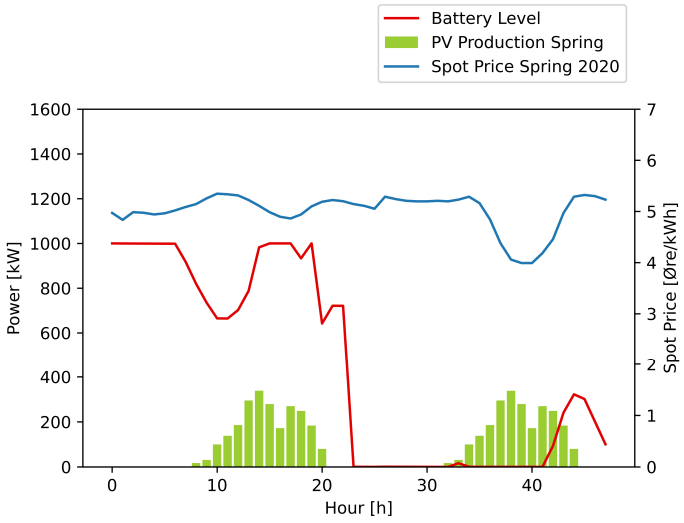

(b) 2020 Spring

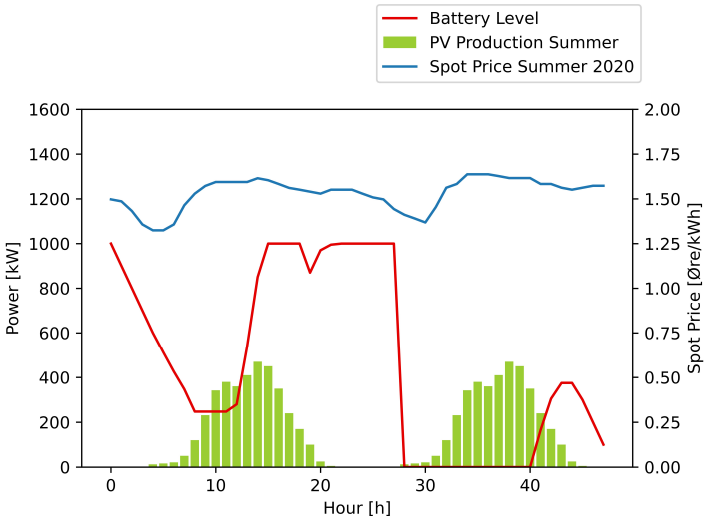

(c) 2020 Summer

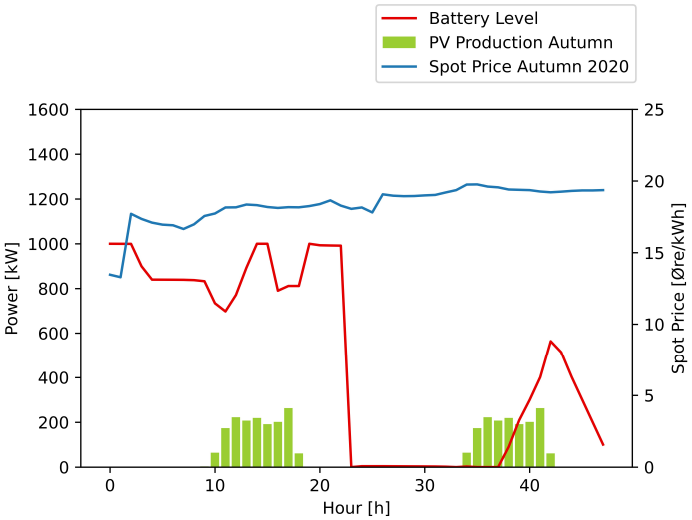

(d) 2020 Autumn

Figure 43: Battery level during winter, spring, summer and autumn in 2020.

In each of the four cases, the battery level changed from fully charged to completely depleted at least once over the course of 48 hours. As shown in figure 43, the installed PV plant was demonstrably more efficient during the summer, with a production peak of 470 kW, compared to the 155 kW peak during winter. As shown in figure 23, the spot price also varied significantly, particularly between summer and autumn, when the spot price was more than 10 times higher. In all four instances, the battery was actively charging and discharging for 48 hours to save money. In all cases, the battery began at 1 000 kWh, and depending on PV production and spot price, it was either utilized or saved. Due to the fact that the PV production fully charged the battery during daylight hours, it was able to sell a large amount of power to the grid during the summer at half the current spot price. Alternatively, the battery was kept at a high level during the night during the winter months, when PV production was relatively low and electricity demand was higher during the day.

As the PV plant generated power during the day, the spot price peaked. The solar power was then split between charging the battery and meeting demand. In all cases, PV production and spot price peaked around twelve o'clock, with the exception of the autumn case, in which the spot price increased gradually throughout the day. The PV production was insufficient to meet demand, resulting in a drop in battery level to cover the total demand.

In the summer case, figure 43 showed a clear correlation between the PV production and the battery level. The total PV production during the 48 hour time period was 7 502 kW, which lead to a fully charged battery during the peak hour at 14:00. For all seasons a general trend could be seen where by the system did not prioritize the charging of the battery during the later hours. This was due to the fact that a cost minimizing function would not necessarily see any utility in charging a battery in the end of the simulation period, as it did not provide economic gain due to the time period. However this would of course be beneficial if a longer time period was simulated.

5.3.2 Load Profile Base Case

The base case load profile was directly derived from the EV charging profile presented in figure 21 as all the connecting EV's have the same charging demand per hour. The complete model outline could be found in Section 4.5. This was evident when comparing the figures 21 and 22, since it was assumed that all vehicles had the same charging demand. In figure 44, the distributed charging pattern for all seasonal cases in 2020 is presented.

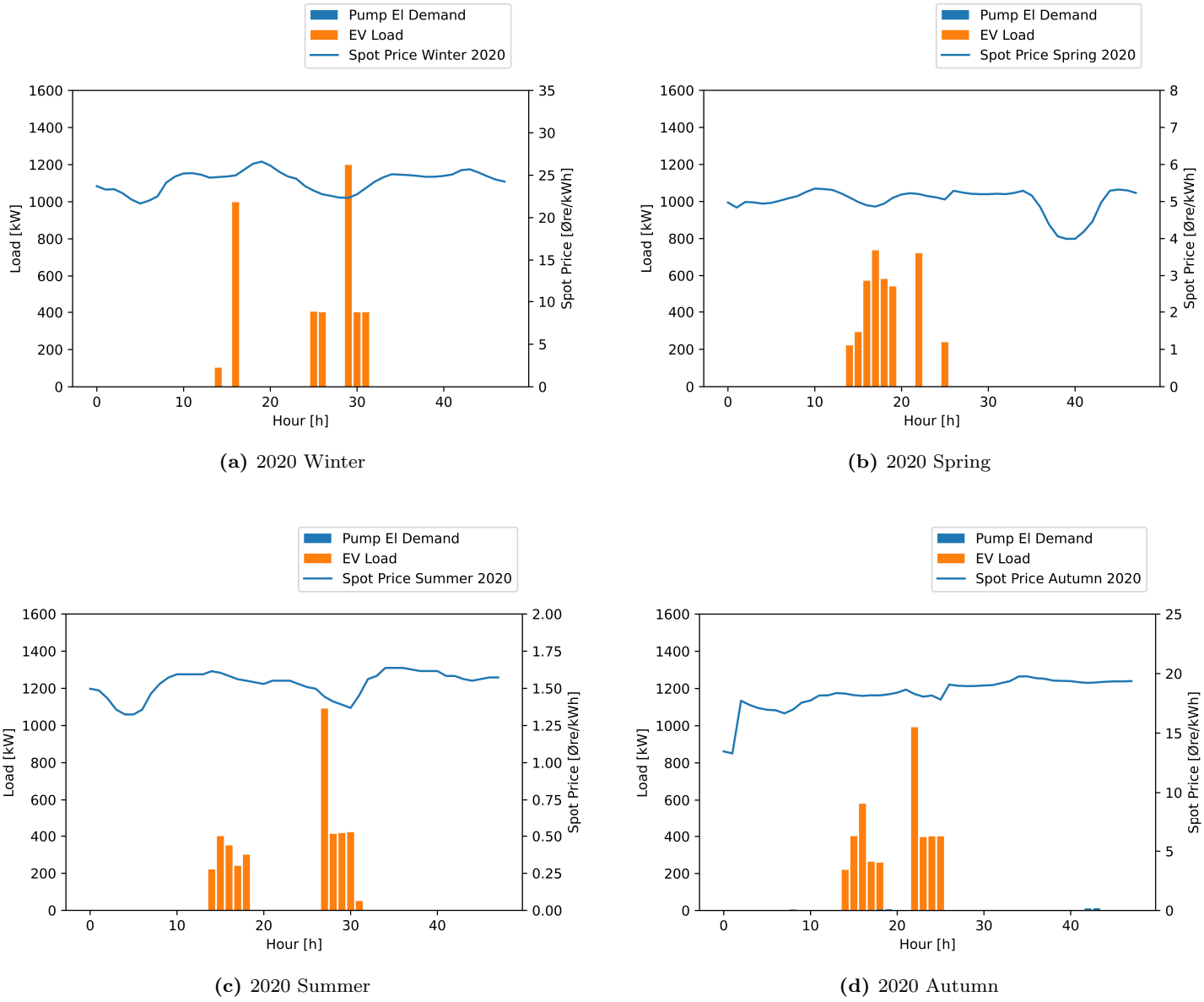

(a) 2020 Winter

(b) 2020 Spring

(c) 2020 Summer

(d) 2020 Autumn

Figure 44: Load profile during winter, spring, summer and autumn in 2020.

As depicted in figure 44, the distribution of loads varied significantly depending on the spot price. As the pump el-demand was almost negligible, it did not have a large impact on the systems ability to move the EV-load where it was most optimal. The daily spot price variation was minimal for all seasons. At approximately hour 30, when the system shifted parts of the charging demand, a

minor price reduction for winter and summer cases could be observed. For the winter and summer scenarios, the charging schedule clearly shifts to price dips to achieve a lower system price, as a charging peak was observed around hour 30. The peaks from the EV-charging could be seen to reach well over a 1000 kW, but this was not a problem as the resulting demand on the external grid was much lower, in accordance with the `transformer capacity` constraint. This could be studied in the next case. Note how all charging was completed within hour 32.

5.3.3 Peak Reduction Base Case

The original load profile resulted in a peak demand of 762.73 kW. It was advantageous to reduce this peak in order to reduce the strain on the power grid and lower costs. The transformer capacity was crucial to reducing peak demand. This was set to 400 kW in all cases. This equates to a peak power reduction of 47.6%. This parameter may be decreased further, but doing so would ultimately increase costs, since the algorithm would have less room to take advantage of favorable price situations. These choices will be further analyzed in Section 5.3.8.

Following the same four case pattern, the `net_transformer_load` variable was plotted with the original load profile consisting of the unaltered EV charging schedule and the pump load. As discussed in Section 4.5, the `net_transformer_load` variable signified the resulting load that needed to be served by the external grid, or sold to the external grid. The results are presented in figure 45. Note that `net_transformer_load` can be negative, this denotes the selling of power to the external grid.

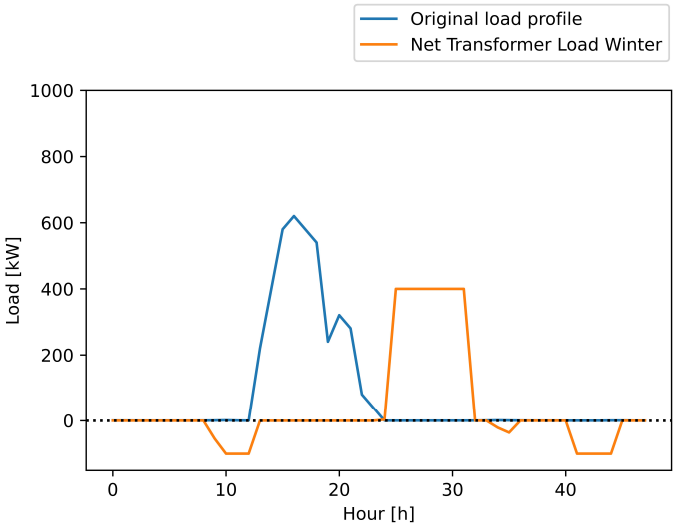

(a) 2020 Winter

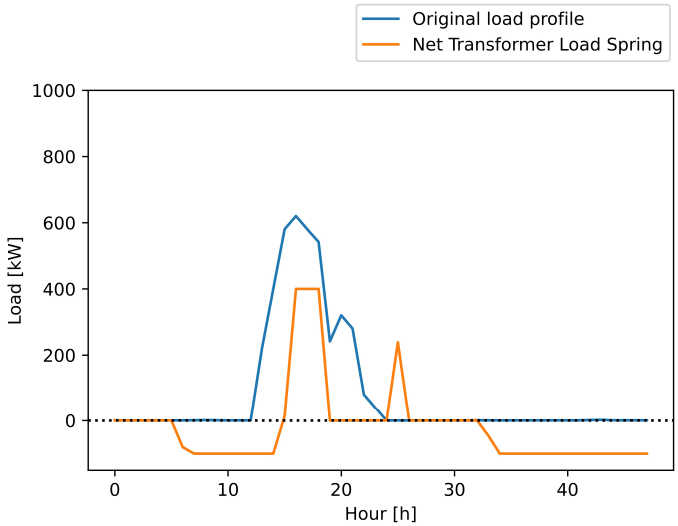

(b) 2020 Spring

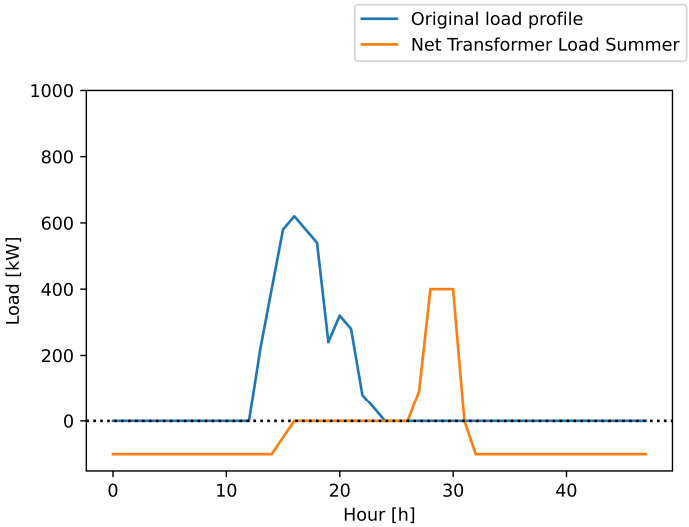

(c) 2020 Summer

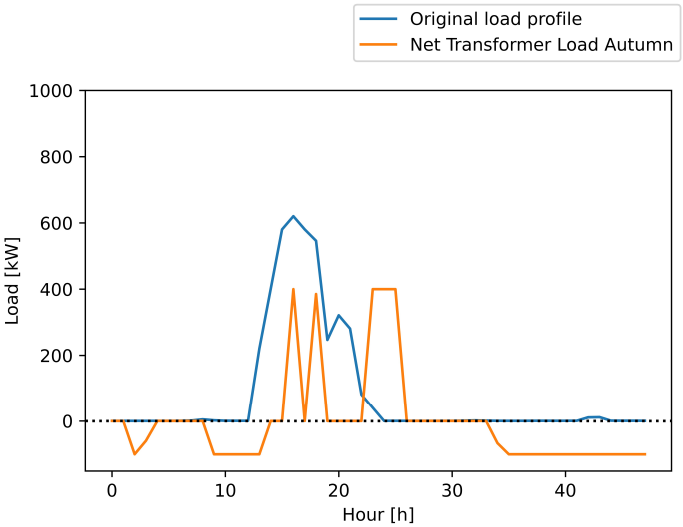

(d) 2020 Autumn

Figure 45: Load profile during winter, spring, summer and autumn in 2020.

As shown in figure 45, a general pattern for `net transformer load` during winter, summer and autumn could be observed. In these three seasons, the `net transformer load` peaked at around hour 25, when the spot price dropped, and the EV load increased, as shown in figure 44. During winter, the `net transformer load` stayed at 400 kW for a long time, due to the low PV production and the high load. On the contrary, the `net transformer load` during the summer period stayed at 400 kW for only a couple of hours when the EV load was at its peak.

The amount of power sold to the external grid directly corresponded to the battery level and PV production illustrated in figure 43 and the EV load shown in figure 44. This resulted in a high quantity of sold power during summer and spring. Most of the power was sold to the external grid at night, when the load was low and the battery level was higher.

Overall, the results were acceptable. The model attempted to invert the resulting power profile by selling power during high spot price hours and importing power during low spot price hours. It attempted, but was limited by the model's constraints, such as PV-production and capacity constraints for both selling and buying.

5.3.4 Battery Level Connected Case

The battery level case from 5.3.1 was re-ran with the aforementioned connection between area 1 and area 2. The results of the simulation was presented in figure 46.

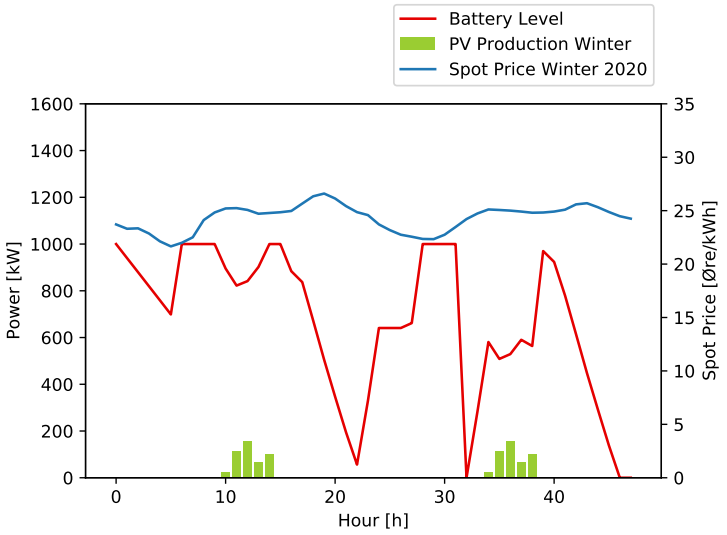

(a) 2020 Winter

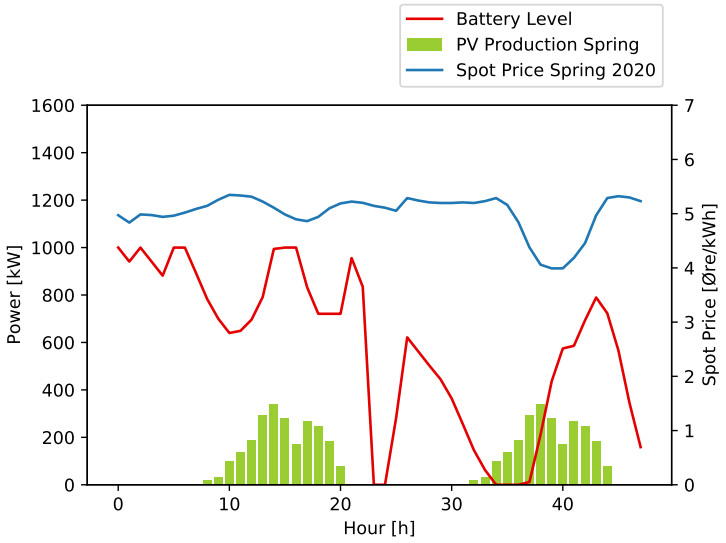

(b) 2020 Spring

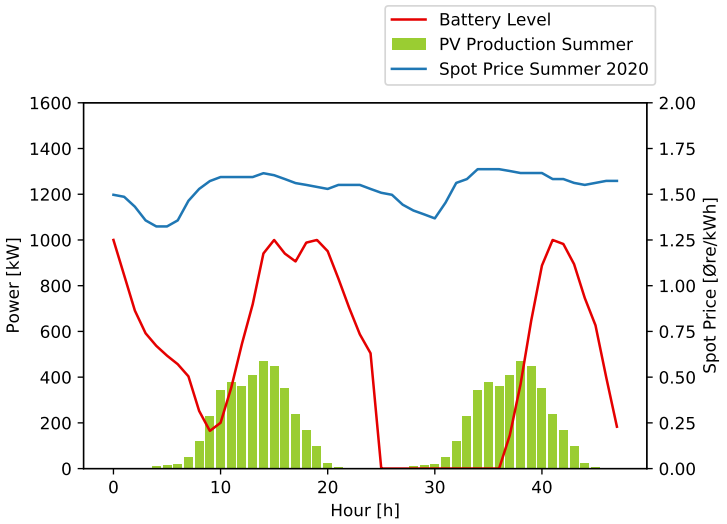

(c) 2020 Summer

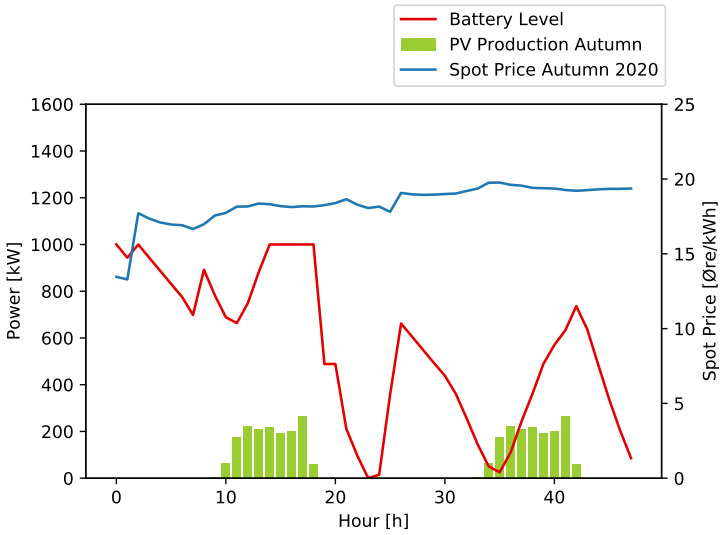

(d) 2020 Autumn

Figure 46: Battery level during winter, spring, summer and autumn in 2020.

The PV production and spot prices remained the same in both cases. Further comparison of the battery level in figure 43 and 46 revealed large differences throughout the day, for all seasons. It can be observed that the battery level was more dynamic in the winter, spring and autumn. For the summer scenario the battery level behaved quite similar, with charging and discharging at approximately the same time. The biggest difference could be seen in the winter scenario, with the battery behaving more dynamic in the connected case compared to the base case. This can be explained by the increased number of loads the battery can serve in the connected case, thus incentivizing increased utilization. By connecting the system, the battery seemed to hold a higher battery level though out the day. This can also be explained by the added loads of the housing stock. As the system can "see" the loads in the later parts of the day, it might make the decision to charge the battery instead of selling off surplus power, as it was needed later.

5.3.5 Load Profile Connected Case

The load profile displayed in figure 47 includes el-demand from both housing stock and the pump. This led to a higher load compared to the base case, where the housing stock el-demand was in area 2 and thus not connected to the PV & battery system. The EV load was also optimized based on the combined system and all its parameters, as described in Section 4.5.2.

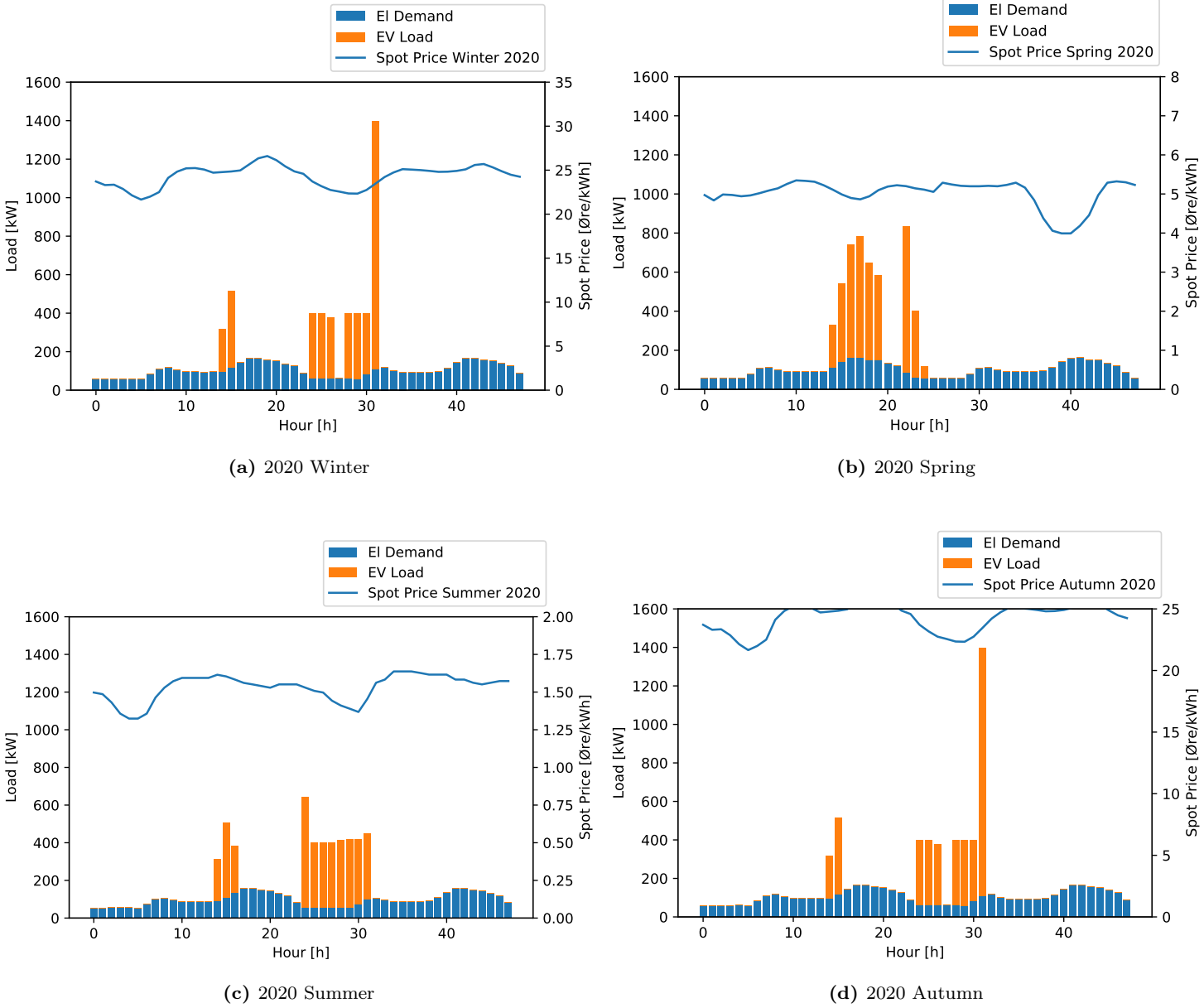

(a) 2020 Winter

(b) 2020 Spring

(c) 2020 Summer

(d) 2020 Autumn

Figure 47: Load profile during winter, spring, summer and autumn in 2020.

As seen in figure 47, the EV load did not shift the EV load solely based on the spot price, as it did in the base case, since the pump load was almost negligible. During winter, the PV peaks in hour 31, although the spot price was at its lowest in hour 29. This was due to the battery dropping in hour 31, as seen in figure 47. The general trend, compared to the base case, is that the EV load was more evenly distributed, especially during summer. This is due to the underlying el-demand, which leaves the system with more constraints in regards to when the EV-demand can be served, and thus the need to distribute the EV-load becomes apparent.

5.3.6 Peak Reduction Connected Case

The peak reduction case presented in figure 45 was run with a connection between the two areas. The results are presented in figure 48.

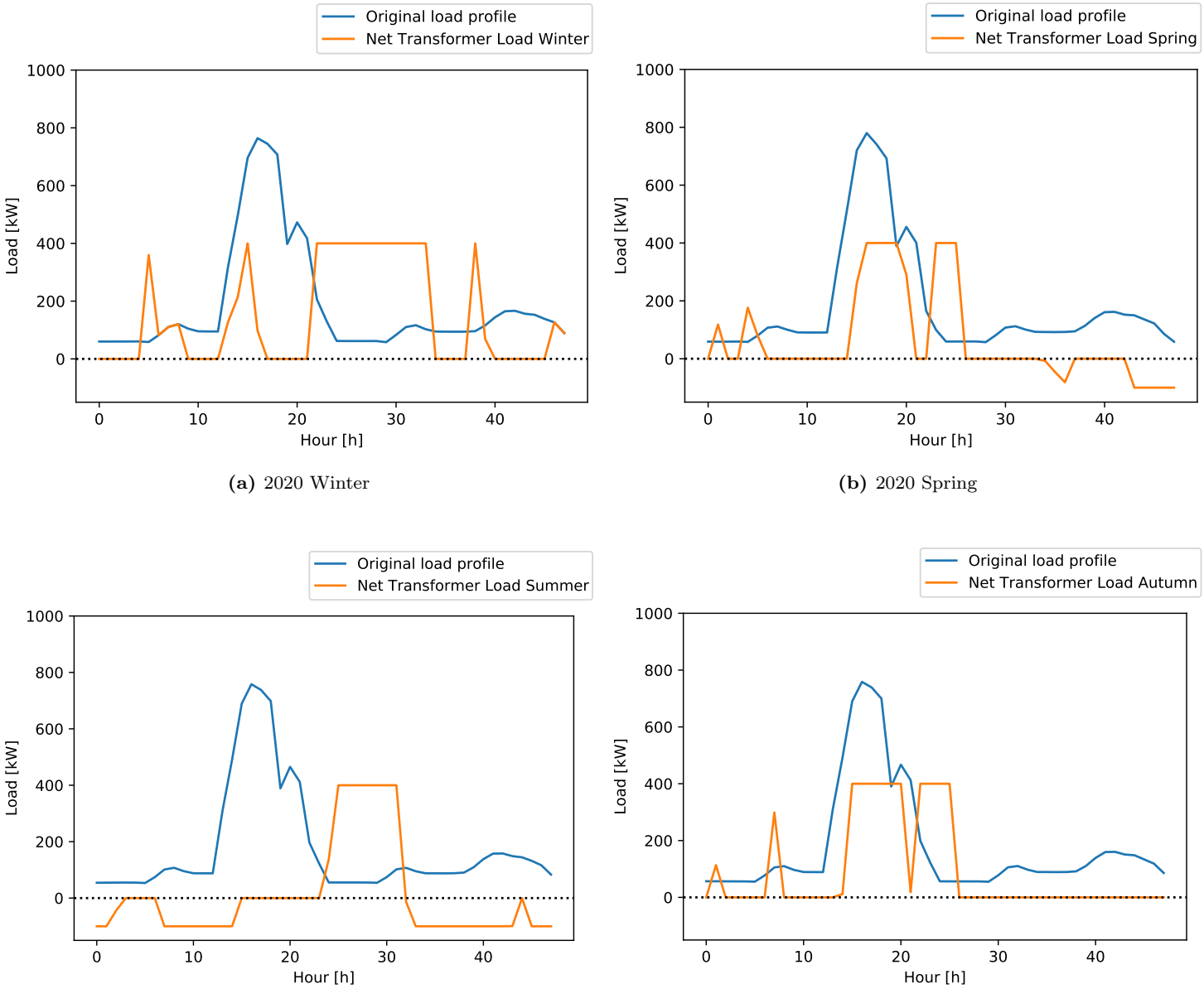

(a) 2020 Winter

(b) 2020 Spring

(c) 2020 Summer

(d) 2020 Autumn

Figure 48: Peak reduction during winter, spring, summer and autumn in 2020.

The first difference that was observed was the load profile. The addition of the housing profile together with the pump and EV demand led to a higher peak, just shy of 800 kW. As the base case profile only contained the EV and pump load, the load profile was very low in the hours when no EV's were charging. As observed in figure 48, the load profile is always greater than zero, with higher peaks than previously.

To continue, the net transformer load behaved differently for the connected case compared to the base case. The two main reasons were the additional load through out the day, and the resulting increased peak. The peak reduction sets a load limit of 400 kW. With the additional load and higher peak, the system needed to shift more of the load in order to remain beneath the limit. A primary observation was that the amount of power sold to the grid decreased drastically. During winter and autumn, no power was sold when running the new load profile. A comparison of the new transformer load for spring and summer also proved a vast decrease in power sold. Another observation is that the system shifted the load to different times through out the day. This was likely due to the variable spot price, which made it more profitable to distribute the load throughout the day.

Despite the differences previously mentioned, some re-occurring trends for each season were observed. The winter and summer case shifted the load for the most part outside the main peak. In contrast, large parts of the spring and autumn load were spread across the peak. In addition, the sales in the summer season were in the same region, mainly before the load peak and after the transformer load shift. A sell-off at the end of each spring season was also observed.

5.3.7 Comparison of Base Case and Connection Case

In order to obtain a better understanding of the cost reduction potential of the base case, the total costs were analyzed and compared for both the base case and the connection case. The total costs are presented in table 20. The different scenarios are presented in Section 4.5.5.

Table 20: Comparison of total costs for both base case and the connected case.

Total Cost Comparison				
	Winter 2020	Spring 2020	Summer 2020	Autumn 2020
Base Case Pump & EV [NOK]	540	14	-6	164
Base Case Only Housing Stock [NOK]	1 276	241	72	876
Base Case Sum [NOK]	1 816	255	66	1 040
Connected Case Sum [NOK]	1 653	171	23	797
Cost Decrease Base Case to Connected Case [%]	**9**	**33**	**65**	**23**

For all four cases, there was a substantial cost reduction when the system was connected. The largest reduction was seen in the summer, with a 65% reduction achieved. The smallest reduction

occurred in the winter with a more modest 9% reduction. Both spring and autumn saw a relative similar reduction at 33% and 23% respectively. The results are reasonable, and what may have been expected. This is due to the PV production being the highest during the summer and lowest during the winter. Since connecting the system meant adding the capabilities of the battery PV combination to the housing stock, the model was able to purchase less energy from the grid. In turn this reduced the overall costs substantially.

Another observation made was that the cost ratio between the different seasons are reasonably proportional in each case. This meant that the system behaves similarly in all cases, regardless of the configuration of the system connection.

5.3.8 Sensitivity Analysis for Transformer Capacity & Battery Constraint

As previously mentioned, the user-selected parameters will have an impact on the results. The grid-to-battery constraint and the transformer capacity constraint were the two most important parameters that were set freely. Both of these constraints worked as a capacity with a set value. The transformer constraint and battery constraint were set to 400 kW and 500 kW, respectively, for all results analyzed in Section 5.3; these values will be referred to as the base case from this point forward.

In this section it was therefore beneficial to perform a small sensitivity analysis based on these parameters. Values both larger and smaller than the base case have been analyzed.

- `gridToBattery : GTB`
- `Transformer_capacity : TC`

Sensitivity Cases

TC_1	270 kW
TC_2	300kW
TC_3	**400** kW
TC_4	550 kW
TC_5	750 kW
GTB_1	100 kW
GTB_2	300 kW
GTB_3	**500** kW
GTB_4	700 kW
GTB_5	1000 kW

Table 21: Small sensitivity analysis for both transformer capacity and grid to battery restriction. This is the cost in NOK over the course of 48 hours during winter 2020.

	GTB_1	GTB_2	GTB_3	GTB_4	GTB_5
TC_1	1 691	1 689	1 689	1 689	1 689
TC_2	1 679	1 678	1 678	1 678	1 678
TC_3	1 655	1 653	**1 653**	1 653	1 653
TC_4	1 631	1 629	1 628	1 628	1 628
TC_5	1 610	1 607	1 607	1 607	1 607

Table 22: Small sensitivity analysis for both transformer capacity and grid to battery restriction. This is the cost in NOK over the course of 48 hours during winter 2021.

	GTB_1	GTB_2	GTB_3	GTB_4	GTB_5
TC_1	4 114	4 105	4 105	4 105	4 105
TC_2	4 027	4 012	4 012	4 012	4 012
TC_3	3 801	3 784	**3 784**	3 784	3 784
TC_4	3 510	3 498	3 493	3 493	3 493
TC_5	3 327	3 311	3 311	3 311	3 311

Table 23: Small sensitivity analysis for both transformer capacity and grid to battery restriction. This is the cost in NOK over the course of 48 hours during summer 2020.

	GTB_1	GTB_2	GTB_3	GTB_4	GTB_5
TC_1	24	24	23	22	22
TC_2	24	24	23	22	22
TC_3	24	24	**23**	22	22
TC_4	24	24	23	22	22
TC_5	24	24	23	22	22

Table 24: Small sensitivity analysis for both transformer capacity and grid to battery restriction. This is the cost in NOK over the course of 48 hours during summer 2021.

	GTB_1	GTB_2	GTB_3	GTB_4	GTB_5
TC_1	847	827	793	784	780
TC_2	847	827	793	784	780
TC_3	847	827	**793**	784	780
TC_4	847	827	793	784	780
TC_5	847	827	793	784	780

Table 21, 22, 23 and 24 displays the effects of the parameter levels for transformer capacity and the grid to battery restriction. All cases were run with data sets for both winter and summer, for 2020 and 2021.

Analysing the edge cases for winter 2020, (GTB_5, TC_5) and (GTB_1, TC_1), a decrease/increase of around 5% was experienced. This was not a very large difference from the base case, and can signify the fact that these parameters did not alter the results to a significant degree. However when analyzing the edge cases for winter 2021 a decrease of around 20% from (GTB_1, TC_1) to (GTB_5, TC_5) was observed. The results were reasonable, as the volatile spot price in 2021 created higher potential for savings when increasing the transformer capacity. Some trends between the data sets for winter and summer were observed. For the summer cases, the change in price was only dependant on the GTB variables. When the GTB was unchanged, the costs remained unchanged regardless of an increased transformer capacity. For the winter cases, the prices were more dependant on the transmission capacity than the GTB variable.

Due to low PV production during the winter as presented in figure 9, the system would benefit more of increased transmission capacity compared to the summer, where PV production was high. In addition, the selling price of electricity back to the grid was set to 50% of the spot price meaning large volatility in price was needed for it to be profitable to buy power from the grid at full price and sell later at 50% of spot price.

5.3.9 Sensitivity Analysis Battery Size

As was done for the construction case on page 77 in table 15, a sensitivity analysis with respect to the size of the battery was performed. As this battery relates to the first stage of the energy central, which corresponds to the middle of phase two of the overall construction effort. This equates to 342 housing units, with a planned construction of almost 600 units. This was described in section 3.1 on page 24. Consequently further expansions of the energy central is planned. To further understand the current state of the battery dimensioning, a sensitivity analysis was performed for the 2020 data sets, for all four seasons. Values both higher and lower than the current size was included.

Table 25: Sensitivity analysis for battery size. Connected case along with 2020 data sets.

	Total El Cost 2020 [NOK]			
Battery Size [kWh]	Winter	Spring	Summer	Autumn
500	1 780	198	37	910
750	1 716	184	29	843
1000	1 653	171	23	797
1 250	1 591	158	18	751
1 500	1 528	145	15	705

As can be seen in table 25, the largest differences are observed in the seasons with the most sun. The winter period exhibited only a 14% decrease in costs from the 500kW case to the 1500kW

case, while the summer season experienced a decrease of almost 60%. This was to be expected, as the larger share of PV production could benefit from larger capacities to store excess energy when the loads were small. Even though cost savings could be achieved by installing a higher capacity battery, it did not appear to be a worthwhile endeavour for the current stage. The summer period would benefit the most from the higher capacity, but the summer period already displayed very low costs, so a percentage-wise large reduction translates to a very small monetary gain. However, this was based on the spot prices from 2020, which were quite low. The 2021 prices were much higher, and can also be analyzed.

Table 26: Sensitivity analysis for battery size. Connected case along with 2021 data sets.

	Total El Cost 2021 [NOK]			
Battery Size [kWh]	Winter	Spring	Summer	Autumn
500	4 129	1 818	1 268	4 050
750	3 955	1 683	1 008	3 724
1 000	3 784	1 559	793	3 503
1 250	3 614	1 436	640	3 286
1 500	3 443	1 315	515	3 075

Studying table 26, all costs were comparatively much higher compared to the 2020 data. The same trends regarding the percentage wise reduction still applied. The winter period exhibited a similar reduction in price from the edge cases of battery size, a 17% decrease in costs from the 500kWh battery to the 1500 kWh battery. The summer period again displayed a 60% decrease in costs. However, as the spot price was overall much higher, the expanded battery yield a much higher associated reduction in monetary costs. This could signify the increasing potential for larger batteries. This could also hold true for the future, as higher volatility and high prices are forecasted for several years in the future [76]. The volatility mentioned is also key. With large discrepancies in pricing throughout the day, a battery can be used to good effect as a balancing tool, as it can both import and export power depending on the need. This already holds true for the 2021 data, as can be seen in figure 23 on page 49. The 2021 data was much more volatile than the 2020 data. Furthermore, as sales of power from the battery to the grid was not sold at spot price, but rather at 50% of the spot price in this thesis, large variations during the day could make it profitable for the battery to purchase power during times of diminished prices, and sell during periods of elevated prices.

5.3.10 Total Cost and Emissions

Total El Cost

The total cost equals the sum of the net transformer load multiplied with the spot price for each of the 48 hours.

Table 27: Total cost during 48 hours.

	Total El Cost			
	Winter	Spring	Summer	Autumn
2020	1 653 NOK	171 NOK	23 NOK	797 NOK
2021	3 784 NOK	1 559 NOK	793 NOK	3 503 NOK

In table 27, the total el cost during summer and spring is clearly cheaper than the winter and autumn. This was to be expected, as the PV had its highest production during these months and could therefore produce a considerable amount of power. During the winter months, the PV produced less energy, resulting in a smaller decrease. Nevertheless, the additions of smart charging and battery + PV had a significant impact, particularly during winter when the spot price was significantly higher.

Emissions Reduction

Considering only the electric demand, the total demand for the 48 hour winter period equated to 8 920 kWh. Assessing only the used power, the new demand equaled 8 920 kWh before subtracting the total PV production during the 48 hours. This resulted in a net demand of 1 072 kWh for the summer period, and 7 995 kWh for the winter period. That is, an 88%, and 10% reduction respectively for the summer and winter period. Consequently, in a simplified manner, this is proportional to the reduction in emissions. The total power and emission reduction by the PV system is presented in table 28.

Table 28: Power and emission reduction from PV over 48 hours.

Season	**Total Demand [kWh]**	**PV Production[kWh]**	**Reduction [%]**	**Emission Reduction [$kgCO_2$]**
Winter	8920	925	10	278
Spring	8768	4677	53	1403
Summer	8576	7504	88	2251
Autumn	8658	3216	37	965

The table displays a large potential for reducing emissions. Using CO_2 equivalent emissions from European electricity at 300 gCO_2e/kWh, the PV system was able reduce up to 2 251 $kgCO_2e$ during the 48 hour phase, proving that the system operates effectively and contributes greatly to achieving zero emission when implemented.

Recommendations

Examining the results in section 5.3.8 and 5.3.9, the current dimensioning can be assessed as adequate, as it strikes a balance between cost reductions, and investment cost. The chosen parameters for power import and and power peak reduction also hold water as a good choice. The battery import capacity does not affect the cost to a large degree, as purchase of power is often not utilized as much, due to the fractional price of selling back to the grid, however, this constraint will become

more relevant if spot prices become more volatile. The constraint on peak power can be further reduced during the summer without affecting the price. During the winter, this constraint does affect the total price, and can be either lowered or raised depending on the desired result. As mentioned, the battery size is adequate for the first stage of the energy central. However, with more buildings being constructed in the area, along with higher spot prices and more volatility, a higher battery capacity can be very beneficial. This also applies to the installment of additional PV-capacity, as higher spot prices allows a much shorter payback time for these systems.

6 Conclusion

An energy supply analysis was conducted both during, and after the construction of a zero emission neighbourhood in Hønefoss, Norway. The area contained a combined energy central of a 500kWp solar array, a 1 MWh battery, and either a 1.1 MW boiler system or connection to a district heating system. The impact of this implementation was mainly considered in regards to cost.

The construction phase took place during a one year period (2021), split into five subsequent phases of construction, with different demand profiles. Each phase was analyzed in regards to the battery and PV system's interaction with the construction site and the external grid, along with the costs this entailed.

After the completion of the construction phase, phase two of the project was considered. This meant a housing stock with both a heating demand as well as an electric demand for the houses and electric vehicles. This systems interaction together with the aforementioned energy central was evaluated over 48 hours. Four instances, including winter and summer for both 2020 and 2021, were analyzed.

Results from the construction phase reveal a clear advantage in operational costs and emissions from utilizing electric construction machinery in conjunction with the PV and battery system, instead of traditional diesel powered machinery. The overall consumption for the duration of construction was 652 788 kWh, which corresponds to approximately 65 278L of diesel. The total emission reduction using electric machinery equaled 171.3 $tCO2e$, or 98%. Taking into consideration the purchased electricity from the grid, the electric machinery resulted in a fuel cost decrease of 530 812 NOK, or 83.6%. Despite a number of obstacles associated with electric construction equipment, most notably the logistics of maintaining a zero-emission building site, the concept has significant potential. It will become a feasible replacement for fossil fueled machinery and contribute to a reduction in construction industry emissions as a result of future investment and development.

After the completion of the construction phase, a decrease of peak power demand of almost 50% was set as a baseline parameter. Even with this major reduction, total cost related to purchase of electricity decreased by 65% during summer. For the winter period, a decrease of 9% was achieved. The added power production from the PV system entailed a decrease of direct emissions related to used power from the external grid by 10% and 88% respectively for the winter and summer period.

In conclusion, the installation of a 500 kWp PV system and a 1 MWh battery will have a significant effect on operational costs and emissions throughout the construction phase and after the project is completed. The installation of this system demonstrates that the construction industry has significant potential to cut emissions, and the residents of Tanberghøgda will benefit considerably from it.

7 Continuation of Thesis Work

Further work on the project includes

- Attaining data for construction machinery to improve accuracy of charging schedule.
- Implement a suitable time schedule for the project time line to achieve improve data accuracy.
- Extend the time period of the optimization model in order to attain a better understanding of long term costs and optimal operation. This will allow the addition of transmission grid fee to the model.

Bibliography

[1] Jonas Dalby, Eskil Kvålsvold, M. A. W. S. 2022. Energi- og klimakonsept for utviklingen av et nullutslipps boligområde – analyse av energiforsyningsløsninger. (1), 93.

[2] BREEAM - The world's leading science-based suite of validation and certification systems for a sustainable built environment. https://bregroup.com/products/breeam/. Accessed: 2022-15-11.

[3] COWI. 2022. Energi- og klimakonsept for Tanberghøgda. 1, 116.

[4] Direktoratet for byggkvalitet. Byggteknisk forskrift (TEK17) med veiledning. https://dibk.no/Templates/DIBK/Pages/Veiledninger/Print/PrintChapter.aspx?chapterId=50488. Accessed: 2022-10-03.

[5] Arbeidstilsynet. Veiledning om arbeid ved dataskjerm. https://radem.no/dok/publikasjoner/AT-540%20-%202006%20Arbeid%20ved%20dataskjerm.pdf. Accessed: 2022-10-03.

[6] Harket, H. T. 2009. ENERGIMERKING AV BYGG. (2), 4. URL: https://publikasjoner.nve.no/faktaark/2009/faktaark2009_02.pdf.

[7] Mosland,T.B. Tekna. Hva er et passivhus, published 26.11.2013. https://www.tekna.no/fag-og-nettverk/bygg-og-anlegg/byggbloggen/hva-er-et-passivhus/. Accessed: 2022-11-11.

[8] Tekna. Krav til passivhus, published 02.01.2021. https://www.tekna.no/fag-og-nettverk/bygg-og-anlegg/byggbloggen/krav-til-passivhus/. Accessed: 2022-11-11.

[9] NVE. Solkraft. https://www.nve.no/energi/energisystem/solkraft/. Accessed: 2022-09-20.

[10] American Solar Energy Society. Monocrystalline vs Polycrystalline Solar Panels, published 20.02.2021. https://ases.org/monocrystalline-vs-polycrystalline-solar-panels//. Accessed: 2022-11-17.

[11] Hanifi, H., Schneider, J., & Bagdahn, J. 09 2015. REDUCED SHADING EFFECT ON HALF-CELL MODULES – MEASUREMENT AND SIMULATION. URL: https://www.researchgate.net/publication/283488492_REDUCED_SHADING_EFFECT_ON_HALF-CELL_MODULES_-_MEASUREMENT_AND_SIMULATION.

[12] Australian Renewable Energy Agency. 2017. Hot-spot cell temperature in half

cell photovoltaic modules. 3. URL: https://arena.gov.au/assets/2017/02/lessons-learnt-pv-mate-half-cell-hotspot.pdf.

[13] Hayibo, K. S., Petsiuk, A., Mayville, P., Brown, L., & Pearce, J. M. 2022. Monofacial vs bifacial solar photovoltaic systems in snowy environments. *Renewable Energy*, 193, 657–668. URL: https://www.sciencedirect.com/science/article/pii/S0960148122006917, doi: https://doi.org/10.1016/j.renene.2022.05.050.

[14] Kostopoulos, E. D., Spyropoulos, G. C., & Kaldellis, J. K. 2020. Real-world study for the optimal charging of electric vehicles. *Energy Reports*, 6, 418–426. URL: https://www.sciencedirect.com/science/article/pii/S2352484719310911, doi: https://doi.org/10.1016/j.egyr.2019.12.008.

[15] Vestwood. 2022. FlexLi-L Series 1MW1MWh BESS Project. *Battery Reports*, 13.

[16] Frederiksen, S. & Werner, S. 2013. *District Heating and Cooling*. Studentlitteratur AB, 1 edition.

[17] Elvia. Hva er nettleie? https://www.elvia.no/nettleie/alt-om-nettleie/hva-er-nettleie/. Accessed: 2022-12-13.

[18] Føie. Nettleie priser og avtaler, published 30.09.2022. https://www.foie.no/viktig-kundeinformasjon/nye-priser-pa-nettleie-fra-17.-oktober. Accessed: 2022-12-10.

[19] NVE. Ny nettleie modell, published 16.12.2021. https://www.nve.no/reguleringsmyndigheten/kunde/nett/ny-nettleie-fra-1-juli-2022/. Accessed: 2022-12-13.

[20] Statkraft. Fjernvarme. https://www.statkraft.no/var-virksomhet/fjernvarme/. Accessed: 2023-04-24.

[21] Ann Christin Bøeng. Stadig mer bruk av fjernvarme, published 14.05.2020. https://www.ssb.no/energi-og-industri/artikler-og-publikasjoner/stadig-mer-bruk-av-fjernvarme. Accessed: 2023-04-24.

[22] FHI. FHI - Legionella, updated 21.11.2022. https://www.fhi.no/nettpub/smittevernveilederen/sykdommer-a-a/legionellose/. Accessed: 2023-04-26.

[23] Nord, N. 2023. Lecture Notes NTNU: "Design and sizing of hydronic systems". Provided by course TEP4245 Klimateknikk . 33.

[24] Enigneer Excel. Pump Efficiency Explained. https://engineerexcel.com/pump-efficiency/. Accessed: 2023-05-03.

[25] Nord, N. 2016. Lecture Notes NTNU: "Economy of Distric heating". Provided by supervisor. 39.

[26] John Siegenthaler (P.E). 2012. *Modern Hydronic Heating*. Cengage Learning, 3 edition.

[27] Vardar Green Energy. Vardar Green Energy - Fjernvarme: Produkter og priser. https://vardar.no/bioenergi/produkter-og-priser/. Accessed: 2023-04-26.

[28] Regjeringen. Regjeringens strømtiltak, updated 16.02.2023. https://www.regjeringen.no/no/tema/energi/regjeringens-stromtiltak/id2900232/?expand=factbox2900261. Accessed: 2023-04-26.

[29] Byggenæringens Landsforening. Om byggenæringen. https://www.bnl.no/om-oss/om-byggenaringen/. Accessed: 2022-11-02.

[30] Asplan Viak. 2019. Bygg- og anleggssektorens klimagassutslipp. 14. URL: https://www.bnl.no/siteassets/dokumenter/rapporter/klimautslipp_bae_2019.pdf.

[31] European Central Bank. Monthy Bulletin May 2009. https://www.ecb.europa.eu/pub/pdf/mobu/mb200905en.pdf. Accessed: 2022-11-07.

[32] Miljødirektoratet. Forbud mot fyring med mineralolje til oppvarming. last updated: 29.01.2021. https://www.miljodirektoratet.no/ansvarsomrader/klima/for-myndigheter/kutte-utslipp-av-klimagasser/fyringsforbud-mineralolje/. Accessed: 2022-11-02.

[33] Tekna. Lavtempererte varmeanlegg, published 03.12.2020. https://www.tekna.no/fag-og-nettverk/bygg-og-anlegg/byggbloggen/lavtempererte-varmeanlegg/. Accessed: 2022-11-07.

[34] Vieira, L. C., Longo, M., & Mura, M. 2021. Are the european manufacturing and energy sectors on track for achieving net-zero emissions in 2050? an empirical analysis. *Energy Policy*, 156, 112464. URL: https://www.sciencedirect.com/science/article/pii/S0301421521003347, doi:https://doi.org/10.1016/j.enpol.2021.112464.

[35] European Commission. A European Green Deal. https://ec.europa.eu/info/strategy/priorities-2019-2024/european-green-deal_en. Accessed: 2022-12-03.

[36] Lin, T., Lin, Y., Ren, H., Chen, H., Chen, Q., & Li, Z. 2020. Development and key technologies of pure electric construction machinery. *Renewable and Sustainable Energy Reviews*, 132, 110080. URL: https://www.sciencedirect.com/science/article/pii/S1364032120303713, doi:https://doi.org/10.1016/j.rser.2020.110080.

[37] Karlsson, I., Rootzén, J., Johnsson, F., & Erlandsson, M. 2021. Achieving net-zero carbon emissions in construction supply chains – a multidimensional analysis of residential building systems. *Developments in the Built Environment*, 8, 100059. URL: https://www.sciencedirect.com/science/article/pii/S2666165921000181, doi:https://doi.org/10.1016/j.dibe.2021.100059.

[38] Carmen, M., Giulia, M., Delia, D., & Paolo, B. 2022. Towards a decarbonised building stock by 2050: The meaning and the role of zero emission buildings (zebs) in europe. *Energy Strategy Reviews*, 44, 101009. URL: https://www.sciencedirect.com/science/article/pii/S2211467X22002036, doi:https://doi.org/10.1016/j.esr.2022.101009.

[39] European Commission. Energy Performance of Building Directive. https://energy.ec.europa.eu/topics/energy-efficiency/energy-efficient-buildings/energy-performance-buildings-directive_en. Accessed: 2022-05-12.

[40] IPCC.Global Warming of 1,5 Degrees Celcius. https://www.ipcc.ch/sr15/. Accessed: 2022-12-06.

[41] Klima- og miljødepartement. Klimaendringer og norsk klimapolitikk, last updated 22.10.2021. https://www.regjeringen.no/no/tema/klima-og-miljo/innsiktsartikler-klima-miljo/klimaendringer-og-norsk-klimapolitikk/id2636812/. Accessed: 2022-12-06.

[42] Samferdselsdempartement. Norge er elektrisk, last updated 10.06.2021. https://www.regjeringen.no/no/tema/transport-og-kommunikasjon/veg_og_vegtrafikk/faktaartikler-vei-og-ts/norge-er-elektrisk/id2677481/. Accessed: 2022-12-06.

[43] Wiik, M. K., Haukaas, N.-O., Ibsen, J. I., Lekanger, R., Thomassen, R., Sellier, D., Schei, O. O., & Suul, J. A. 2020. Nullutslippsgravemaskiner. (1), 56. URL: https://www.sintefbok.no/book/index/1252/nullutslippsgravemaskin_laeringsutbytte_fra_elektrifisering_av_anleggsmaskiner.

[44] Sintef. Alt ligger til rette for utslippsfrie byggeplasser i Oslo, published 24.05.2022. https://www.sintef.no/siste-nytt/2022/alt-ligger-til-rette-for-utslippsfrie-byggeplasser-i-oslo/. Accessed: 2022-12-06.

[45] Fufa, S. M., Mellegård, S., Wiik, M. K., Flyen, C., Hasle, G., Bach, L., Gonzalez, P., Løe, E. S., & Idsøe, F. 2018. Utslippsfrie byggeplasser. (1), 72. URL: https://www.sintefbok.no/book/index/1190/utslippsfrie_byggeplasser_state_of_the_art.

[46] Amundsen, A. Reduserte utslipp fra anleggsmaskiner, published 2021. https://www.tiltak.no/c-miljoeteknologi/c1-drivstoff-og-effektivisering/reduserte-utslipp-fra-anleggsmaskiner/. Accessed: 2022-11-08.

[47] Tekna. Passivhusstandard, published 02.01.2021. https://www.tekna.no/fag-og-nettverk/bygg-og-anlegg/byggbloggen/krav-til-passivhus//. Accessed: 2022-11-08.

[48] Fossheim, M. KlimaOslo. Utslippsfri byggeplass med el-gravemaskiner,

published 20.03.2019. https://www.klimaoslo.no/2019/03/20/utslippsfri-byggeplass-med-el-gravemaskiner/. Accessed: 2022-11-08.

[49] Nasta. Nasta ZE85. https://www.nasta.no/anleggsmaskiner/anleggsmaskin/zeron-ze85/. Accessed: 2022-11-09.

[50] Nasta. Nasta ZE160LC. https://www.nasta.no/anleggsmaskiner/anleggsmaskin/zeron-ze160/. Accessed: 2022-11-09.

[51] ur Rehman, H., Korvola, T., Abdurafikov, R., Laakko, T., Hasan, A., & Reda, F. 2020. Data analysis of a monitored building using machine learning and optimization of integrated photovoltaic panel, battery and electric vehicles in a central european climatic condition. *Energy Conversion and Management*, 221, 113206. URL: https://www.sciencedirect.com/science/article/pii/S0196890420307500, doi:https://doi.org/10.1016/j.enconman.2020.113206.

[52] Wegener, Moritz, Isalgué, Antonio, Malmquist, Anders, Martin, & Andrew. 2019. 3e-analysis of a bio-solar cchp system for the andaman islands, india—a case study. *Energies*, 12(6). URL: https://www.mdpi.com/1996-1073/12/6/1113, doi:10.3390/en12061113.

[53] Moelven Pellets AS. Moelven Pellets. https://www.moelven.com/no/om-moelven/moelven-pellets/. Accessed: 2022-02-12.

[54] Vardar Green Energy. Vardar Fjernvarme. https://www.vardar.no/bioenergi/. Accessed: 2022-12-02.

[55] Fossen Utvikling AS. Tanberghøgda. https://www.fossenutvikling.no/prosjekter/tanberghogda/. Accessed: 2022-11-01.

[56] Frederik W. Skarstein (Fossen Utvikling AS). Tanberghøgda Ny bydel i Hønefoss. https://fagus.no/wp-content/uploads/2020/11/12.-Frederik-Skarstein.pdf. Accessed: 2023-05-10.

[57] COWI. I dette området vil 600 boliger være selvforsynte med energi, published 18.03.2022. https://www.cowi.no/om-cowi/nyheter-og-presse/i-dette-omraadet-vil-600-boliger-vaere-selvforsynte-med-energi. Accessed: 2022-11-11.

[58] Ringerike Kommune (26.10.2022). Detaljregulering for 495 - Tanbergdansen - oppstart av planarbeid for solcelleanlegg. https://www.ringerike.kommune.no/globalassets/bilder-blokker-og-filarkiv/bilder-og-dokumenter/samfunn/areal-og-byplan/pagaende-planprosesser/varsel-om-oppstart/495---tanbergdansen/detaljregulering-for-495---tanbergdansen---oppstart-av-planarbeid-for-solcelleanlegg.pdf. Accessed: 2023-05-16.

[59] Naturvernforbundet - er solkraft og sau framtidas klimaløsning? https://naturvernforbundet.no/oppland/nyheter/er-solkraft-og-sau-framtidas-klimalosning-article42495-1052.html. Accessed: 2022-11-11.

[60] COWI. 2022. KOSTNADSBEREGNING FOR VARMESENTRAL TANBERGHøGDA. *Internal documents*, 4.

[61] Roland, E. W. 2022. Energiforsyning for utslippsfri byggeplass. (1), 77. URL: https://ntnuopen.ntnu.no/ntnu-xmlui/handle/11250/3020767.

[62] Hansen, J. S. 2013. Analyse av energiytelser til sirkulasjonspumper i bygninger. (1), 148. URL: https://ntnuopen.ntnu.no/ntnu-xmlui/handle/11250/241791.

[63] Haugsbø, M. S., Ellis, I. O., & Johansson, M. Reisevaner i Ringeriksregionen 2013/14. Published 11.08.2015. https://s3.eu-west-1.amazonaws.com/rr-urbanet/Filer-Dokumenter/UArapport_59_RVU_Ringeriksregionen.pdf. Accessed: 2022-11-03.

[64] Bråthen, H. Statistisk Sentralbyrå. To av tre nye personbiler er elbiler, published 25.03.2022. https://www.ssb.no/transport-og-reiseliv/landtransport/statistikk/bilparken/artikler/to-av-tre-nye-personbiler-er-elbiler. Accessed: 2022-11-03.

[65] Eco Cost Savings. Average Electric Car KWh Per Mile [Results From 231 EVs]. https://ecocostsavings.com/average-electric-car-kwh-per-mile/. Accessed: 2022-12-09.

[66] Statnett. Om strømpriser. https://www.statnett.no/om-statnett/bli-bedre-kjent-med-statnett/om-strompriser/. Accessed: 2023-05-09.

[67] Mjønerud, I. Plusskunde – spørsmål og svar, last updated 17.11.2019. https://strÃÿm.no/plusskunde. Accessed: 2022-11-02.

[68] Norsk klimaservicesenter. Observasjoner og værstatistikk. https://seklima.met.no/observations/?fbclid=IwAR1gzRKs4NpdqPrgToa_r3bRBwCKYSCsW4dnvERZkcPjx-XIzCF3FVEz5LM. Accessed: 2022-12-03.

[69] Standard Norge. NS-EN 303-5:2021 + A1:2022. https://www.standard.no/no/Abonnement/Standarder/. Accessed: 2023-05-04.

[70] Jach-Nocoń, M., Pełka, G., Luboń, W., Mirowski, T., Nocoń, A., & Pachytel, P. 2021. An assessment of the efficiency and emissions of a pellet boiler combusting multiple pellet types. *Energies*, 14(15). URL: https://www.mdpi.com/1996-1073/14/15/4465, doi:10.3390/en14154465.

[71] NVE-RME. Høring - Forslag om innføring av modell for deling av overskuddsproduksjon. https://www.nve.no/reguleringsmyndigheten/regulering/regelverk-og-hoeringer/horinger/hoeringer-reguleringsmyndigheten-for-energi-rme/

hoering-forslag-om-innfoering-av-modell-for-deling-av-overskuddsproduksjon/. Accessed: 2023-03-22.

[72] NordPool. Day-ahead prices. https://www.nordpoolgroup.com/en/Market-data1/Dayahead/Area-Prices/NO/Daily1/?view=table. Accessed: 2022-10-12.

[73] Kennedy, R. PV Magazine. How long do residential energy storage batteries last? published 21.09.2021. https://pv-magazine-usa.com/2021/09/21/how-long-do-residential-energy-storage-batteries-last//. Accessed: 2022-06-12.

[74] SSB. Sal av petroleumsprodukt og flytande biodrivstoff. https://www.ssb.no/statbank/table/09654/tableViewLayout1/. Accessed: 2022-12-15.

[75] Michelin. How To Calculate Your Fleet's Carbon Footprint, published 27.10.2022. https://connectedfleet.michelin.com/blog/calculate-co2-emissions. Accessed: 2022-12-08.

[76] Gunnar G. Løvås (NVE). 2023. Langsiktig markedsanalyse. 80. URL: https://www.statnett.no/for-aktorer-i-kraftbransjen/planer-og-analyser/langsiktig-markedsanalyse/?fbclid=IwAR0RDllpdkYgJgOXXEJaCDsrnwfgIAKSGGtALYd_amrCaFv7OGBXsVbh6wg.

A Appendices

A.1 Python Code for Energy Needs and Costs During Construction Phase

```
"""
Created on Sat Oct  8 09:21:16 2022
"""
import matplotlib.pyplot as plt
import numpy as np
import pandas as pd

"-------------------------------------------------ARRAY-----------------------------------
time = np.arange(0,8760) #8760 hours in one year

#import the excel file with the necessary spot price data
import_prices=pd.read_excel('/Users/jonas/Downloads/Excel-data-byggeplass.xlsx','Spot_price')
import_prices.head()
type(import_prices.to_numpy())
import_prices.to_numpy()[0]
spot_prices = import_prices.to_numpy()

#import the excel file with the necessary PV prod data
import_pv_prod = pd.read_excel('/Users/jonas/Downloads/Excel-data-byggeplass.xlsx', 'PV_prod')
import_pv_prod.head()
type(import_pv_prod.to_numpy())
import_pv_prod.to_numpy()[0]
pv_prod = import_pv_prod.to_numpy()

#Demand for each hour, calculated with energy supply needs
#for machines in each stage of construction
demand_groundwork = np.zeros(8760)
demand_building   = np.zeros(8760)
demand_facade     = np.zeros(8760)
demand_internal   = np.zeros(8760)
demand_outdoors   = np.zeros(8760)
"-----------------------------------------------DATAINIT----------------------------------
battery_cap = 1000 # maximum 1000kW
battery_charge = np.zeros(8760)
battery_discharge = np.zeros(8760)
sum_charge = np.zeros(8760)
cost_array = np.zeros(8760)
grid_battery_pv = np.zeros(8760)
chosen_demand = np.zeros(8760)
available_battery = np.zeros(8760)
pv_battery_combined = np.zeros(8760)
deficit = np.zeros(8760)
surplus = np.zeros(8760)
sell = np.zeros(8760)
buy = np.zeros(8760)
totalSales = np.zeros(8760)
totalPurchase = np.zeros(8760)
power_waste = np.zeros(8760)
"-----------------------------------------------MENU--------------------------------------
ans=-1
length = 0
while ans == -1 : #The menu. Choosing which phase we want to analyse.
    print ("""
    1.Groundwork
    2.Building
    3.Facade
    4.Internal
    5.Outdoors
    """)
    ans= input("Choose your model!")
    if ans=="1":
```

```
      chosen_demand = demand_groundwork
      length = 24
      sheet = "demand_groundwork"
    elif ans=="2":
      chosen_demand = demand_building
      length = 15
      sheet = "demand_building"
    elif ans=="3":
      chosen_demand = demand_facade
      length = 15
      sheet = "demand_facade"
    elif ans=="4":
      chosen_demand = demand_internal
      length = 15
      sheet = "demand_internal"
    elif ans=="5":
      chosen_demand = demand_outdoors
      length = 9
      sheet = "demand_outdoors"
    elif ans !="":
      print("\n Not Valid Choice Try again")

"-----------------------------------------EXCEL-----------------------------------------
# First, collecting the values from the data file in
#Excel and distribute them into belonging sets
df = pd.read_excel('/Users/jonas/Downloads/Excel-data-byggeplass.xlsx', sheet)

demand_data = {'Maskintype': [], 'Betegnelse': [], 'Energiforsyning': [],
               'Kablet effekt [kW]': [],'Batteristørrelse [kWh]': [],
               'Maks ladeeffekt [kW]': [], 'Ladesyklus [antall/døgn]': [],
                'Ladeeffekt natt [kW]': [], 'Ladetimer natt [h]': []}

# Implementing data from excel file to generator dictionary
for i in range(9):
    key = df.iat[1, i]
    for l in range(length):
        a = df.iat[l+2, i]
        demand_data[key].append(df.iat[l+2, i])

# Create dictionary called demand_data
betegnelse = dict(zip(demand_data['Maskintype'], demand_data['Betegnelse']))
energiforsyning = dict(zip(demand_data['Maskintype'], demand_data['Energiforsyning']))
kablet_effekt = dict(zip(demand_data['Maskintype'], demand_data['Kablet effekt [kW]']))
batteristørrelse = dict(zip(demand_data['Maskintype'], demand_data['Batteristørrelse [kWh]']))
maks_ladeeffekt = dict(zip(demand_data['Maskintype'], demand_data['Maks ladeeffekt [kW]']))
ladesyklus = dict(zip(demand_data['Maskintype'], demand_data['Ladesyklus [antall/døgn]']))
ladeeffekt_natt = dict(zip(demand_data['Maskintype'], demand_data['Ladeeffekt natt [kW]']))
ladetimer_natt = dict(zip(demand_data['Maskintype'], demand_data['Ladetimer natt [h]']))
demand_dict = {'Betegnelse': betegnelse, 'Energiforsyning': energiforsyning,
               'Kablet effekt [kW]': kablet_effekt,  'Batteristørrelse [kWh]': batteristørrelse,
               'Maks ladeeffekt [kW]': maks_ladeeffekt,'Ladesyklus [antall/døgn]': ladesyklus,
               'Ladeeffekt natt [kW]': ladeeffekt_natt, 'Ladetimer natt [h]': ladetimer_natt}

 #The machines who have to charge twice a day
 #have to charge with max charging effect during lunch.
for t in range(length):
    if demand_dict['Ladesyklus [antall/døgn]'][t] == 2:
        chosen_demand[11] = chosen_demand[11] + demand_dict['Maks ladeeffekt [kW]'][t]
        chosen_demand[35] = chosen_demand[35] + demand_dict['Maks ladeeffekt [kW]'][t]

#The machines have to charge after work.
```

```
for t in range(length):
    while demand_dict['Ladetimer natt [h]'][t] > 0:
        for k in range(16,33): #timene mellom arbeidsdagen slutter og starter igjen, dag 1
            chosen_demand[k] = chosen_demand[k] + demand_dict['Ladeeffekt natt [kW]'][t]
            demand_dict['Ladetimer natt [h]'][t] = demand_dict['Ladetimer natt [h]'][t] - 1
            if demand_dict['Ladetimer natt [h]'][t] == 0:
                demand_dict['Ladeeffekt natt [kW]'][t] = 0

for i in range(16,24):
    chosen_demand[i+24]=chosen_demand[i]   #Setting demant at the evening equal to each other.

for i in range(11,8712):
    chosen_demand[i+48]=chosen_demand[i]   #looping the demand from the first 48 hours.

for i in range(120,168):
    chosen_demand[i] = 0   #Setting the demand during weekends equal to zero.

#looping the demand the first week.
for i in range(1,8592):
    chosen_demand[i+168] = chosen_demand[i]

"----------------------------------------INITIALIZING-----------------------------------------
#setting the battery level equal to 1000 kW in the first hour.
available_battery[0] = battery_cap
for t in time:
    sum_charge[t] = pv_prod[t]-chosen_demand[t] #charge sum is PV prod - demand [kW]
for t in time:
    if sum_charge[t] >= 0:
        surplus[t] = sum_charge[t]        #battery_charge to surplus
    else:
         deficit[t] = sum_charge[t]       #battery_discharge to deficit

'----------------------------------------Charging----------------------------------------------
for t in time:
    if sum_charge[t] > 0 :
        if  (t<8759) and (available_battery[t] + surplus[t] >= battery_cap):
            available_battery[t+1] = battery_cap #Setting the battery level to max.
            #selling excess power to the grid.
            sell[t] = available_battery[t] + surplus[t] - battery_cap
            if sell[t] > 100:
                power_waste[t] = sell[t] - 100 #cannot sell more than 100 kW each hour
                sell[t] = 100
            battery_charge[t] = battery_cap - available_battery[t]
        if  (t<8759) and (available_battery[t] + surplus[t] < battery_cap):
            battery_charge[t] = surplus[t] #charging the battery
            available_battery[t+1] = available_battery[t] + battery_charge[t]
    if sum_charge[t] < 0 :
        if  (t<8759) and (abs(deficit[t]) < available_battery[t]):
            battery_discharge[t] = deficit[t] #discharging the battery
            available_battery[t+1] = available_battery[t] + battery_discharge[t]
        if  (t<8759) and (abs(deficit[t]) > available_battery[t]):
            battery_discharge[t] = available_battery[t]
            #have to buy power from grid when the battery is empty.
            buy[t] = deficit[t] + battery_discharge[t]
            available_battery[t+1] = 0
    if (t<8759) and (deficit[t]==0) and (surplus[t]==0):
        available_battery[t+1] = available_battery[t] #nothing happens to the battery level.

'----------------------------------------COST----------------------------------------------
for t in range(0,8760):
    cost_array[t] = np.multiply(spot_prices[t], 0.5*sell[t])
```

```
    + np.multiply(spot_prices[t], buy[t])
    #sell power for 0.5 times the spot price.
    totalSales[t] = np.multiply(spot_prices[t], 0.5*sell[t])
    totalPurchase[t]=np.multiply(spot_prices[t], buy[t])

totalcost_array = np.multiply(cost_array, 0.01) #going from NOK/kWh to øre/kWh
sumCost = sum(totalcost_array)
sumPV = sum(pv_prod)

if sumCost < 0:
    print("Total cost of:", round(abs(sumCost)), "NOK") #printing the cost
if sumCost > 0:
    print("Total gain of:", round(abs(sumCost)), "NOK") #printing the gain

print('Total gain of selling power:',sum(totalSales)*0.01, 'NOK')
print('Total cost of buying power:',abs(sum(totalPurchase)*0.01), 'NOK')
print('Total unused power:', np.round(sum(power_waste)), 'kWh')
print('Total power production:', np.round(sumPV), 'kWh')

'-----------------------------------------ADDITIONAL-PLOTTING-------------------------------
for t in time:
    pv_battery_combined[t] = pv_prod[t] + abs(battery_discharge[t]) #only for plotting.


"-----------------------------------------------PRINT/PLOT-----------------------------------
#plot for demand, PV prod, spot prices and sales. Comment out the irrelevant variables.
t = [i for i in range(0,8760)]
plt.figure(dpi=1200)
fig, ax1 = plt.subplots()

#plotting the maximum transformer capacity
ax1.plot(t,chosen_demand, color='r', label = 'Demand')
ax1.plot(t, available_battery, label = 'Available Battery')
ax1.plot(t, pv_prod, color='y', label = 'PV prod')
#ax1.plot(t, grid_battery_pv, color = 'c', label = 'Combined Power Discharge')
#ax1.plot(t, spot_prices, color='c', label = 'Spot prices')
#ax1.plot(abs(actual_battery_discharge))
#ax1.plot(abs(battery_discharge))
ax1.set_xlim(0,8760)
ax1.set_ylim(0,2100) # Setting y-axis plot limit
ax1.set_ylabel('Loading Demand [kW]') # Setting label for y-axis
ax1.set_xlabel('Hour [h]') # Setting label for x-axis
#ax2 = ax1.twinx()
#ax2.set_ylabel('Spot Price [Øre/kWh]', color='g')
#ax2.set_ylim(50,300)
#ax2.plot(t, spot_prices, color = 'g', label = 'Spot Price')
#ax2.plot(spot_prices)
fig.legend(bbox_to_anchor=(0.5, 1.07), loc='upper left', borderaxespad=0)

plt.savefig('filename.png', dpi=1200, bbox_inches='tight')

plt.show()
```

A.2 Python Optimization model for Energy Use After Completed Construction

```python
# -*- coding: utf-8 -*-
"""
Created on Mon Feb 20 09:44:58 2023

@author: maxim
"""

"Authors: Maximilian A W Sletbakk, Jonas Dalby, Eskil Kvålsvold"
# PV BATTERY LOAD EV
import matplotlib.pyplot as plt
import numpy as np
import pandas as pd
from gurobipy import GRB
import pyomo.environ as aml
from pyomo.environ import ConcreteModel,Set,RangeSet,Param,Suffix,Reals,NonNegativeReals,NonPositiveReals,Binary,Objective,minimize,maxim
from pyomo.core import Constraint,Var,Block,ConstraintList
from pyomo.opt import SolverFactory, SolverStatus, TerminationCondition
from pyomo.environ import *
from pyomo.core.expr.current import value
'-------ARRAYS ARE COMMENTED IN AND OUT DEPENDING ON WHEN THEY ARE USED----------------------'
'-----------------------------------El-DEMAND-----------------------------------------'
time = np.arange(0, 48)

# Winter demand data
# transformer_load = [59.70,59.55,59.69,59.69,59.94,57.94,81.22,108.49,113.93,
#                     102.14,94.42,94.12,94.10,94.47,95.81,115.72,143.88,164.30,
#                     164.87,155.05,151.92,137.24,125.48,88.77,61.65,61.46,61.44,
#                     61.45,61.48,57.56,82.70,109.51,114.61,101.67,94.24,93.95,
#                     93.79,93.99,95.81,115.57,143.86,164.55,165.13,154.77,
#                     152.19,138.24,126.09,89.04]
# # Spring demand data
# transformer_load = [58.91,58.74,58.87,59.18,57.94,79.72,106.85,110.77,99.06,
#                     90.57,90.39,90.36,90.50,92.16,111.83,139.66,159.76,160.66,
#                     151.13,148.32,135.21,120.71,84.87,59.34,59.19,59.31,59.45,
#                     59.57,57.13,80.69,107.48,111.99,100.45,92.63,92.22,91.97,
#                     92.39,94.45,113.26,140.55,160.82,161.86,151.80,149.31,
#                     135.71,121.94,85.47,58.72]
# #Summer demand data
# transformer_load = [54.33,54.59,54.83,55.02,54.83,53.34,74.18,101.28,107.32,
#                     95.41,88.00,87.81,87.79,87.99,90.91,109.51,138.06,157.68,
#                     158.37,149.04,145.12,131.97,116.51,82.82,55.41,55.28,55.28,
#                     55.32,55.16,54.17,74.33,101.76,107.19,95.13,87.91,87.82,
#                     87.75,88.05,90.45,109.45,138.04,157.61,158.11,148.73,
#                     144.53,132.05,116.29,83.21]

# #Autumn demand data
transformer_load = [56.61,56.45,56.29,56.15,56.00,55.08,76.54,104.25,109.27,
                    96.58,89.10,88.87,88.81,89.01,91.72,110.32,138.37,158.23,
                    159.02,150.04,146.68,132.30,118.44,82.93,56.35,56.11,56.04,
                    55.96,56.00,54.60,77.04,104.35,109.49,97.22,89.04,88.95,
                    88.78,89.14,91.42,110.29,138.73,158.90,159.46,150.54,
                    147.96,133.21,118.44,85.58]

# transformer_load = np.zeros(48)


'-----------------------------------PUMP-----------------------------------------------'
#Winter pump Jan (480h)
# transformer_load_pump = [0.459,0.491,0.528,0.555,0.545,0.539,0.828,2.180,
#                          6.285,2.500,1.047,0.917,0.811,0.716,0.650,0.465,0.416,
#                          0.594,2.673,2.684,0.806,0.603,0.639,0.662,0.445,0.367,
#                          0.365,0.367,0.388,0.348,0.392,0.817,1.930,0.953,0.465,
#                          0.352,0.327,0.337,0.315,0.310,0.264,0.333,1.469,1.685,
#                          0.564,0.440,0.420,0.416]

# #Spring pump mar (1837h)
# transformer_load_pump = [0.210,0.213,0.172,0.186,0.170,0.204,0.325,0.608,
#                          1.036,0.479,0.214,0.172,0.193,0.307,0.329,0.287,0.219,
#                          0.279,1.274,1.051,0.336,0.247,0.236,0.203,0.188,0.170,
#                          0.144,0.154,0.140,0.147,0.176,0.279,0.431,0.268,0.163,
#                          0.131,0.184,0.242,0.255,0.175,0.123,0.159,0.564,0.635,
#                          0.257,0.202,0.199,0.167]

# # Summer pump 10.june
# transformer_load_pump = np.zeros(48)

#Autumn pump Oct (7080h)
transformer_load_pump = [0.193,0.203,0.204,0.186,0.197,0.295,0.570,1.123,
                         0.640,0.296,0.198,0.162,0.144,0.151,0.133,0.108,0.127,
                         0.619,0.792,0.347,0.304,0.286,0.277,0.237,0.234,0.245,
                         0.248,0.227,0.231,0.349,0.711,1.479,0.842,0.402,0.329,
                         0.275,0.200,0.187,0.185,0.128,0.146,0.653,0.829,0.312,
                         0.288,0.289,0.270,0.247]
'-------------------------------------------------------------------------------------------------'

#Transformer_load array allows the use of auxillary power consumption
# transformer_load = np.zeros(48)
```

```
# Number of EVs connecting at which time step.
# 5 means that 5 EVs connect at that time step.
Number_of_EVs_connecting = [0,0,0,0,0,0,0,0,0,0,0,0,22,40,58,62,58,54,24,
                            32,28,8,4,0,0,0,0,0,0,0,0,0,0,0,0,0,0,0,0,0,0,0,0
                            ,0,0,0,0,0]

#Adds together the electric load from housing and the electric load for the pump
for t in time:
    transformer_load[t] = transformer_load[t] + transformer_load_pump[t]

print('NUMBER OF EVs:', sum(Number_of_EVs_connecting))



'---------------------------------SPOT PRICES AND PV-----------------------------------------'

'-----------------------------2021-SPOT--------------------------------------'
# # 2021 Winter   24 jan.
# Spot_price = [53.53,45.45,46.93,43.07,42.52,41.84,42.66,47.10,63.90,72.20,
#               78.00,82.18,77.31,74.47,71.19,69.11,67.98,68.09,69.47,75.77,
#               73.75,67.12,64.49,57.00,51.70,41.82,43.94,43.67,43.55,43.12,
#               45.48,51.39,60.43,73.01,76.31,74.02,76.27,74.30,72.24,68.02,
#               68.45,70.33,70.95,76.09,72.61,65.17,62.42,56.69]

# # 2021 Spring 26,27. march
# Spot_price = [60.00,51.73,51.13,48.71,48.53,48.16,49.12,51.72,59.31,80.71,
#               79.67, 56.84,51.15,50.19,48.61,46.61,45.99,47.42,49.27,52.17,
#               59.10,58.58,56.49,57.97,52.41,48.31,47.17,46.50,47.09,47.95,
#               49.01,52.28,69.58,79.31,83.29,67.98,54.60,51.61,49.67,49.57,
#               50.96,54.43,56.09, 63.76, 65.36,73.86,63.46,60.81]

# # # 2021 Summer   10.juni.
# Spot_price = [50.22,48.63,49.11,49.10,47.51,46.81,48.99,48.85,51.78,57.27,
#               58.64,58.71,58.69,58.68,59.15,58.77,57.71,57.20,57.18,57.18,
#               57.18,57.15,57.30,53.04,52.08,50.15,49.82,49.38,49.17,49.08,
#               48.85,49.06,49.75,52.65,57.29,57.22,56.33,52.87,52.89,52.11,
#               51.09,50.48,51.29,52.12,51.84,51.42,50.88,50.68]


# #2021 Autumn
# Spot_price = [89.41,89.19,84.47,81.88,81.03,80.93,81.04,81.18,85.79,90.45,
#               91.68,89.11,87.49,86.52,80.39,77.19,79.61,84.42,88.65,90.89,
#               93.45,92.86,92.59,91.27,88.12,88.96,83.88,79.93,75.51,74.51,
#               74.49,75.57,77.71,81.61,85.51,85.43,88.57,87.12,83.51,80.16,
#               83.23,84.29,89.31,90.88,95.43,101.13,93.74,90.70]

'-----------------------------2020-SPOT--------------------------------------'

#2020 Winter 16 jan:
# Spot_price = [23.711,23.305,23.347,22.862,22.13,21.656,21.992,22.506,24.119,
#               24.831,25.207,25.237,25.069,24.712,24.782,24.851,24.97,25.662,
#               26.345,26.602,26.137,25.425,24.861,24.584,23.713,23.179,22.748,
#               22.56,22.352,22.333,22.748,23.47,24.213,24.737,25.113,25.064,
#               25.004,24.915,24.806,24.826,24.915,25.093,25.588,25.697,25.321,
#               24.876,24.48,24.252]

# # #2020 Spring 6,7 April
# Spot_price = [4.971,4.835,4.986,4.974,4.941,4.963,5.02,5.087,5.144,5.256,5.347,
#               5.335,5.313,5.223,5.11,4.986,4.896,4.862,4.941,5.099,5.189,5.223,
#               5.2,5.144,5.11,5.053,5.288,5.242,5.208,5.197,5.197,5.208,5.197,
#               5.231,5.288,5.162,4.844,4.378,4.059,3.991,3.991,4.185,4.457,
#               4.969,5.288,5.322,5.299,5.231]

# # 2020 Summer  24.juni:
# Spot_price = [1.497,1.486,1.432,1.357,1.324,1.324,1.357,1.464,1.529,1.572,
#               1.594,1.594,1.594,1.594,1.615,1.604,1.583,1.561,1.551,1.54,1.529,
#               1.551,1.551,1.551,1.529,1.508,1.497,1.443,1.411,1.39,1.368,1.454,
#               1.562,1.583,1.637,1.637,1.637,1.627,1.616,1.616,1.616,1.583,1.583,
#               1.562,1.551,1.562,1.573,1.573]

# #2020 Autumn 14,15 oktober
Spot_price = [13.464,13.289,17.714,17.358,17.099,16.958,16.915,16.656,16.98,
              17.563,17.736,18.157,18.167,18.362,18.319,18.189,18.124,18.178,
              18.167,18.254,18.394,18.653,18.286,18.06,18.157,17.811,19.074,
              18.977,18.945,18.955,18.999,19.031,19.204,19.366,19.754,19.765,
              19.614,19.56,19.409,19.387,19.366,19.269,19.215,19.258,19.312,
              19.344,19.344,19.366]

'-----------------------------PV-PROD----------------------------------------'
#WINTER
# PV_Prod = [0,0,0,0,0,0,0,0,0,0,22.37,114.191,155.34,67.76,102.36,0,0,0,0,0,0,0,
#            0,0,0,0,0,0,0,0,0,0,0,22.37,114.91,155.34,67.76,102.36,0,0,0,0,0,
#            0,0,0,0]

# # SPRING      12.April
# PV_Prod = [0,0,0,0,0,0,0,2.13,17.06,30.54,99.78,138.08,185.73,294.96,338.11,
```

```
#             278.69,172.25,269.46,248.44,183.51,79.62,0,0,0,0,0,0,0,0,0,0,2.13,
#             17.06,30.54,99.78,138.08,185.73,294.96,338.11,278.69,172.25,269.46,
#             248.44,183.51,79.62,0,0,0]

# # SUMMER
# PV_Prod = [0,0,0,0,12,16,21,50,120,231,342,380,360,410,470,450,350,240,170,
#             100,25,5,0,0,0,0,0,0,12,16,21,50,120,231,342,380,360,410,470,450,
#             350,240,170,100,25,5,0,0]

# # AUTUMN   20.Oktober
PV_Prod = [0,0,0,0,0,0,0,0,0,3.54,64.23,173.86,222.36,207.36,219.47,191.41,
           201.46,262.83,61.42,0,0,0,0,0,0,0,0,0,0,0,0,3.54,64.23,173.86,
           222.36,207.36,219.47,191.41,201.46,262.83,61.42,0,0,0,0,0]

# PV_Prod = np.zeros(48)
Battery_Charge = np.zeros(48)
Charge_Status = np.zeros(48)
Discharge_Status = np.zeros(48)
PV_togrid = np.zeros(48)
Data = {}

'---------------------------------DICTIONARY---------------------------------'
Data["Transformer_load"] = {}
Data["Number_of_EVs_connecting"] = {}
Data["Spot_price"] = {}
Data["PV_Prod"] = {}

for t in time:
    Data["Transformer_load"][t] = transformer_load[t]
    Data["Number_of_EVs_connecting"][t] = Number_of_EVs_connecting[t]
    Data["Spot_price"][t] = Spot_price[t]
    Data["PV_Prod"][t] = PV_Prod[t]

Data["Transformer_capacity"] = 400
# Electric vehicle charging information
Data["Energy_per_EV"] = 10
# Total EV charge need
Data["Total_charge_need"] = Data["Energy_per_EV"]*\
    sum(Data["Number_of_EVs_connecting"][t] for t in range(len(time)))

'-----------------------------------MODEL-----------------------------------'

def getModel(Data): # Function where we extract the model
    ## Defining model type
    model = ConcreteModel() # Creating the model
    model.Data = Data
    ## Creating sets
    # Set representing the time steps, 48 hours
    model.t = Set(initialize=np.arange(0, 48), ordered=True)
    model.t1 = Set(initialize=np.arange(1, 48), ordered=True)
    # Set representing the time steps until all vehicles must be fully charged
    # which is 32 hours
    model.c = Set(initialize = np.arange(0,32), ordered=True)

        # Creating parameters
    def load_data_rule(model, t):
        return Data["Transformer_load"][t]
    def pv_prod_rule(model, t):
        return Data["PV_Prod"][t]
    model.Load = Param(model.t, rule=load_data_rule)
    model.Pv = Param(model.t, rule = pv_prod_rule )
    def EV_demand_rule(model, t):
        return np.multiply(Data["Number_of_EVs_connecting"][t]\
                           , Data["Energy_per_EV"])
    model.Original_EV_demand = Param(model.t, rule=EV_demand_rule)
    def Spot_price_rule(model, t):
        return 0.01 * Data["Spot_price"][t] # Spot prices converted to NOK/kWh
    model.Spot_price = Param(model.t, rule=Spot_price_rule)
    def Total_charge_need_rule(model):
        return Data["Total_charge_need"]
    model.Total_charge_need = Param(rule=Total_charge_need_rule)
    model.Transformer_capacity = Param(initialize=Data["Transformer_capacity"])
    model.Energy_per_EV = Param(initialize=Data["Energy_per_EV"])


                    #VARIABLES
    model.net_transformer_load = Var(model.t) #Can be negative
    # Variable to track how much we charge each hour
    model.charged = Var(model.t,within=NonNegativeReals)
    # Variable to track the total charge need per hour
    model.charge_need =Var(model.t,within=NonNegativeReals)
    model.pvtogrid = Var(model.t, within=NonNegativeReals)
    #variable to track the power that goes from PV(solar) to direct supply
    model.batteryCharge = Var(model.t, within = NonNegativeReals)
    #variable to track the power that goes from PV(solar) to charge the battery
    model.batteryDischarge = Var(model.t, within = NonNegativeReals)
    #variable to track the power that discharges from the battery to supply
```

```
    model.batteryLevel = Var(model.t, within = NonNegativeReals)
    #variable that tracks the battery level
    model.chargeDecision = Var(model.t, within = Binary)
    model.dischargeDecision = Var(model.t, within = Binary)
    model.gridToBattery = Var(model.t, within = NonNegativeReals)
    model.pvtowaste = Var(model.t, within = NonNegativeReals)



    ## Constraints
    eps =0.001
    M = 1000 + eps

# create new variables to represent positive and negative values of net_transformer_load
    model.positive_transformer_load = Var(model.t, within=NonNegativeReals)
    model.negative_transformer_load = Var(model.t, within=NonPositiveReals)

# define constraints to ensure that the positive and negative variables sum up to the original net_transformer_load
    def transformer_load_constraint_rule(model,t):
        return model.positive_transformer_load[t] \
            + model.negative_transformer_load[t]\
                == model.net_transformer_load[t]
    model.transformer_load_constraint = Constraint(model.t, rule=transformer_load_constraint_rule)

# define additional constraints to ensure that each variable represents only positive or negative values
    def positive_transformer_load_constraint_rule(model,t):
        return model.positive_transformer_load[t] >= 0
    model.positive_transformer_load_constraint = Constraint(model.t, rule=positive_transformer_load_constraint_rule)

    def negative_transformer_load_constraint_rule(model,t):
        return model.negative_transformer_load[t] <= 0
    model.negative_transformer_load_constraint = Constraint(model.t, rule=negative_transformer_load_constraint_rule)

    def zero_sum_constraint_rule(model, t):
        return model.positive_transformer_load[t] * model.negative_transformer_load[t] == 0
    model.zero_sum_constraint = Constraint(model.t, rule=zero_sum_constraint_rule)



    def charge_rule(model,t):
        return model.batteryCharge[t] >= 0 + eps - M * (1\
                                        - model.chargeDecision[t])
    model.charge_rule = Constraint(model.t, rule=charge_rule)

    def charge_rule2(model,t):
        return model.batteryCharge[t] <= 0 + M * model.chargeDecision[t]
    model.charge_rule2 = Constraint(model.t, rule=charge_rule2)

    def discharge_rule(model,t):
        return model.batteryDischarge[t] >= 0 + eps - M * (1\
                                       - model.dischargeDecision[t])
    model.discharge_rule = Constraint(model.t, rule=discharge_rule)

    def discharge_rule2(model,t):
        return model.batteryDischarge[t] <= 0 + M * model.dischargeDecision[t]
    model.discharge_rule2 = Constraint(model.t, rule=discharge_rule2)

    def battery_decision_rule(model,t):
        return model.chargeDecision[t] + model.dischargeDecision[t] <= 1
    model.battery_decision =  Constraint(model.t, rule=battery_decision_rule)

    def energy_balance_rule(model, t):
        return model.net_transformer_load[t] == model.Load[t] +\
            model.charged[t] -model.pvtogrid[t] - model.batteryDischarge[t]\
          + model.gridToBattery[t]
    model.energy_balance_c = Constraint(model.t, rule=energy_balance_rule)

    def battery_test_rule(model,t):
        return model.batteryLevel[t] == model.batteryLevel[t-1]\
            +model.batteryCharge[t-1]-model.batteryDischarge[t-1]\
           + model.gridToBattery[t-1] #Hour t denotes beginning of hour t
    model.battery_test_rule = Constraint(model.t1, rule = battery_test_rule)

    # The sum of EV charge load must equal the total charge need
    def tot_charge_need_rule(model, t):
        return model.Total_charge_need == sum(model.charged[t] for t in model.c)
    model.tot_charge_need = Constraint(model.c, rule=tot_charge_need_rule)
            # The amount of charging per hour must be less than the
            # total charge need for all connected vehicles through hour t,
            # minus total amount already charged.

    def max_charge_rule(model,t):
        return model.charged[t] <= sum(model.Original_EV_demand[i]\
         for i in range(t))- sum(model.charged[i] for i in range(t))
    model.max_charge = Constraint(model.c, rule =max_charge_rule)

    def max_charge_needed_rule(model,t):
```

```
        return  model.Total_charge_need == sum(model.charged[t] for t in model.t)
    model.max_charge_needed = Constraint(model.t, rule = max_charge_needed_rule)

    def battery_discharge_rule(model,t):
        return model.batteryCharge[t] + model.pvtogrid[t] + model.pvtowaste[t] \
            == model.Pv[t]
    model.battery_discharge = Constraint(model.t, rule = battery_discharge_rule)

    def battery_discharge_rule2(model,t):
        return model.batteryDischarge[t] <= model.batteryLevel[t]
    model.battery_discharge_rule2 = Constraint(model.t, rule = battery_discharge_rule2)

    def transformer_capacity_rule(model,t):
        return model.net_transformer_load[t] <= model.Transformer_capacity
    model.max_transformer_capacity = Constraint(model.t, rule = transformer_capacity_rule)

    def battery_start_rule(model,t):
        return model.batteryLevel[0] == 1000    #starts with a full battery
    model.battery_start_rule = Constraint(model.t, rule = battery_start_rule)

    def battery_level_rule1(model,t):
        return model.batteryLevel[t] <= 1000      #capacity of battery is 1MWh
    model.battery_level1 = Constraint(model.t, rule = battery_level_rule1)

    def selling_capacity_rule(model,t):
        return model.net_transformer_load[t] >= -100   #Selling cap
    model.selling_capacity_rule = Constraint(model.t, rule = selling_capacity_rule)

    #arbitrary cap, just to limit the strain on external grid
    def grid_to_battery_cap_rule(model,t):
        return model.gridToBattery[t] <= 500
    model.grid_to_battery_cap_rule = Constraint(model.t, rule = grid_to_battery_cap_rule)

    model.halved_negative_transformer_load = Expression(model.t, rule=lambda model, t: model.negative_transformer_load[t] / 2)
    # halve the negative variable model, so that it can be used directly in the obj. function

    def objective_function(model):
        cost = sum(model.positive_transformer_load[t] * model.Spot_price[t] for t in model.t) +
        sum(model.halved_negative_transformer_load[t] * \
                model.Spot_price[t] for t in model.t)
        return cost
    model.objective = Objective(rule=objective_function, sense=minimize)
    return model
# Solving the created model
model = getModel(Data) # Getting the model from the getModel function
opt = SolverFactory('gurobi', solver_io = 'python')
results = opt.solve(model, tee=True) # Results are saved
model.write('model.lp')    #writes an .lp file to review and analyze

'----------------------------------PLOTTING-----------------------------------------------'
model.solutions.load_from(results)
Load = np.zeros(48)
old_EV_load = np.zeros(48)
new_EV_load = np.zeros(48)
battery_discharge_array = np.zeros(48)
battery_charge_array = np.zeros(48)
battery_level_array = np.zeros(48)
pvtogrid_array = np.zeros(48)
c_decision_array =np.zeros(48)
d_decision_array = np.zeros(48)
net_transformer_load_array = np.zeros(48)
net_traf_neg_array = np.zeros(48)
net_traf_pos_array = np.zeros(48)
gridToBattery_array = np.zeros(48)
old_load_combined = np.zeros(48)
new_load_combined = np.zeros(48)
net_traf_neg_array_half = np.zeros(48)
pvtowaste_array = np.zeros(48)

#Write the values from the pyomo models to arrays
for t in time:
    Load[t] = model.Load[t]
    old_EV_load[t] = model.Original_EV_demand[t]
    new_EV_load[t] = model.charged[t].value
    battery_level_array[t] = model.batteryLevel[t].value
    battery_charge_array[t] = model.batteryCharge[t].value
    battery_discharge_array[t] = model.batteryDischarge[t].value
    pvtogrid_array[t] = model.pvtogrid[t].value
    c_decision_array[t] = model.chargeDecision[t].value
    d_decision_array[t] = model.dischargeDecision[t].value
    net_transformer_load_array[t] = model.net_transformer_load[t].value
    net_traf_pos_array[t] = model.positive_transformer_load[t].value
    net_traf_neg_array[t] = model.negative_transformer_load[t].value
    gridToBattery_array[t] = model.gridToBattery[t].value
    old_load_combined[t] = model.Original_EV_demand[t] + model.Load[t]
    new_load_combined[t] = model.charged[t].value + model.Load[t]
    net_traf_neg_array_half[t] = value(model.halved_negative_transformer_load[t])
```

```
    pvtowaste_array[t] = model.pvtowaste[t].value

sumBought = 0
for t in time:
    if  net_transformer_load_array[t] > 0:
        sumBought = sumBought + net_transformer_load_array[t]
    else:
        sumBought = sumBought



#\%\%  Plot setup
t=[i for i in range(0,48)]
plt.figure(dpi=1100)
fig, ax1 = plt.subplots()
ax1.set_xlabel('Hour [h]') # Setting label for x-axis
ax1.set_ylabel('Power [kW]') # Setting label for charging-axis
ax1.tick_params(axis='y')
ax1.set_ylim(0,1600) # Setting y-axis plot limit
ax2 = ax1.twinx() # initiate second axis for spot price
ax2.set_ylabel('Spot Price [Øre/kWh]') # Setting label for price-axis
ax2.tick_params(axis='y')
ax2.set_ylim(0,35) # Setting y-axis plot limit

## Plotting values
# ax1.plot(t, transformer_load_pump, label = ' Pump El-Demand Winter') # Plotting base load
# ax1.plot(t, transformer_load_pump2, label = ' Pump El-Demand Spring') # Plotting base load
# ax1.plot(t, transformer_load_pump3, label = ' Pump El-Demand Summer') # Plotting base load
# ax1.plot(t, transformer_load_pump4, label = ' Pump El-Demand Autumn') # Plotting base load

# ax1.plot(t, Load, label = ' El Demand') # Plotting base load
# ax1.bar(t, new_EV_load, bottom = Load, label = 'EV Load')
# ax1.bar(t, old_EV_load, bottom = Load, label = 'Original EV Load Profile')
# ax1.bar(t, transformer_load, label = 'Housing Stock El-Demand Autumn')
# ax1.bar(t, transformer_load_pump, label = 'Pump El-Demand Autumn')
# ax1.bar(t, old_load_combined, label = 'Original load profile')
# ax1.bar(t, new_load_combined, label = 'New load profile')
# ax1.bar(t, gridToBattery_array, label = 'Battery charging from external grid')
ax2.plot(t, Spot_price, label = 'Spot Price Autumn 2020')
# ax2.plot(t, Spot_price, color='g', label = 'Spot Price Spring 2020')
ax1.plot(t,battery_level_array, color = '#E50000', label = 'Battery Level')
ax1.bar(t,PV_Prod, color ='#9ACD32', label = 'PV Production Autumn')
# ax1.plot(t,net_transformer_load_array, label = 'Net Transformer Load Autumn')
# ax1.plot(t,battery_charge_array, label = 'Charging')
# ax1.plot(t,battery_discharge_array, label = 'Discharge')
# ax1.plot(t,pvtogrid_array, label = 'PV to grid')

# ax1.axhline(y=0, color='#000000', linestyle='dotted')
# ax1.plot(t,[Data["Transformer_capacity"]]*(max(t)+1),
#           color='r', label = 'Max transformer capacity')
# fig.legend()
fig.legend(bbox_to_anchor=(0.54, 1.08), loc='upper left', borderaxespad=0)
plt.savefig('conBatteryAutumn.pdf', dpi=1100, bbox_inches='tight')
plt.show()
print('TOTAL BOUGHT POWER', sumBought, 'kWh')
sumUsed = sum(old_load_combined) -sum(PV_Prod)
print('Total used power', sumUsed,'kWh')
print('OLD LOAD', sum(old_load_combined), 'kWh')
print('SUM PV', sum(PV_Prod), 'kWh')
print('Total wasted power',sum(pvtowaste_array), 'kWh' )
```

A.3 MatLab Heating Code Hønefoss: Eivind W. Roland (Reproduced with permission)

```
%{
Dette programmet tar inn vÃ¦rdata fra excel-dokumentet "Weather-data.xlsx"
og beregner energibehov for Ã¥ oppnÃ¥ Ã¸nsket innvendig temperatur pÃ¥ byggeplass. For Ã¥
endre prosjekt, mÃ¥ du endre input-verdiene Ã¸verst i koden. Excel-arket "Weather-data.xlsx"
inneholder timeopplÃ¸st temperatur for Oslo-omrÃ¥det i gjennomsnitt fra 2010
til 2021 i perioden november til mars.

Programmet er skrevet av Eivind W Roland som en del av fordypningsprosjekt
hÃ¸sten 2021.
%}

clear all;
clc;

%Inputs:

Rehab_logic = 0; %1 if project is rehabilitation of existing concrete structure

Facade_logic = 0; %1 if project is in need of heating facade

Envelope_area = 11154; %Area of building envelope

BuildingVolume = 82080; %Volume of building

Set_temp = 15; %Temperature desired inside building.



%Allocations and fixed values


U_value = 1.9; %U-value of building envelope (Dynamic value for a building site). Approximated value.

Infiltration = 0.7; %Hourly air exchange in building (Dynamic value for a building site)

Facade_power = 0.003; %Power needed for facade heating on average [kW/m^3]. DNVGL-report.

c = 0.33; %Heat capacity air

Temperatures = xlsread('Weather_data_Hønefoss','P:P'); %Vector with temperatures for given period.

EnergyLossEnvelope = 0; %Allocation

EnergyLossAir = 0;%Allocation

MaxThermalW = 0; %Allocation
```

```
MaxInfiltrationW = 0; %Allocation

Heat_index = []; %Vector that contains 0 for hours not in need of heating, 1 otherwise.

Power_vector_thermal = []; %Vector that contains power for thermal loss for each timestamp

Power_vector_infil = []; %Vector that contains power for infiltration for each timestamp

Hours = [];

Heating_factor = 1; %Can be reduced if project is rehabilitation

%change energy needs if rehab
if Rehab_logic == 1
    Heating_factor = 0.82; %value approximated by UCO
end


%Find what hours are in need of heating and store them in vector.
for i=1:length(Temperatures)
    Hours(i,1)=i;
    if Temperatures(i)>= Set_temp
        Heat_index(i)=0;
    else
        Heat_index(i)=1;
    end
end

%Use U-value to calculate thermal loss through Envelope

for k=1:length(Temperatures)
    if Heat_index(k)==1
        ThermalHeatLoss = Heating_factor*(U_value*(Set_temp-Temperatures(k)) *Envelope_area)/1000;
        EnergyLossEnvelope = EnergyLossEnvelope + ThermalHeatLoss;  %Energyloss in kWh since temperatures are hourly
        Power_vector_thermal(k,1) = ThermalHeatLoss;
        if ThermalHeatLoss > MaxThermalW
            MaxThermalW = ThermalHeatLoss;
        end
    end
end

%Use infiltrationvalue to calculate loss
for k=1:length(Temperatures)
    if Heat_index(k)==1
        InfiltrationHeatLoss = Heating_factor*(c*Infiltration*(Set_temp-Temperatures (k))*BuildingVolume)/1000;
        EnergyLossAir = EnergyLossAir + InfiltrationHeatLoss;  %Energyloss in kWh since temperatures are hourly
```

```
        Power_vector_infil(k,1) = InfiltrationHeatLoss;
        if InfiltrationHeatLoss > MaxInfiltrationW
            MaxInfiltrationW = InfiltrationHeatLoss;
        end
    end
end

%Energy used facade heating
if Facade_logic == 1
    Facade_power_total = Facade_power*BuildingVolume;
    Facade_Energy = Facade_power*BuildingVolume*length(Temperatures);
else
    Facade_Energy = 0;
    Facade_power_total = 0;
end



TotalE_heating_inside = EnergyLossEnvelope + EnergyLossAir;  %total inside heating↙
power

Power_vector = Power_vector_thermal+Power_vector_infil+Facade_power_total;  %total↙
power demand



Power_heatpump = Power_vector;

%Heat pump
for j=1:length(Power_heatpump)
    if Temperatures(j) <= -15
        COP = 1.25;
        Power_heatpump (j) = Power_heatpump (j)/COP;
    end
    if Temperatures(j) <= -7 && Temperatures(j) > -15
        COP = 1.98;
        Power_heatpump (j) = Power_heatpump (j)/COP;
    end
    if Temperatures(j) <= 2 && Temperatures(j) > -7
        COP = 2.38;
        Power_heatpump (j) = Power_heatpump (j)/COP;
    end
    if Temperatures(j) <= 7 && Temperatures(j) > 2
        COP = 2.775;
        Power_heatpump (j) = Power_heatpump (j)/COP;
    end
    if Temperatures(j) <= 12 && Temperatures(j) > 7
        COP = 3.175;
        Power_heatpump (j) = Power_heatpump (j)/COP;
    end
    if Temperatures(j) > 12
        COP = 4;
        Power_heatpump (j) = Power_heatpump (j)/COP;
```

```
    end
end



%Writing to Excel

%Inside heating
xlswrite('Results.xlsx',TotalE_heating_inside,'Energy and Power','I4');

%Facade_energy
xlswrite('Results.xlsx',Facade_Energy,'Energy and Power','I5')

%Powers for all hours
xlswrite('Results.xlsx',Hours,'Energy and Power','A2');
xlswrite('Results.xlsx',Power_vector,'Energy and Power','B2');

%Volume and envelope
xlswrite('Results.xlsx',Envelope_area,'Energy and Power','F9');
xlswrite('Results.xlsx',BuildingVolume,'Energy and Power','F10');

%Heat pump results
xlswrite('Results.xlsx',Hours,'Heat pump','A2');
xlswrite('Results.xlsx',Power_heatpump,'Heat pump','B2');
```

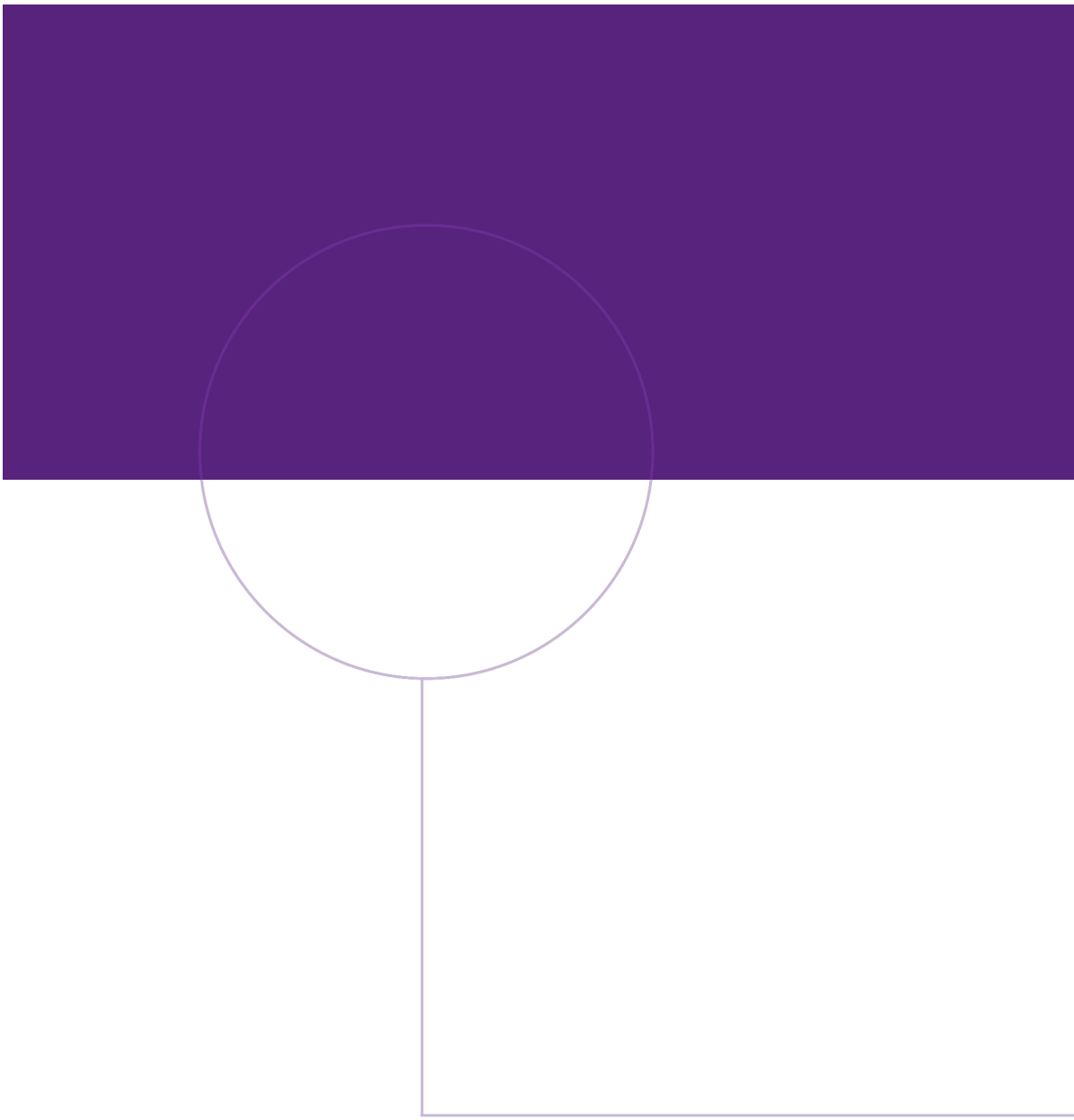

NTNU

Norwegian University of
Science and Technology